

SECURITY (red)

REPORT DOCUMENTATION PAGE

READ INSTRUCTIONS
BEFORE COMPLETING FORM

1. REPORT NUMBER MTL TR 92-10	2. GOVT ACCESSION NO.	3. RECIPIENT'S CATALOG NUMBER									
4. TITLE (and Subtitle) DEVELOPMENT AND TESTING OF ADVANCED EM ACCELERATOR BORE MATERIALS		5. TYPE OF REPORT & PERIOD COVERED Interim Report - 10/1/87 - 9/30/91									
		6. PERFORMING ORG. REPORT NUMBER LJ91-077-TR									
7. AUTHOR(s) R. Daniel Stevenson, Stuart N. Rosenwasser, and John W. McCoy		8. CONTRACT OR GRANT NUMBER(s) DAAL04-86-C-0045									
9. PERFORMING ORGANIZATION NAME AND ADDRESS Sparta, Inc. 9455 Towne Centre Drive San Diego, CA 92121-1964		10. PROGRAM ELEMENT, PROJECT, TASK AREA & WORK UNIT NUMBERS									
11. CONTROLLING OFFICE NAME AND ADDRESS U.S. Army Materials Technology Laboratory ATTN: SLCMT-PRA Watertown, Ma 02172-0001		12. REPORT DATE February 1992									
		13. NUMBER OF PAGES 142									
14. MONITORING AGENCY NAME & ADDRESS (if different from Controlling Office)		15. SECURITY CLASS. (of this report) Unclassified									
		15a. DECLASSIFICATION/DOWNGRADING SCHEDULE									
16. DISTRIBUTION STATEMENT (of this Report) Approved for public release; distribution unlimited.											
17. DISTRIBUTION STATEMENT (of the abstract entered in Block 20, if different from Report)											
18. SUPPLEMENTARY NOTES Robert Fitzpatrick, COR											
19. KEY WORDS (Continue on reverse side if necessary and identify by block number) <table style="width: 100%; border: none;"> <tr> <td style="width: 33%;">Railguns</td> <td style="width: 33%;">Electromagnetic launcher</td> <td style="width: 33%;">Aluminum oxide</td> </tr> <tr> <td>Ceramics</td> <td>Bore materials</td> <td>Fracture toughness</td> </tr> <tr> <td>Insulators</td> <td>Fracture (mechanics)</td> <td>Hot pressing</td> </tr> </table>			Railguns	Electromagnetic launcher	Aluminum oxide	Ceramics	Bore materials	Fracture toughness	Insulators	Fracture (mechanics)	Hot pressing
Railguns	Electromagnetic launcher	Aluminum oxide									
Ceramics	Bore materials	Fracture toughness									
Insulators	Fracture (mechanics)	Hot pressing									
20. ABSTRACT (Continue on reverse side if necessary and identify by block number) (SEE REVERSE SIDE)											

DTIC
 ELECTE
 MAR 11 1992
 S B D

Block No. 20

ABSTRACT

Electromagnetic railguns are being considered for a number of potential Strategic Defense, Theater Missile Defense and tactical missile applications. Bore materials, particularly insulators, limit the performance and lifetime of current railguns. A program was undertaken to develop improved advanced ceramic insulators. The program aim was to: analytically determine the property goals required of bore insulators to meet railgun systems requirements; select and design initial candidate materials using micro-architectural tailoring; fabricate and test panels of the selected materials; iterate compositions and processing parameters to improve properties; and down-select to an optimal material and scale it up to a size required for near-term railguns. From the start of the program it was realized that ceramics alone possessed the necessary properties to meet the system requirements. Through a combination of mechanical and electrical tests a large number of ceramic materials were screened. Microstructurally toughened aluminum oxide based ceramics gave the best combination of mechanical and electrical properties. The addition of chromia to the base alumina-zirconia-yttria composition improved the electrical properties with no compromise in mechanical properties. The alumina-chromia material was successfully scaled up to 1.5 x 4 x 18 inch pieces, representative of large railgun bore insulators. These scaled up pieces also met the mechanical and electrical goal properties for railgun insulator operation. The additional work required to produce and qualify these insulator materials for reliable and cost effective high-energy railgun utilization was recommended.



US ARMY
LABORATORY COMMAND
MATERIALS TECHNOLOGY LABORATORY

MTL TR 92-10

AD

DEVELOPMENT AND TESTING OF ADVANCED EM ACCELERATOR BORE MATERIALS

February 1992

R. DANIEL STEVENSON, STUART N. ROSENWASSER,
and JOHN W. McCOY

Sparta, Inc.
9455 Towne Centre Drive
San Diego, CA 92121-1964

INTERIM REPORT

Contract DAAL04-86-C-0045

Approved for public release; distribution unlimited.

Prepared for

U.S. ARMY MATERIALS TECHNOLOGY LABORATORY
Watertown, Massachusetts 02172-0001

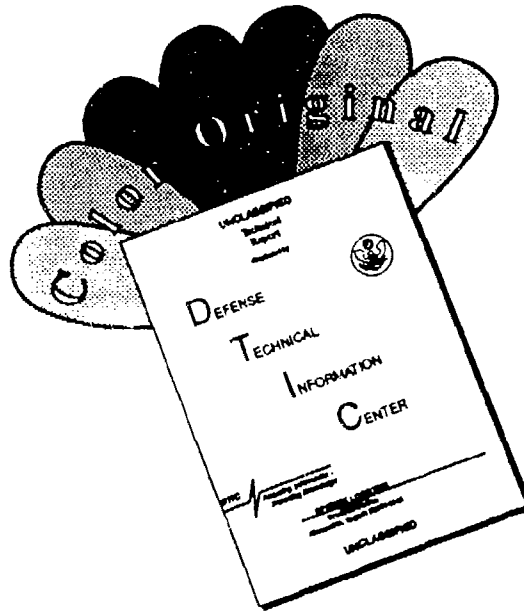
The findings in this report are not to be construed as an official Department of the Army position, unless so designated by other authorized documents.

Mention of any trade names or manufacturers in this report shall not be construed as advertising nor as an official indorsement or approval of such products or companies by the United States Government.

DISPOSITION INSTRUCTIONS

Destroy this report when it is no longer needed.
Do not return it to the originator.

DISCLAIMER NOTICE



THIS DOCUMENT IS BEST QUALITY AVAILABLE. THE COPY FURNISHED TO DTIC CONTAINED A SIGNIFICANT NUMBER OF COLOR PAGES WHICH DO NOT REPRODUCE LEGIBLY ON BLACK AND WHITE MICROFICHE.

FOREWORD

This document is an Interim Technical Report for 22 October 1991 covering work performed under U.S. Army Materials Technology Laboratory (MTL) contract DAAL04-86-0045. The MTL contracting officer technical representatives are Mr. John Dignam and Dr. Robert Fitzpatrick. This work was sponsored by the Strategic Defense Initiative Organization / U.S. Army Strategic Defense Command Office (SDIO/USASDC) at Huntsville, Alabama. The work was monitored by the Electric Gun Branch at the U.S. Army Armament Research, Development and Engineering Center (ARDEC), where railgun testing of the materials was also performed. Maj. Noble Johnson and Lt.-Col. Gary Hagen were the Product Managers, and Mr. Stanley Smith was the Project Engineer at SDIO/USASDC.

The effort centered on the development, test and application of advanced ceramic insulator materials to electromagnetic launchers (EMLs). The environment of the bore insulating materials in high-power EMLs was evaluated and goal properties set. A wide variety of ceramic materials were produced and tested, and two compositions, one alumina (Al_2O_3) based and one silicon nitride (Si_3N_4) based were down selected. The alumina based material (with the addition of chromium oxide [Cr_2O_3]) was then chosen to be scaled up to the size needed for state-of-the art EMLs. The material still met the mechanical, electrical and producibility goals after scaling up. Limited testing was performed in a small EML.

Major contributions to this program were made by Richard Palicka and Andre Ezis, President and Vice-President of Cercom, Inc. of Vista, California. They provided essential support in the selection of material compositions and processing conditions. They fabricated most of the advanced ceramic insulator materials discussed in this report.

The authors extend their thanks to Bob Washburn (retired), Jim Black, Rudy Akin, and Galyn Thompson of SPARTA for their assistance in selection of compositions, processing conditions, and for testing and analysis. Two separate University groups, headed by Dr. Kris Kristiansen at Texas Tech University in Lubbock, Texas and Dr. Jenn-Ming Yang at the University of California, Los Angeles; provided expert assistance in the areas of electrical testing of insulator and conductor materials and mechanical testing and analysis of ceramic materials respectively.

Accession For	
NTIS GRA&I	<input checked="" type="checkbox"/>
DWIC TAB	<input type="checkbox"/>
Unannounced	<input type="checkbox"/>
Justification	
By	
Distribution/	
Availability Codes	
Dist	Avail and/or Special

92-06115



[This page is intentionally left blank]

CONTENTS

	PAGE
1.0 INTRODUCTION.....	1
1.1 The Limitations of Current Railgun Bore Materials	1
1.2 Program Objectives	5
2.0 SURVEY OF EM GUN BORE MATERIALS EXPERIENCE	9
2.1 Sources Surveyed	9
2.2 Results of Survey	12
2.3 Survey Summary and Conclusions	21
2.3.1 General	21
2.3.2 Conductor Bore Materials	22
2.3.3 Insulator Bore Materials	23
2.3.4 Design	23
3.0 DEFINING GUN DESIGNS AND BORE ENVIRONMENTS	25
4.0 ANALYTICAL MODELING TO DEFINE PROPERTY REQUIREMENTS	29
4.1 Bore Insulators	30
4.2 Conductor Rails	41
5.0 MATERIALS DESIGN, FABRICATION AND SCREENING	45
5.1 Advanced Ceramic Insulator Design Approach	45
5.2 Fabrication of Ceramic Insulator Materials	50
6.0 TESTING OF MATERIALS	75
6.1 Mechanical Testing	76
6.2 Electrical Testing	86
6.2.1 Candidate Ceramic Insulator Materials	87
6.2.2 Electrical Testing of Other Insulator Materials	108
6.2.3 Conductor Materials	118
6.3 Testing in the FLINT Railgun	125
6.3.1 Analysis and Modification of FLINT Gun Configuration	125
6.3.2 Testing of Insulator Samples in FLINT	129
7.0 SUMMARY AND CONCLUSIONS	133
8.0 RECOMMENDATIONS FOR FUTURE WORK	139
REFERENCES	141

FIGURES

		PAGE
1.1	Schematic of Electromagnetic Accelerator Operation. Bore Insulators (Not Shown) Separate the Conductor Rails	2
1.2	Bore Measurement (Insulator and Conductor) After Single High-Energy Shot in ARDEC/SPARTA Advanced Composite Railgun	4
1.3	Flow Chart Illustrating Major Components of This Program	
	References to Report Sections	7
2.1	The Report Form Used to Conduct EM Gun Bore Materials Experience Survey	13
3.1	Schematic of Structural, Thermal and Electrical Environment Experienced by Electromagnetic Launcher Bore Materials.....	26
3.2	Baseline Barrel Configuration Used in Analytical Modeling Studies	26
3.3	ARDEC/DARPA Advanced Composite Railgun and Pertinent Operating Parameters	28
4.1	Finite Element Models of Bore Radial Displacement for High- and Low-Modulus Materials Systems	31
4.2	Sensitivity Study of the Bore Component Displacement To Material Stiffness for Solid Armature EMLs	32
4.3	Active Prestress Load Transfer Efficiency To the Rail/Bore Insulator Interface	34
4.4	Probability of Detection of a Flaw As a Function of Thickness Sensitivity (Flaw Size Divided by Section Thickness).....	36
4.5	Effects of Bore Insulator Modulus on the Maximum Insulator Hoop Stress for Different Current Densities	37
4.6	Required Fracture Toughness of Advanced Bore Insulators as a Function of Conductor Rail Current Density and Insulator Moduli	38
4.7	Required Fracture Toughness of Advanced Bore Insulators as a Function of Minimum Detectable Crack Depth and Conductor Conductor Rail Current Density	38
4.8	The Range of Fracture Toughness Values for Some Ceramics and Ceramic Matrix Composites	39
4.9	Axial Variations of the Rail and Insulator Maximum Displacements Due to Plasma Armature Pressure	39
4.10	Axial Variations of the Maximum Axial Hoop Stresses in the Conductor Rails and Insulators Due to Plasma Armature Pressure	40
4.11	Thermal Model of Rail Showing Localized Melting on the Rail Corners During the Electrical Pulse	42

FIGURES - (Cont.)

	PAGE
4.12 Sensitivity Trade-Off of Rail Conductivity (% I.A.C.S.) On the Overall EML (Electromagnetic Launcher) Efficiency.....	42
4.13 Thermal/Electrical Current Diffusion Analysis for EML Rails	43
4.14 Evaluation Trade-Off Between Rail Cladding Thermal and Electrical Properties and the Cladding/Rail Substrate Temperature	44
5.1 Cutting Map for Consolidated 6 x 6 Inch Advanced Ceramic Panels	52
5.2 Determination of Candidate Ceramic Allowable Design Stresses Utilizing Weibull Statistics	57
5.3 The Effect of Weibull Modulus on the Ratio of Design Strength to Average MOR Strength for Different Values of Probability of Failure	58
5.4 Designs of Three Types of Mechanical Test Specimens Used in This Program: a) Chevron Notch Short Beam Fracture Toughness Test Specimen. B) Single Edge Notched Beam (SENB) Fracture Toughness Test Specimen. C) Modulus of Rupture (MOR) Flexural Strength Test Specimen. (All Dimensions In Inches)	60
5.5 Weibull Curves and Calculated Data for the Four Different Advanced Ceramic Insulator Materials Used for Testing in the Modified FLINT Gun Barrel	62
5.6 Weibull Curve for Advanced Ceramic Insulator $AlN-0.4Y_2O_3 - 25\ v/o\ SiC_w$	65
5.7 Cutting Map for Ceramic Plates, Type 1	69
5.8 Cutting Map for Ceramic Plates, Type 2	70
5.9 Photomicrograph of Typical Microstructure of $Al_2O_3-8ZrO_2-5.0Cr_2O_3-0.25Y_2O_3$ Advanced Ceramic Insulator Material and Explanation and Implications of Features (1500X)	72
5.10 Photomicrograph of Typical Microstructure of $Si_3N_4 - 8.0Y_2O_3 - 1.0Al_2O_3 - 15\%SiC_w$ Advanced Ceramic Insulator Material and Explanation and Implications of Features (1500X)	73
6.1 Mechanical Properties of Commercial Silicon Carbide Whisker (Made By ACMC) Loaded Alumina Plates	79
6.2 Typical Microstructure of 25% SiC Whisker (ACMC) Reinforced Alumina Material (1000X)	80
6.3 Typical Fracture Surface of 25% Silicon Carbide Whisker (ACMC) Loaded Alumina Material Revealing Whisker Pull-Out (5000X)	80

FIGURES - (Cont.)

		PAGE
6.4	Cutting Map for Mechanical Test Specimens From Full Sized 1.5 x 4 x 18 in. (3.8 x 10.2 x 45.7 cm) Alumina-Zirconia-Chromia Insulator Block	84
6.5	Representative Micrograph of Alumina-Chromia Block Consolidated To Demonstrate Retainment of Mechanical Properties in Full Scale Pieces. Evidence of Mixed Mode Failure is Shown By Sharp Grains (Intergranular) and Arrows Indicating Areas of Transgranular Failure (and Thus High Toughness) (3,500X)	86
6.6	Schematic Diagram of the SDS III Test Facility at Texas Tech University	88
6.7	Drawings of the Capacitor Bank and the Surface Discharge Switch Used for Testing Insulator Materials	89
6.8	Rep-Rated (1 Hz) Standing Arc Exposure Test Facility (SDS III) for Advanced Insulators at Texas Tech University	90
6.9	Closeup Photograph of Test Section Revealing Test Block With Electrodes Clamped On It's Surface	90
6.10	Surface Breakdown Voltage as a Function of Number of Discharges For Tested Railgun Bore Insulator Materials. Current Level of Approximately 300 kA With Pulse Repetition Rate of 1 Hz	91
6.11	Photomicrograph of the Exposed Surface of Transformation- Toughened Zirconia (TTZ by Coors Ceramics) After One Pulse (200X)	94
6.12	Photomicrograph of the Exposed Surface of Partially-Stabilized Zirconia (PSZ by Nilcra, Inc.) After One Pulse (200X)	95
6.13	Photomicrograph of the Exposed Surface of Alumina-Zirconia (TZ3Y by Ceramtec, Inc.) After One Pulse (200X)	95
6.14	Photomicrograph of the Exposed Surface of Alumina-25% SiC _w After 166 Pulses (200X)	96
6.15	The Response of Ceramic Insulator Materials to Repeated Arc Exposures. Surface Standoff Voltage Is Plotted for Each Arc Pulse in a Series of 100 For Six Different Materials	98
6.16	Micrograph of Al ₂ O ₃ -0.25Y ₂ O ₃ -8ZrO ₂ (483-2) After Exposure to Greater Than 100 Pulses in Arc Test Facility. Microcrack Network and Limited Spalling is Seen (400X)	100
6.17	Micrograph of Al ₂ O ₃ -8ZrO ₂ -0.25Y ₂ O ₃ -5Cr ₂ O ₃ (483-2) After Exposure to Greater Than 100 Pulses in Arc Test Facility. Microcrack Network and Limited Spalling is Seen (400X)	100

FIGURES - (Cont.)

	PAGE
6.18 Micrograph of Al_2O_3 -8ZrO ₂ -0.25Y ₂ O ₃ -25 v/o SiC(Platelets) (484-4) After Exposure To Greater Than 100 Pulses In Arc Test Facility. Microcrack Network and Metallic Nodules (Si) Are Seen (400X)	101
6.19 Micrograph of Al_2O_3 -8ZrO ₂ -0.25Y ₂ O ₃ -30 v/o SiC _w (484-3) After Exposure to Greater Than 100 Pulses in Arc Test Facility. No Microcrack Network is Seen, But Metallic Nodules (Si) Are Present (400X)	101
6.20 Micrograph of Si ₃ N ₄ - 30 v/o Mullite After Exposure To Greater Than 100 Pulses in Arc Test Facility. No Microcrack Network Is Seen, But Silicon Metal Nodules Are Present (400X)	102
6.21 Voltage Holdoff Degradation Performance of Alumina-Chromia Materials, a) 4-253-4, b) 4-253-6, c) 4-253-1, d) 4-253-5, e) 4-253-3	104
6.22 Voltage Holdoff Degradation Performance of Silicon Nitride /SiC _w Materials a) 4-265-3, b) 4-265-4, c) 4-265-6, d) 4-265-1, e) 4-265-5	105
6.23 Voltage Holdoff Strength Versus Number of Pulses for Al_2O_3 -15ZrO ₂ -35%SiC _w (AMI008-1)	106
6.24 Voltage Holdoff Strength Versus Number of Pulses for Si ₃ N ₄ -8Y ₂ O ₃ -1Al ₂ O ₃ -35%SiC _w (S-340-2)	106
6.25 Summary of Breakdown Voltage Resistance of Advanced Ceramic Insulator Materials Taken From Optimum Quality Panels	107
6.26 Spectrum Intensity vs. Wavelength (UV region) For Molybdenum and Graphite Electrodes	109
6.27 Effect of Graphite vs. Molybdenum Electrodes and Treating of G-10 With Benzophenone On the Voltage Stand-Off Capability of G-10 Insulators	110
6.28 Voltage Holdoff Recovery Behavior of Mullite Ceramic As Measured At SDS III Facility At TTU	111
6.29 Voltage Holdoff Recovery Behavior of Cordierite Ceramic As Measured At SDS III Facility At TTU	112
6.30 Voltage Holdoff Recovery Behavior of Steatite Ceramic As Measured At SDS III Facility At TTU	112
6.31 Voltage Holdoff Strength Versus Number of Pulses For Torlon 4203 Polymer	114
6.32 Voltage Holdoff Strength Versus Number of Pulses For Ultem 1000 Polymer	115

FIGURES - (Cont.)

		PAGE
6.33	Voltage Holdoff Strength Versus Number of Pulses For Ultem 4001 Polymer	115
6.34	Surface Voltage Breakdown vs. Number of Pulses For AD994 Alumina	116
6.35	Surface Voltage Breakdown vs. Number of Pulses For Mycalex 400 Glass/Mica Composite	117
6.36	Surface Voltage Breakdown vs. Number of Pulses For Mycalex 1100 Glass/Mica Composite	117
6.37	Stationary Arc Erosion Test Results for Four Copper-Based Hemispherical Electrode Materials Tested In the MAX I Apparatus At TTU	120
6.38	Stationary Arc Erosion Test Results for Flat Electrodes As a Function of the Effective Charge Per Shot for Five Different Conductor Materials	121
6.39	Stationary Arc Erosion Test Results For Hemispherical Electrodes As a Function of the Effective Charge Per Shot for CuW + Re	121
6.40	Stationary Arc Erosion Test Results For Hemispherical Electrodes As a Function of the Effective Charge Per Shot for Tungsten Alloy W#1	122
6.41	Stationary Arc Erosion Test Results For Hemispherical Electrodes As a Function of the Effective Charge Per Shot for Tungsten Alloy W#2 With It's Grains Aligned Perpendicular To the Electrode Surface	122
6.42	Stationary Arc Erosion Test Results for Hemispherical Electrodes as a Function of the Effective Charge Per Shot for Dornier Tungsten Alloy W#3	123
6.43	Stationary Arc Erosion Test Results for Hemispherical Electrodes as a Function of the Effective Charge Per Shot for Supercon, Inc. Cu-Nb Composites	123
6.44	Stationary Arc Erosion Test Results for Hemispherical Electrodes as a Function of the Effective Charge Per Shot For Cu-Nb Compared to CuW + Re	124
6.45	Cross-Section of Modified FLINT Gun Used for Testing of Advanced Ceramics as Bore Insulators	127

FIGURES - (Cont.)

	PAGE
6.46 Finite Element Models of the Cross-Section of the Modified FLINT Gun Barrel for Testing of Advanced Ceramic Insulator Materials. Two Different Elastic Moduli for the Test Bore Insulator Were Used as Inputs for the Finite Element Runs; 25 and 50 Mpsi (175 and 345 GPa), With a Poisson Ratio of 0.21 (Typical Value for Ceramic Materials). The Rest of the Barrel Including the Bolts and the Top, Bottom and Side Plates Were Modelled Using the Properties of Steel	128
6.47 Photograph of the First Pair of Rails (N081) After Three Shots In FLINT Gun at ARDEC	130

TABLES

		PAGE
1.1	Summary of Bore Material Issues and Their Effect On the Operation of Railgun Systems	3
2.1	List of Sources for Railgun Materials Survey	10
2.2	Features of EML Systems Existing at Time of survey	14
2.3	Advanced EM Accelerators systems of Special Interest	16
3.1	Environmental Loads Experienced by Electromagnetic Accelerator Bore Materials	27
4.1	Summary of Bore Insulator Property Requirements	41
5.1	Micro-Architectural Tailoring of Advanced Ceramic Insulators	47
5.2	Ceramics Consolidated In the First Hot Press Run	50
5.3	Panels Consolidated in Runs #2 and #3	51
5.4	Modulus of Rupture Results From Run #2	53
5.5	Panels Consolidated in Runs #4 and #5	53
5.6	Modulus of Rupture Results From Hot-Pressing Runs #4 & 5	54
5.7	Modulus of Rupture Values Used for Weibull Modulus Determination	56
5.8	Results of Chevron Notch Short Beam Fracture Toughness Tests	61
5.9	MOR Results for Hot-Pressed Ceramic Insulator Materials With and Without HIP Processing	64
5.10	8 X 8 in. (20 X 20 cm) Ceramic Panels Fabricated January to September 1989	67
5.11	Processing Conditions Used to Hot-Press 8 x 8 in. (20 X 20 cm) Panels	68
5.12	Compositions and Densities of Two Scaled-Up Thickness Blocks of Advanced Ceramic Composite Insulators for Electromagnetic Launchers	71
6.1	Mechanical Test Results from 8 x 8 in. (20 X 20 cm) Ceramic Panels	77
6.2	Compositions and Densities of Scaled-Up Blocks of Advanced Ceramic Composite Insulators for Electromagnetic Launchers	83
6.3	Results of Modulus of Rupture and Fracture Toughness Tests on Scaled-Up Advanced Ceramic Insulators Materials	85
6.4	Summary of Arc Erosion Tests on First Six Ceramic Insulator Materials	93
6.5	Insulator Surface Breakdown Data	96
6.6	Initial Test Results of Surface Breakdown for Si_3N_4 - 30% Mullite	97
6.7	Arc Exposure Data on Three Conventional Engineering Ceramics	111

TABLES (Cont.)

	PAGE
6.8 Results of SDS Standing Arc Tests of Advanced Organic Insulator Materials	113
6.9 MAX I High-Coulomb Stationary Arc Test Results	119
6.10 Composition and Origin of Electrode Test Materials	120
6.11 Three Ceramic Insulator Samples Tested In the FLINT Gun	130
7.1 Measured vs. Goal Properties of Alumina-Zirconia-Chromia Bore Insulator Material	135

[This page is intentionally left blank]

INTRODUCTION

Electromagnetic accelerators (EMAs) are being developed for a number of potential Strategic Defense, Theater Missile Defense, and tactical missile applications. The railgun, the most mature type of EMA, accelerates projectiles to velocities of 3-6 km/sec or higher by applying large electromagnetic forces to an armature that pushes the projectile as shown schematically in Figure 1.1. This process requires large electric currents on the order of several mega-amperes, to be conducted down one conductor rail, across a solid or plasma armature and back through the other rail. The conductor rails are separated by insulators, and these four components are confined together to form the bore assembly. The performance and lifetime of the bore is a major design and operational issue. This program addresses the development of advanced bore materials, concentrating on improved bore insulators.

1.1 The Limitations of Current Railgun Bore Materials

The development of materials with the necessary properties to perform successfully as bore insulators and conductors in EMAs is a major challenge to the Materials Technologist. The bore component design requirements imposed by the extreme thermal, electrical and mechanical stresses of the railgun environment dictate a set of properties that cannot be fully met by any commercially available materials. Included in Table 1.1 is a listing of bore material issues, their implications, and the effect they have on the operation of railgun systems. As the table indicates, the shortcomings of current railgun bore materials seriously limit the performance of railgun systems. This fact was recognized at the beginning of the program, but during its performance, significant additional operational data was acquired that made the railgun community more acutely aware of the vital importance of railgun bore material performance, especially the insulator materials.¹ This additional knowledge was derived from experiences with smaller laboratory railguns, and more importantly, from the following 90 mm bore diameter high-energy guns:

- The Single Shot Gun (SSG) at the University of Texas Austin - Center for Electromechanics (UT - CEM)
- The SSG at the DNA/Maxwell Green Farm Facility in San Diego, California
- The Advanced Composite Railgun barrel built by SPARTA for the U.S. Army Armament Research, Development and Engineering Center (ARDEC) in Picatinny Arsenal, New Jersey and fired at the Green Farm facility.

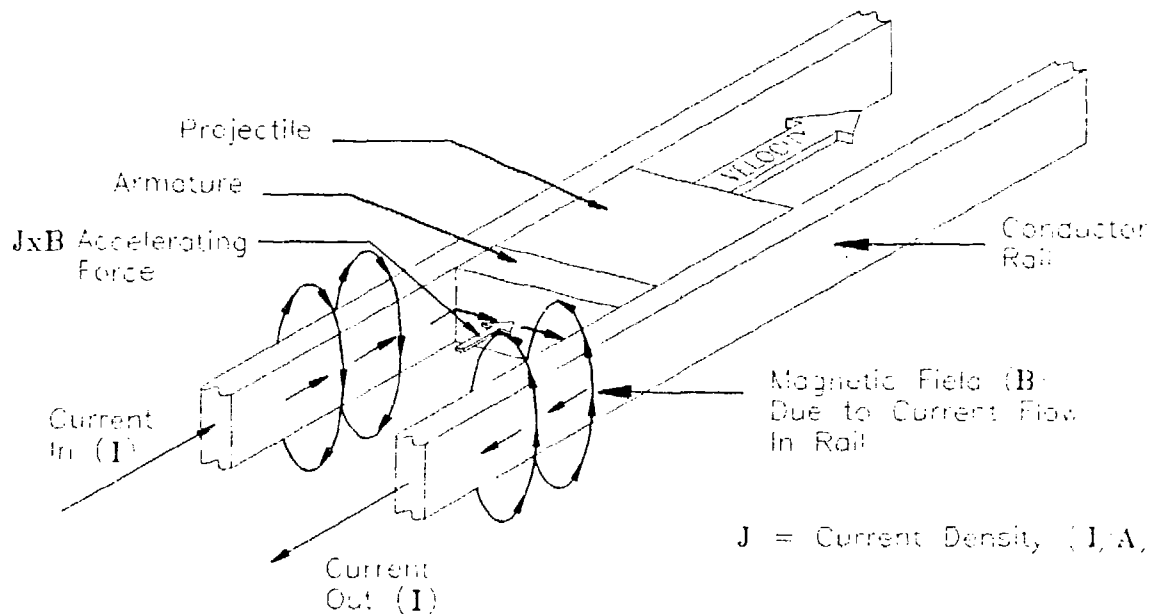


Figure 1.1 Schematic of electromagnetic accelerator operation. Bore insulators (not shown) separate the conductor rails.

All currently operating high-energy railguns use glass fiber reinforced polymers as the bore insulators. The fibers are in the form of cloth or laid-up plies. The matrices commonly used include epoxy, melamine, and polyester.^{2,3} The two most commonly used standard materials are "G-9" and "G-10". These materials are fabricated to specifications set by the National Electrical Manufacturing Association (NEMA). Both materials use the same plain weave E-glass cloth (62% by volume). The difference is that the G-10 utilizes epoxy resin as the matrix whereas G-9 utilizes melamine resin as the matrix. The G-10 material is stronger and has better interlaminar shear strength than the G-9, however, the G-9 possesses the special feature of being relatively cleanly ablating, that is, it leaves a minimum of solid residue when its surface is ablated by a passing arc plasma. Any carbonaceous residue deposited on the bore insulator may provide a conductive path which produces a short in the gun, so these guns must typically be cleaned after every shot. Clearly, this requirement is unacceptable for a device which would be used in the field as a weapon. The G-9 leaves less residue than other resin-matrix composites which have been tested, but it still produces enough conductive residue to require cleaning after each shot when a high-power plasma armature is used.

There are four major types of armatures presently utilized for high-energy railguns. A "plasma armature" railgun configuration is one in which the current that accelerates the projectile flows through an electric arc which connects the two conductor rails. An alternative configuration is referred to as a "solid armature". In this situation, a conductive

Table 1.1 Summary Of Bore Material Issues And Their Effect On The Operation Of Railgun Systems

BORE MATERIAL ISSUE	IMPLICATION	RAILGUN SYSTEM EFFECT
Ablation and Erosion of Insulators	Increases Diameter of Bore Adds Parasitic Mass to Launch Package	Changes Fit of Projectiles, or Causes Need for Varied Size Projectiles; Decreases Barrel Lifetime Decrease Efficiency (Velocity)
Gouging, Divotting, Abrasion, and Delamination (Insulators Only) of Bore Materials	Increases Roughness of Bore Causes Projectile Balloting Increases Honing Frequency Requires Repair Makes Bore Rider Sealing More Difficult	Causes Damage To Projectiles (Possible In-Bore Failures); Increases Projectile Dispersion and Reduces Accuracy; Limits Barrel Lifetime, Increases System Life-Cycle Costs due to Refurbishment; Reduces Efficiency Because of Plasma Blow-By
Conductive Residue in Bore After Shot	Second Shot Not Possible Without Cleaning	Rep-Rated Operation Impossible or Very Difficult
Low Modulus Insulators	Increased Deflection of Bore, Increasing Plasma Blow-By and Deforming Barrel Shape	Decreases System Efficiency (Lower Velocity) and Increases Projectile Scatter (Dispersion)
Insulator Thermal Properties	Better Thermal Conductivity Gives Better Heat Sink	Increases Allowable Rep-Rate

metal bridge provides a current path between the rails and pushes the projectile (or is itself the projectile). The solid armature configuration presents a less challenging environment for the bore insulators because there is no arc present. It is usually a less efficient design because of the parasitic mass of the metal armature and it is difficult to prevent arc formation at velocities in excess of one to two km/sec. There are two additional types of armatures under development including those that start as solid metal and transition in a controlled manner to plasma as the metal vaporizes (thus a "transitioning armature"), and a "hybrid armature" which is part plasma and part metallic by design. Both of these armature types reduce exposure of the bore insulator to the intense plasma radiation (10,000 to 40,000K). The purpose of discussing these armature types, as will be shown later, is that the type of armature utilized effects the bore environment and thus impacts the property requirements of bore insulator material.

A second shortcoming of glass fiber composites for use as bore insulator materials is the excessive erosion and divoting that they experience due to a combination of arc erosion and mechanical erosion/ablation/abrasion and projectile balloting (lateral acceleration). Shown in Figure 1.2 are results from an actual bore diametral measurement taken after a high power shot with the Advanced Composite Railgun. The bore had been honed before the shot and it is seen that the glass-epoxy insulator rails experience a great deal more ablation and erosion than the bare copper conductor rails. This dimensional instability, as shown in Table 1.1, seriously compromises railgun system operation.

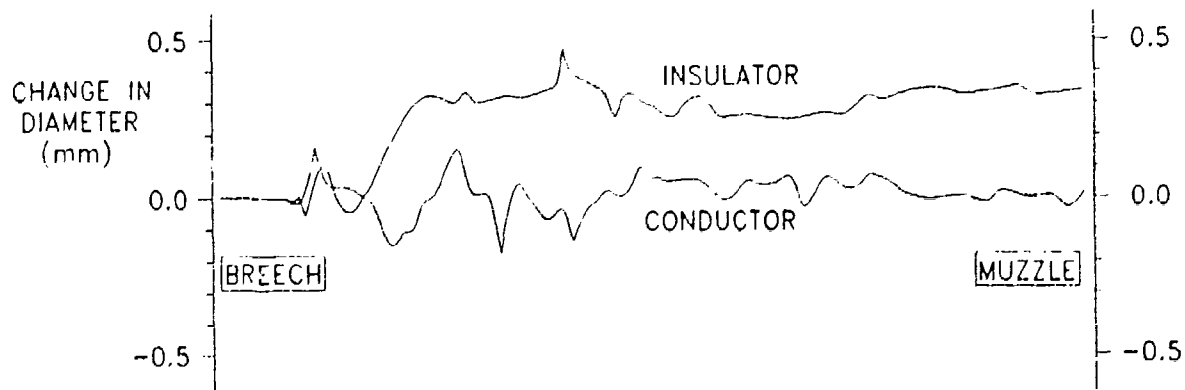


Figure 1.2 Bore measurement (insulator and conductor) after single high-energy shot in ARDEC/SPARTA advanced composite railgun

Current railguns accelerate projectiles up to as much as 6 km/sec, while maintaining close tolerances between projectile and bore. The projectile undergoes "balloting" during its axial acceleration. Balloting, or lateral acceleration, produces repeated collisions of the projectile with the bore of the gun. This balloting causes both impact and abrasion damage to the bore. The amount of balloting is a function of the smoothness (and straightness) of the bore. This balloting can cause in-barrel damage or failure of the projectile. EM guns constructed with glass fiber composite insulators must be routinely patched with epoxy or a filled epoxy compound to fill in gouges and delaminated areas, and to build up eroded surfaces. They must also be honed frequently to provide a smooth sealing surface for the projectile. Since the next generation of railguns will be designed for multiple shots per minute, this kind of maintenance constraint becomes entirely unacceptable. Another disadvantage is that the mass added to the armature/projectile package due to entrained erosion and ablation of insulator material substantially reduces the efficiency of the gun.

The third drawback of a glass fiber reinforced composite insulator is its relatively low compressive modulus. The efficiency of an electromagnetic gun is in part related to the radial stiffness of the barrel.¹ A plasma armature creates a pressure wave as it travels down the barrel. The radial deflection of the barrel in response to this pressure dissipates energy which would otherwise be imparted to the projectile. The deflection can also

produce plasma leakage around the projectile (blow-by), which seriously degrades gun efficiency. Most modern railguns are externally pressurized or prestressed to keep the bore components in compression, so the material property that is required to minimize internal radial deflection is high compressive modulus. High loading fractions of glass in the composite keep the modulus relatively high for a polymer-based composite, but if a ceramic substitute could be found, gun efficiencies would improve significantly because ceramics possess moduli that are twenty to thirty times higher than glass fiber composites.

Ceramics appear to be a promising alternative to the presently used glass fiber reinforced polymer insulators, but no commercially available ceramic can provide the required mechanical strength and fracture toughness under the dynamic loading conditions and the necessary multi-shot high voltage surface breakdown resistance. Thus the development of such an insulating ceramic material needed to be carried out in order to meet the requirements imposed by a railgun bore environment.

For conductor rails, copper or copper alloys have been the materials of choice. But these materials have proved to be too soft and have too low a melting point to perform very well under multiple shots in high energy railguns. Bare copper surfaces are easily damaged by the abrasion and impacts of high-speed projectiles and melted by the combined effects of the rail and arc current. Harder, more refractory metals such as molybdenum, tungsten and tantalum or their alloys have significantly higher electrical resistivities than copper alloys and generally have limited fracture resistance. There are some conductive ceramics which might be refractory enough to resist ablation, and able to withstand impact damage and abrasion far better than copper because of their hardness. Conductive ceramics, as well as some new combinations of more refractory metals, were evaluated in this investigation. However, this work was much more limited than the work on ceramic insulators which was the major focus of this program.

The lack of a durable bore insulator material is one of the most significant technical problems in railgun development today. All of the large research guns now in operation require significant maintenance after almost every firing, due primarily to ablation and/or physical erosion of the insulators. This maintenance may consist of cleaning, patching, or honing, but even in the most minor procedures, it may consume hours or days of labor. Railgun technology will have difficulty establishing any credibility as a practical weapon or launching system of the future until a low maintenance, long lifetime bore insulator material is developed.

1.2 Program Objectives

It is clear that polymer-based materials are not ideal selections for railgun insulators, and it is widely believed that a ceramic material will eventually provide the ultimate solution to this problem.⁴ The choice of a conductor material is not as critical an issue as the insulators, which are the primary obstacle to multi-shot capability, but there is con-

siderable room for improvement in this area nonetheless. The first objective of this program was to ascertain the specific mechanical properties which would be required of such materials in a large railgun of advanced design. This was accomplished by the application of continuum mechanics and finite element analysis to an advanced railgun model. This analysis provided the strength, strain, and modulus requirements, but was not sufficient to determine dynamic fracture toughness requirements. A subsequent fracture mechanics analysis considered such issues as flaw detection limits and Weibull statistics in order to establish a fracture toughness criterion for the candidate materials.

Having established a set of mechanical property goals for the bore materials, the next step was to evaluate and select candidate materials which could be expected to meet these goals, and which would warrant experimental evaluation. A survey was performed that collected manufacturers' product literature, and scientific literature pertaining to new experimental research in high-toughness ceramics. It also included a survey of the EM gun development community to collect reports of previous experiences with bore materials. This community is composed of military, government, industrial, and academic groups.

Once a primary set of candidate materials had been selected, the material was designed (using microstructural tailoring) with respect to chemical composition, constituent sizes and architecture. Each material was then fabricated in a plate form, from which a variety of test samples were cut. These samples were used to measure density, modulus of rupture strength, Weibull modulus, fracture toughness, and surface breakdown voltage. The properties were correlated to microstructure and iterative development carried out. Parts cut from selected plates were also tested as actual railgun insulators in a small electromagnetic gun. After identifying the ceramic compositions which exhibit the best combination of properties, the materials were scaled up to a size representative of state-of-the-art, or next generation railguns. These larger size pieces were then subjected to the same series of evaluations to confirm that adequate properties were maintained in the scale-up process.

A schematic diagram that illustrates the approach utilized in this program is given in Figure 1.3. The details of the work performed are discussed in Chapters 2 through 6 of this report as indicated in the diagram. Conclusions and recommendations for further work are discussed in Chapters 7 and 8, respectively.

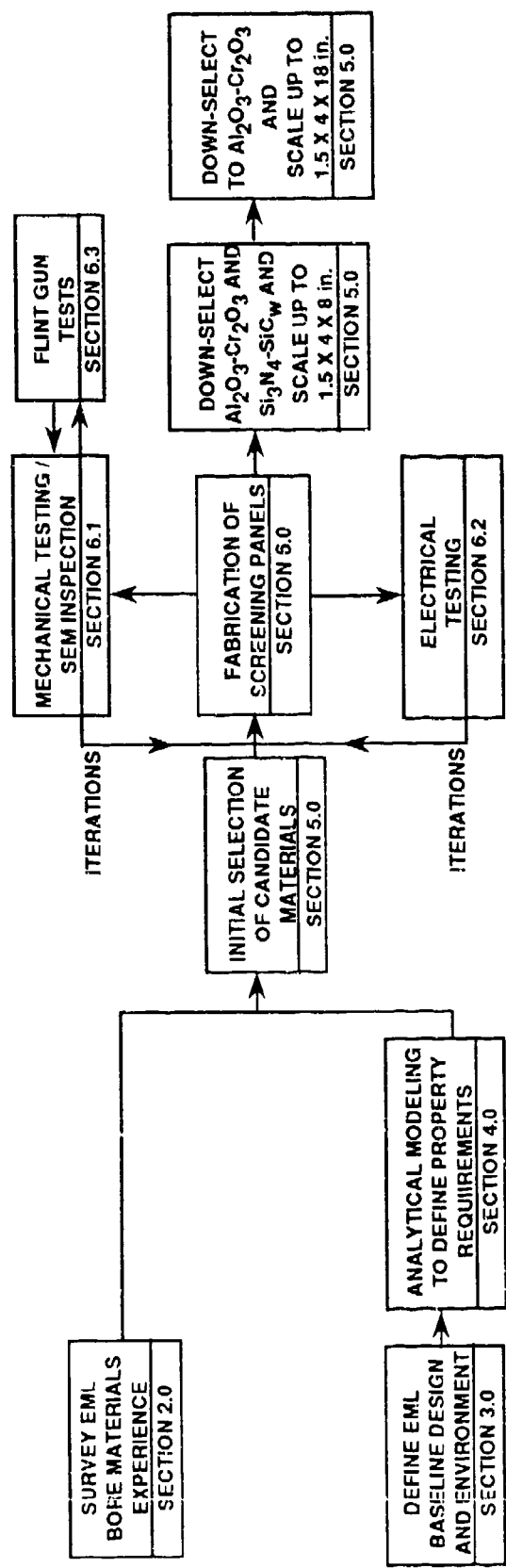


Figure 1.3 Flowchart illustrating major components of this program with references to report sections.

This page is intentionally left blank.

SURVEY OF EM GUN BORE MATERIALS EXPERIENCE

Early in this program, a survey was conducted of all the organizations in the United States presently or formerly engaged in railgun research. The purpose of this survey was to collect information on their experience with railgun bore materials. Three categories of questions were posed:

1. What bore materials have been used in the past for both insulators and rails?
2. How have these materials performed?
3. What will be the requirements for materials in the next generation of railgun designs?

During the survey, information was also gathered on: most pertinent contact at the facility, name of operating gun(s), physical and operating characteristics of the gun(s), containment method and stiffness of barrel, bore conductor rail material experience, bore and backup insulator material experience, and armatures used (type and materials), armature/bore interaction experience, and near-term experimental plans. All of this information was collected in the Spring and Summer of 1988. It represents the state-of-the-art at the time this program was initiated, and it explains the context in which the program was conducted.

2.1 Sources Surveyed

Shown in Table 2.1 is a listing of the sources surveyed, key contact and phone number, and comments on the areas of primary focus at that facility. The list of sources to be contacted was compiled by a combination of

1. SPARTA contacts with electromagnetic railgun facilities/experimenters
2. Papers given at past Electromagnetic Launch Technology Symposia^{4,5,6,7&8}
3. Contributors to other conferences on electromagnetic accelerator technology

TABLE 2.1 - List of Sources for Railgun Materials Survey

Organization	Point of Contact and Phone Number	Materials Relevant Work
ARDEC (US Army) Picatinny Arsenal, NJ	Greg Colombo Tom Coradeschi 201-724-3353	Developing wrapped barrels (Benet) and solid armatures
Astron Research San Jose CA	Charles Powars 408-297-2926	Analyzing and developing advanced material insulator and conductor rails for test
Auburn Univ. Auburn, AL	Gene Clothiaux Ray Askew 205-826-5894	Development of advanced diagnostic techniques
Ballistic Research Laboratory (US Army) Aberdeen, MD	Keith Jamison Alex Zielinski 301-278-5687	Development of advanced diagnostic techniques; test of advanced bore materials and development of projectiles
Benet Weapons Lab Watervliet Arsenal Watervliet, NY	Pete Aalto Pat Vottis 518-266-5595	Development and fabrication of wrapped composite barrels
Boeing Aerospace Seattle, WA	John Schrader 206-773-2914	Development and test of solid armature designs
Eglin Air Force Base Eglin AFB, FL	Ed Bradley Lt. Dan Jensen Lt. Jeff Martin 904-882-0207	Development and test of multishot insulator and conductor rails, solid and plasma armature development. Conventional and Marc IV railgun tests
Electromagnetic Launch Research Inc. Cambridge, MA	Henry Holm 617-661-5655	Development and fabrication of coil guns (including power supplies)
FMC Corp Minneapolis, MN	Steve French 617-337-3269	Design and development of composite barrels, materials for use in electro-thermal guns
Ford Aerospace, Aeronutronics Div Newport Beach, CA	Bill Creighton 714-720-6098	No work currently being performed on advanced bore materials, development of advanced projectile structures
General Atomics Corp San Diego, CA	Leo Holland Fred Chamberlain 619-455-3043	System thermal management; solid armature design
General Dynamics Corp Valley Systems Div Rancho Cucamonga, CA	Jaime Cuadros 714-945-8370	No longer working with railguns
GT Devices Alexandria, VA	Rod Burton Doug Witherspoon 703-642-8150	Ceramic materials for use in electro-thermal guns
IAP Research, Inc Dayton, OH	John Barber Tim McCormick 513-296-1806	Development of solid armature and switch materials; laminated, stiff railgun barrels

TABLE 2.1 - Continued

Organization	Point of Contact and Phone Number	Materials Relevant Work
Lawrence Livermore Labs Livermore, CA	Ron Hawke 415-422-8679	All work is being performed at Sandia
Los Alamos Nat'l Labs Los Alamos, NM	Jerry Parker Bill Condit 505-667-3119	Development of advanced diagnostic techniques and analytic models. Design and fabrication of Sialon ceramic-backed railgun
LTV Aerospace Dallas, TX	Mike Tower George Jackson 214-266-7435	Not currently doing any advanced bore materials work.
Maxwell Labs San Diego, CA	Mike Holland Rolf Dethlefsen 619-576-7887	Development and test of projectiles. Design, fabrication and operation of 90 mm bore single shot (B) gun
MER Corp Tucson, AZ	Raof Loutfy 602-746-9442	Development of advanced reinforced ceramic matrix rail materials
Physics International San Leandro, CA	Ron Gellatly 415-577-7119	No current work on bore materials
Sandia National Labs Albuquerque, NM	Jim Asay 505-844-1506	Materials equation of state development
Science Applications International Eglin AFB, FL	Ed O'Donnell 904-883-0389	ETA contractor at Eglin Development of bore ablation model
SPARTA, Inc San Diego, CA	Stuart Rosenwasser R. Daniel Stevenson 619-455-1650	Advanced insulator and conductor materials, actively cooled conductor rails, stiff, high prestress barrels
Supercon Inc Shrewsbury, MA	Eric Gregory 617-842-0174	Development and test of Cu-Nb conductor rails
Texas Tech Univ Lubbock, TX	Kris Kristiansen Greg Engel 806-742-2224	Development/test of switch contact, electrode, and insulator materials
Univ of Texas Austin, TX	Bill Weldon Ray Zawortz 512-471-4496	Design, fabrication and operation of stiff, actively pressurized 90 mm vertically oriented single shot (B) railgun. Use of ceramics in railguns
Westinghouse Marine Div Sunnyvale, CA	Jeff Fletcher Jeff Anderson 408-735-7400	Thunderbolt railgun design and fabrication development effort
Westinghouse R&D Center Pittsburgh, PA	John Spitznagel Dan Duis 412-256-1481	Selection and test of advanced bore materials and fabrication methods for Thunderbolt through SUVAC II gun testing

2.2 Results of Survey

A copy of the survey form used to record information from each source contacted is shown in Figure 2.1. A listing of the U.S. railgun systems identified during the survey along with some of their key design and performance parameters, and primary armature type and baseline bore materials are given in Table 2.2. A listing of railgun barrels without their own power supplies that had been fabricated and tested up until the time of the survey is shown in Table 2.3. They are included because of interesting advanced designs or the use of advanced materials.

A brief summary of the advanced materials investigated by each source is shown in Table 2.4. Included below is a discussion of the railgun work relevant to bore materials carried out at each of the organizations.

ARDEC - ARDEC has four rail guns either operational or under fabrication:

- i.* EMACK - a 5 m long, 50 mm square bore gun (under modification)
- ii.* TOPAZ - 2.6 m long with 50 mm square bore
- iii.* FLINT - 1 m long with 1 cm square bore
- iv.* Benet Barrel - 1.2 m long 50 mm round bore, fiberglass overwrap.
To be succeeded by a 5 m long version.

At this time, the TOPAZ gun and the Benet Barrel are operating while the EMACK power supply is being upgraded and the FLINT gun assembled. The EMACK gun will be available for testing shortly. Much of the work involves penetrator/projectile studies and solid armature development. Shortly, a 4 m barrel produced by ARES using cast alumina ceramic in an epoxy organic matrix for the bore insulator will be tested. The Benet barrel is being used for projectile studies. A 5 m graphite fiber/epoxy wrapped barrel with a 50 mm round bore was under fabrication at Benet for delivery to ARDEC in June, 1988. ARDEC is sponsoring the development of light-weight, fiber-wrapped barrels for railguns. All of the above barrels use conventional bore materials. These include copper or copper alloy conductor rails and G-9, G-10, or G-11 insulator rails. No advanced bore material studies are underway, although the FLINT gun will be used to test advanced materials under development.

Astron Research - Astron is supplying advanced conductor and insulator rails for test at Eglin Air Force Base. Rails currently under development (for test in Eglin's PUG Gun) include: plasma-sprayed Mo and W coated copper rails, chemical vapor deposited (CVD) coated W copper rails, rails with graphite strips brazed to the bore facing surface, solid Mo and W rails, hot-pressed Si₃N₄ insulator rails (24 in. (61 cm) long) which survived exposure in the Eglin PUG gun without fracture, although a partially conductive surface coating was formed, and glass-reinforced polyimide and quartz cloth reinforced polyimide insulating rails.

SURVEY OF EM GUN BORE MATERIALS EXPERIENCE
CONTRACT DAAL04-86-C-0045

Location: _____

Contact and Other Key Personnel: _____

Address and Phone #: _____

Type and Name of Gun: _____

Barrel Construction, Dimensions/Operating Parameters (mass, peak acceleration, peak current, injection velocity, final velocity, pre-stress, max. pressure)

Conductor Rail Materials Tested and Results: _____

Insulator Materials Tested and Results: _____

Armature Types, Materials, and Bore Interactions: _____

Figure 2.1 The report form used to conduct EM Gun Bore Materials Experience Survey.

TABLE 2.2 — Features of EML Systems Existing at Time of Survey

Location	Gun Name/Type	Power Supply	Dimensions	I (Peak) [kA]	Typical Proj. Mass	Injection Velocity	Armature Type(s)	Baseline Bore Materials	Backing Materials	Comments
ARDEC	EMACK	Homopolar Gen. 30 MJ	5m x 50mm round	1500	350-700g	none	solid	Cu-110 + G-11	G-11	Power supply being refurbished
ARDEC	TOPAZ	Homopolar Gen. 20 MJ	2.6m x 50mm square	1500	700g	none	solid	copper + G-11	G-11	
ARDEC	FLINT	Capacitor Bank 250 kJ	1m x 1cm square	150	10g	300m/s	plasma	copper + G-11	G-11	Copy of Eglin PUG I Gun
ARDEC	Benet Barrel Composite Tube	200 kJ Cap. Bank - 20 MJ Homopolar	1.2m x 50mm round	1300	350g	0-250m/s	solid	copper + G-10	G-11	Composite Tube, will be replaced with 5m long barrel to be HPG driven
Army-BRL	Test Gun	Capacitor Bank 400 kJ	1 to 2m x 3.5 cm square	500	1g	200m/s	solid	Al-60 + G-9 or ceramic	G-10	E-T Injector, uses 1A? confinement barrel
Eglin AFB	PUG I, Mk I	Capacitor Bank 400 kJ	0.6m x 1cm square	240	5-15g	350m/s	plasma	Cu-110 + G-9	G-10	
Eglin AFB	PUG II, Mk II	Capacitor Bank 5 MJ	3.65m x 75mm square				plasma			
Eglin AFB	MIDI-III	Capacitor Bank	1.64m x 9.5mm square	150	Free Arc to 1g	none	plasma	Cu-110 + G-9	G-10	
Eglin AFB	5A AEMG Barrel	Homopolar Gen. 10 MJ to be replaced by 110 MJ battery supply system which in turn will be upgraded in energy by the addition of more batteries	5m x 50mm square	1500	150g	300-500m/s	solid plasma	CuCr + G-9	glass-resin barrel	Water cooled by holes in conductor rails
Eglin AFB	5D AEMG Barrel		5m x 50mm square	1500	150g	300-500m/s	solid plasma	Cu-110 + G-10		Will be sent to Netherlands, water cooled by holes in conductor rails
Eglin AFB	5E AEMG Barrel		5m x 50mm square	1500	150g	300-500m/s	solid plasma	Cu-110 + S_3N_4		Augmented rail, LINI cooled, bore is vacuum
Eglin AFB	AP AEMG Barrel		3m x 50mm square	750 (1500 design)	150g	300-500m/s	solid plasma	Cu-110 + G-10	G-10	Parallel augmented turn currently not in use
FMC Corp.	Electro-Thermal Gun									(proprietary information)
General Atomics	Lab. Gun I	Capacitor Bank	1m X 1.27cm square	250	3-10g	500m/s	solid	CuCr + G-9	G-10	
General Atomics	Lab. Gun II	Capacitor Bank	2m X 5cm square	1300	150-200g	500m/s	solid	CuCr + G-9	G-10	
GI Devices	J-2 GEDI Gun	Capacitor Bank 1.4 MJ	0.9 and 3.6m	260	0.5-1.0	1-1.5 km/s	plasma	Cu-110 + titanium or ceramic	G-10	Electro-thermal hybrid

TABLE 2.2 (Continued)

Location	Gun Name/Type	Power Supply	Dimensions	I (Peak) (kA)	Typical Proj. Mass	Injection Velocity	Armature Type(s)	Baseline Bore Materials	Backing Materials	Comments
IAP, Inc.	15mm Gun	Capacitor Bank 210 kJ	1m x 15mm square	400	15g	none	plasma solid	Cu-110 + G-10	G-10	320 kJ bank to be added
IAP, Inc.	50mm Gun	Capacitor Bank 210 kJ	1m x 50mm square	600	150g	none	plasma solid	Cu-110 + G-10	G-10	320 kJ bank to be added
Los Alamos	HIDI-11	Capacitor Bank 300 kJ	1.64m x 9.5mm square	150	free arc to 1g	none	plasma	Cu-110 + G-9	G-10	Duplicate of this barrel built for Eglin
LTV	DCS gun (5 stages)	Capacitor Bank 640 kJ in five modules	2.7m x 20mm square	500	7 to 60	500-1000 m/s	plasma	Cu-110 + glass-polyester	G-10	Barrel is in storage.
Maxwell Labs	CHECMATE	Capacitor Bank 6 MJ	5m x 5.1cm square	2000	75 to 150	500-700 m/s	plasma	MZC ¹ + G-10	G-10	the power supply was never finished
Maxwell Labs	HYVEL	Capacitor Bank 300 kJ	1m x 1cm square	420	10	600 m/s	plasma	Cu-110 + G-10	G-10	Deactivated
Maxwell Labs	SSG, B-gun	Capacitor Bank 32 MJ	8m x 9cm round	3200	1 to 3 kg	600 m/s	plasma solid	MZC + G-10	G-10	
Sandia ML	HELEOS	Capacitor Bank	2.4m x 1.27cm round	100	1 g	6-8 km/s	plasma	Al-15 ² + Lexan		
U. of Texas	GED1 a) Bolt Up Structure	1 MJ Cap. Bank, 6 MJ HPG or 1 to 6 10 MJ Balcones HPG	3 or 2m x 25mm square	550	2 to 3 g	none	solid	Cu110 + Quartz Layers on G-10	Glass-Epoxy Tube	
U. of Texas	GED1 b) Ring Fedder Structure	1 MJ Cap. Bank, 6 MJ HPG or 1 to 6 10 MJ Balcones HPG	1 or 2m x 25mm square	550	2 to 3 g	none	solid	Cu110 + Quartz Layers on G-10	Glass-Epoxy Tube in Steel Tube	
U. of Texas	GED1 c) Hydraulically Pressurized Bore	1 MJ Cap. Bank, 6 MJ HPG or 1 to 6 10 MJ Balcones HPG	1 or 2m x 25mm square	550	2 to 3 g	none	solid	Solid Mo + Granite or Al ₂ O ₃	Al ₂ O ₃ Rings	
U. of Texas	SSG Prototype	1 to 6 10MJ Balcones HPG's	3m x 45mm round	1600	125-313 g	none	solid	OFHC Copper Fiberglass-epoxy	Al ₂ O ₃	Support design/fab of B-gun barrel
U. of Texas	SSG, B-Gun	1 to 6 10MJ Balcones HPG's	10m x 90mm round	3200	1 to 2.5 kg	none	solid	OFHC Copper Fiberglass-epoxy	Al ₂ O ₃	Currently in fabrication

TABLE 2.2 (Continued)

Location	Gun Name/Type	Power Supply	Dimensions	I(Peak) (kA)	Typical Proj. Mass	Injection Velocity	Armature Type(s)	Baseline Bore Materials	Backing Materials	Comments
Westinghouse Marine Div.	CAP Gun	Capacitor Bank	1m x 10mm square	400	1.5 g	none	plasma	variable	G-11	
Westinghouse Marine Div.	"Lab Gun"	Homopolar Gen.	4m x 33mm square	2000(design) 1000(avail.)	100-300g	400-500 m/s	solid	A1-60 ² + G-9	G-10	
Westinghouse Marine Div.	THUNDERBOLT (3 segments)		14m x 5.6cm round	2000		1000 m/s	plasma	A1-60 ² + G-9	G-10	in fabrication
Westinghouse R&D Center	SUVAC I	Capacitor Bank	2m x 1cm square	460	1g	none	plasma	Mo coated Cu Lexan	G-10	
Westinghouse R&D Center	SUVAC II	Capacitor Bank	up to 14m x 2cm round					Mo coated Cu Lexan		OES type gun

1 HZC is Cu-0.05 Mg-0.10 Zr-0.6 Cr alloy produced by Amax Specialty Metals Corporation

2 A1-15 and A1-60 are grade of Al₂O₃ dispersion strengthened copper produced by SCM Metal Products in Cleveland, OH.

TABLE 2.3 — Advanced EM Accelerator Systems of Special Interest

Location	Gun Name/Type	Dimensions	I(Peak) (kA)	Typical Proj. Mass	Injection Velocity	Armature Type(s)	Baseline Bore Materials	Backing Materials	Comments
FMC Corp.	Subscale Area "C" Barrel	1m x 50mm round	1600	220g	450m/s	plasma	HZC Cu alloy, glass epoxy	A1-0 ₃	Tested with Maxwell CHECMATE Power Supply
Los Alamos	LTS Barrel Transformer Driven	22m x 25mm round	970	20g	1-6 km/s	plasma	Cu-110 + Lexan	G-10	Barrel in Storage, Power Supply Never Fabricated
SPARTA, Inc.	Suscale Area "C" Barrel	1m x 50mm round	1500	200g	450 m/s	plasma	Mo clad A1-15 G-9 Hoop Wrap	A1-0 ₃	Tested with Maxwell CHECMATE Power Supply

Auburn University - They are using a 30 cm long in-house gun for the development of advanced diagnostic techniques and will be receiving a copy of the Los Alamos MIDI-II gun from Eglin for the development of soft x-ray diagnostic techniques. No materials development work is currently being performed.

Ballistic Research Lab (US Army) - The majority of BRL's work is centered on development of advanced diagnostic techniques for railguns. They have a small 1 cm square bore gun that is used to prove out diagnostic techniques and has been used to expose advanced conductor and insulator materials produced by SPARTA. SPARTA produced a 1 m long, 1 cm square bore barrel with provision for quick change out of 12 in. (30.5 cm) long materials test sections for use by BRL.

They also have an in-house 100 kJ (capacitive storage) electrical-thermal (ET) type gun. Its capacitors are tailored to give a ramp current to 100 kA in 800 milliseconds. It uses round bores ranging from 9.5 to 15.9 cm diameter by 15 cm in length. In September 1988, a 1 MJ (stored) bank was installed with a maximum current of 350 to 800 kA. The device is currently not used for materials studies, but for development and application of advanced diagnostics and understanding of the physics of ET guns (including internal ballistics).

Benet Weapons Lab - Benet is designing and fabricating composite-wrapped barrels for test at ARDEC. These barrels are made from graphite or glass fiber/epoxy matrix materials. These resin matrix composite materials are wrapped over 110 copper alloy or Glidcop conductor rails and G-10 insulating rails.

Boeing Aerospace - They have been doing work on the development of solid armature designs and are currently not active in the area of advanced rail gun bore materials.

Eglin Air Force Base - Eglin is currently using their PUG Mark I gun with a 0.6 m long barrel and 1 cm square cross-section for test of advanced materials that are produced by various companies (see sections on Astron, MER Corp. and SPARTA). Eglin themselves are developing advanced solid armatures and rail configuration designs. Some of these results are featured in the PUG Mark IV railgun design. There are other, larger guns at Eglin (including the four Tier 1 barrels built by General Electric, General Atomics, General Dynamics, and IAP) but they are not used for materials development or testing. The large majority of the shots are made with copper alloy 110 conductor rails and G-10 insulating rails. The refractory alloy clad rails have performed very well with very low total system (bore conductors and insulators) mass loss even after multiple shots. Conventional plasma-sprayed refractory metal coated rails tend to crack and spall. However, rails coated with tungsten by a vacuum plasma deposition process did perform well.

Electromagnet Launch Research - They are active in the area of research, design, and fabrication of coil guns (linear synchronous launchers). Advanced materials including spiral inductors made from SiC fiber reinforced aluminum, copper alloy/Inconel laminated inductors, and barrels made from laminated copper and stainless steel utilizing graphite-epoxy as an insulator.

FMC Corp. - FMC has been surveying and testing insulator and conductor materials for use in the breech end of electro-thermal guns. The main emphasis on electro-thermal gun materials is materials that exhibit low mass loss (erosion), while plasma sealing considerations are not as important. A listing of the materials they are investigating is not available because it is proprietary. They also fabricated a 1 m long, 50 mm bore barrel tested at Maxwell's CHECMATE facility. This barrel utilized Al_2O_3 backup insulators and a graphite fiber-wrapped barrel for light weight and stiffness.

Ford Aerospace - Ford is currently doing no work in the area of advanced railgun bore materials. They are designing and fabricating projectiles that are being tested at Maxwell and the University of Texas. Carbon-carbon is the major advanced material being utilized in these components.

General Atomics - They have not fired any of their 50 mm bore guns recently. They are using two different square bore in-house guns for the development of thermal management techniques and plasma brush armatures. A 50 mm square bore Tier 1 gun was fabricated using epoxy pressure injected behind the bore component in order to provide precompression at the bore component interfaces to reduce plasma leakage. In addition, coolant passages were gun-drilled in the Cu-Cr conductor rails in order to provide active cooling.

General Dynamics - General Dynamics is no longer working with railguns.

GT Devices - They have tested 6 in. (15 cm) and 18 in. (46 cm) lengths of 0.5 in. (1.27 cm) diameter Al_2O_3 and Si_3N_4 ceramic rods as insulators in their 3 ft. (0.91 m) long hybrid electro-thermal/electromagnetic gun. This gun uses an ET injector together with a plasma arc and conductor rails. Measured ablation on the ceramic rods was 10 times less than measured using Lexan insulators. However, deeper arc tracking was observed on the Al_2O_3 dispersion-strengthened copper (Glidecop Al-15) conductor rails when using the ceramic insulators, a phenomenon that they plan to investigate further. Some of the 18 in. (46 cm) long ceramic rails broke during test.

IAP Inc. - The two main areas of work are solid armatures and various types of switches. In addition, a stiff laminated steel containment barrel concept has been developed to maximize induction gradient. This 50 mm gun has copper alloy rails and G-10 insulators. In addition, a test bed to measure the properties of solid armature contact materials under controlled conditions of velocity, current and contact pressure has been set up.

Lawrence Livermore Laboratories - L.L.L. does not currently have any working railguns. Some of their personnel are involved with the railgun program at Sandia National Laboratories.

Los Alamos - Most of the railgun work currently underway at Los Alamos is concerned with problems of diagnostics and plasma arc / bore materials interactions. No advanced materials are currently being investigated, although analytical studies are being conducted on advanced bore materials. The only gun currently operating at Los Alamos is the

MIDI-II gun (1.64 m long with a 9.5 mm square bore). Los Alamos fabricated a duplicate of the MIDI-II gun and it is currently being fired at Eglin Air Force Base and will later be sent to Auburn University.

LTV Aerospace - They are not currently performing any work in the area of advanced bore materials. Their distributed energy gun (DES) is not currently being used but could be put into operation rather quickly. They are concentrating in the area of guided projectiles.

Maxwell Labs - The CHECMATE gun facility is no longer being used. The large (8 m by 90 mm round bore) SSG B-gun is being used to develop projectiles. The B-gun uses copper alloy MZC rails and G-10 insulators. Multiple shots have been conducted at half power without intershot bore cleaning.

MER Corp. - They produced a pair of 6 in. (15 cm) long insulator rails (for test in Eglin's Mark I PUG gun) made from toughened Al_2O_3 . The toughening was due to the inclusion of SiC whiskers and a HfC transformation toughening phase. The resistivity of the rails was relatively low, but methods are being developed to increase the resistivity by breaking up the path between the SiC whiskers. They are also looking at reinforced TiB_2 matrix conductor rails.

Physics International - No work is currently being performed on bore materials. All efforts are on fabrication of power supplies for the Thunderbolt railgun.

Sandia National Laboratories - They are using their HELEOS (2.4 m long, 12.7 mm round bore) gun to study materials equations of state. A two-stage light gas gun (2SLGG) is used as a preaccelerator (6 to 8 km/sec) into the railgun. Dispersion-strengthened copper (Glidecop) conductor rails and Lexan insulator rails are used. To date, only low levels of current have been used, resulting in little bore materials damage.

Science Applications International - They have a SETA role at Eglin Air Force Base. In addition, they operate the MIDI-II type railgun at Eglin with the purpose of measuring plasma armature bore drag. They are also developing models to predict bore ablation. They are not performing any advanced bore materials work.

SPARTA - SPARTA is active in the areas of designing, fabricating, and testing advanced conductor and insulator rail materials; advanced active cooling techniques, solid armature materials and designs; and barrel prestressing and stiffening designs. Examples of conductor rails include W, Mo, Mo-TZM, and W-Re clad (using solid-state bonding) copper rails; detonation gun coated WC rails; and TiB_2 and ZrB_2 matrix conductive ceramic rails (including reinforced grades). Solid molybdenum rails have been exposed but exhibited cracking after multiple shots (greater than five). Examples of insulator rails include: advanced organic composites (using glass, quartz and alumina reinforcement), high toughness tailored ceramics, and whisker and fiber reinforced ceramics. Conductor rails with internal coolant passages for active cooling have been developed (using solid state bonding to consolidate the rails) and tested. A 50 mm by 1 m railgun barrel prestressed using hydraulic pressurization to prevent plasma leakage has been designed, fabricated

and tested. This barrel has demonstrated the use and survival of ceramic backup insulators and their dramatic effect in minimizing bore deflections. The barrel demonstrated that at currents up to 1.5 MA that Mo-clad rails eroded only slightly, and that glass-reinforced melamine cleanly ablated at about 0.001 in. (0.025 mm) per shot.

Supercon - They are pursuing the development of niobium filament reinforced copper rails for use as railgun bore conductors. This work (performed under a Phase I Air Force SBIR) offers the possibility of decreased bore erosion because of the electron emission properties of the niobium filaments.

Texas Tech Univ. - Much effort is directed toward the development and test of advanced switch and contact materials, many of which can also be used as railgun conductor materials. Three different test beds are used to expose materials to stationary and moving arcs to determine ablation resistance of both conductors and insulators and rapid-fire voltage standoff degradation of insulators. In conjunction with the current SPARTA contract, a program has been initiated to screen a variety of advanced insulator and conductor materials, including a large number of reinforced ceramic materials for use as advanced railgun bore materials.

Univ. of Texas at Austin - The GEDI gun (1 m and 2 m versions with 12.7 mm square bores) is actively used with sprayed Mo on copper 110 conductor rails. At 550 kA/cm, some spalling occurs of the Mo coating. In addition, another GEDI barrel has solid molybdenum conductor rails. The barrel is honed between every shot. Quartz strips are bonded to a G-10 substrate and used for bore insulators. They fracture on every shot and are replaced, but ablate very little. A 3 m, 45 mm round bore gun is currently being used to test projectile designs. This gun uses 35 kpsi (241 MPa) hydraulically-pressurized ceramic cylinders to transmit precompression to the bore components and to minimize bore deflections. The rails are made from pure copper and the bore insulators are E-glass polyester. The 3 m gun is a prototype of the SSG B-gun (10 m, 90 mm bore) currently in fabrication. The use of high-modulus ceramics and molybdenum rails has been demonstrated to minimize bore deflections and thus plasma leakage. Effort has also been placed on the development of solid armatures that minimize damage to the conductor rail surfaces.

Westinghouse Marine Div. - Two railguns are currently in operation at the Marine division, the lab gun and the CAP gun. The lab gun is a single prototype segment of the Thunderbolt System. These guns are used to test out materials, designs, and fabrication methods of pertinence to the Thunderbolt System. The Thunderbolt System (3 segments) is currently being assembled.

Westinghouse R&D Center - Much of the Westinghouse R&D effort on advanced materials has been directed toward selection and verification of materials and processes for the Thunderbolt gun which is under fabrication. They currently are using two different guns for their development tests: SUVAC I (2 m with 1 cm square bore) and SUVAC II (varying lengths to 14 m with 2 cm round bore) that are used to test Thunderbolt materials and concepts. The following are being investigated:

- a. Control of plasma chemistry through selection of bore materials
- b. Solid state bonded refractory alloys clad to copper substrates
- c. Graphite fiber-epoxy as a bore insulator
- d. DuPont FP alumina fiber in epoxy insulators
- e. Low and high carbon content Mo-TZM cladding for conductor rails
- f. Al_2O_3 particulate-loaded epoxy (up to 80% by volume) for use as a bore insulator material. As the epoxy ablates, the alumina particulate may feed the plasma and reduce erosion of the conductor rails.
- g. Pyrolytic BN chemical vapor deposited on graphite, extracted as cylindrical segments, and bonded to G-9 for use as a bore insulating material.

2.3 Survey Summary and Conclusions

Although the extent of this survey was limited by the resources and time duration allocated to it, SPARTA believes that the results give an accurate picture of the status of railgun materials usage, performance, and development work at the beginning of this program (in 1988). The information was obtained from conversations with the key investigators at the pertinent organizations, from the literature, and from recent symposia and meetings. The following items summarize the important findings and conclusions:

2.3.1 General

- There are about 36 railgun barrel subsystems in the United States either existing or under construction. Several of these are operated off common power supplies and at least three do not have their own power supplies.
- With a few exceptions, the existing guns are designed and/or operated in a single shot mode with some bore maintenance/cleaning required between each shot.
- The bore materials of choice for a majority of the existing railguns and for a very large fraction of the railgun shots that have been made are bare copper or copper alloy conductor rails and glass reinforced resin matrix composite insulators.
- With the exception of some excellent work on plasma armature / bore material interactions, there has been little effort expended in analytically predicting which materials properties most dominate railgun performance and lifetime. There has been almost no work in quantifying property goals for railgun bore materials.
- There have been recent programs (most funded through the DoD Small Business Innovative Research (SBIR) Program) to develop specific advanced materials or materials concepts. These have been aimed at improved rail or insulator plasma armature erosion / ablation resistance.

- The emerging “conventional wisdom” of the railgun community is that lower radial deformation, higher stiffness bores will benefit the performance of both solid and plasma armature railguns. However, this effect has not been either experimentally or analytically verified.
- The requirements for plasma armature railgun materials have been given more attention than those for solid armature railgun bores. Contamination of the plasma, secondary restrike, insulator breakdown, and ablation/erosion of the rails and especially the insulators are most often mentioned as key issues for plasma armature railgun materials. Rail gouging, armature contact loss, and bore deformation effects on contact loss were most often mentioned as key solid armature railgun materials issues.

2.3.2 Conductor Bore Materials

- The large majority of railgun shots have been made using pure copper or copper alloy rails including OFHC, alloy 110, oxide dispersion-strengthened copper (Glidcop) or MZC (magnesium-zirconium-chromium) copper. Since most guns have been cleaned and/or honed between shots, the ablation and melting that occurs with copper alloy rails has been more or less acceptable for experimental railguns.
- Several organizations (Astron, SPARTA, Univ. of Texas, and Westinghouse) have investigated solid or clad refractory alloy (Mo, Mo-TZM, W, W-Re, W-Cu, Nb, etc.) rails. The claddings and coatings have been applied by plasma-spray, CVD, detonation gun spray, and solid state bonding. Both SPARTA/Army BRL and Westinghouse have noted fracture in solid molybdenum rails after repeated (greater than five) shots. Spallation and/or cracking of sprayed, CVD, or detonation gun coated rails has been noted, but copper rails coated by the vacuum plasma deposition process have performed well on limited tests. Generally, if the cladding or coating adheres to the substrate in plasma armature guns, erosion and melting are significantly reduced. The use of refractory metal rails for solid armature guns has been very limited.
 MER Corp., SPARTA, and Texas Tech have done limited work with conductive ceramic rails. Methods to toughen these rails by use of whiskers, chopped fibers, or continuous reinforcing filaments are underway. Much additional work is needed, and obtaining conductivities that will be acceptable from a system efficiency consideration is a key issue with plasma armatures.
- Very limited testing of graphite rails has been conducted by Astron/Eglin. Additional work will be done in order to fully understand the merit of this concept.
- Multiple shots (up to five) have been fired on refractory alloy clad rails without need for cleaning or honing.

2.3.3 Insulator Bore Materials

- The large majority of railgun shots have been made with G-9, G-10, or G-11 type insulating rails. In general, G-9 (glass-reinforced melamine) has performed best in plasma armature guns because it tends to be cleanly ablating and does not require cleaning of conductive char or soot between shots. Melamine also aids in reducing arc restrike.
- Astron, GT Devices, MER, SPARTA, University of Texas, and Westinghouse have tested ceramic bore insulating rails and/or backup insulators. Although structural failures have been noted, survivability has been demonstrated under proper prestress and/or lower linear current densities.
- Very little testing of the most advanced toughened, reinforced ceramics have been conducted
- Deterioration of surface voltage standoff has been noted on some ceramics, and is an issue for multishot railguns

2.3.4 Design

- Design of the railgun barrel has been shown to be an integral factor in the performance of the railgun bore materials. Groups including General Atomics, SPARTA, and the University of Texas have developed barrel designs (and fabricated them) with the purpose of minimizing bore deflections, maintaining brittle ceramics under compression, and in the case of plasma armatures, minimizing leakage.
- Barrel designs at FMC Corp., Los Alamos, SPARTA, and University of Texas have made increasing use of ceramics as backup insulating materials in order to increase the overall radial stiffness of the barrel to reduce bore deflections.

Although this survey was conducted in late 1988, little has changed in the area of bore materials since that time, so it portrays a relatively accurate picture of the current state of the art.

This page is intentionally left blank.

DEFINING GUN DESIGNS AND BORE ENVIRONMENTS

A schematic drawing which illustrates the environment of the bore materials in a current electromagnetic railgun is shown in Figure 3.1. The specific structural, thermal and electric loads, many of which act simultaneously on the bore conductor and insulator rails, are listed in Table 3.1. The time scale over which each of these loads acts is also described.

In order to define the exact mechanical and thermal loads which electromagnetic launcher (EML) bore insulator rails experience, it was necessary to develop a representative analytical model of a railgun design. The EML cross-section shown in Figure 3.2 was selected as the baseline on which to conduct the analytical studies of Section 4.0, which resulted in the selection of railgun insulator goal properties (requirements). This hydraulically prestressed railgun design has been utilized on a number of existing high-energy railguns, including those manufactured by SPARTA and the University of Texas - Center for Electromechanics (UT-CEM). The configuration is comprised of a round bore with an external prestress uniformly applied on the backup insulators. This configuration represents a prototypical weaponlike rep-rated system. The EML performance (efficiency and bore deflection) was examined for a wide variation in presumably achievable material properties for the rail, bore insulator and backup insulators. A photograph of an EML manufactured by SPARTA for ARDEC based on this design approach is included as Figure 3.3, along with its operational parameters.

The EML environment for both solid and plasma armatures were considered to determine their effects on the bore material requirements. The loading for these two cases consists of a peak uniform pressure (plasma induced) occurring adjacent to the rear of the projectile and dropping off to a rail repulsion (electromagnetic) force several bore diameters aft of the projectile for the plasma armature, and a nonsymmetric rail repulsion force (i.e. acting only on the conductor rails) only for the solid armatures. Thermal loading also is dramatically affected by armature type. Since both types of armatures are considered for future EML applications, and because solid armatures transition to "plasma brushes" at velocities above about 1.5 km/sec, the implication of armature type on the loads experienced by EML insulator rails were evaluated.

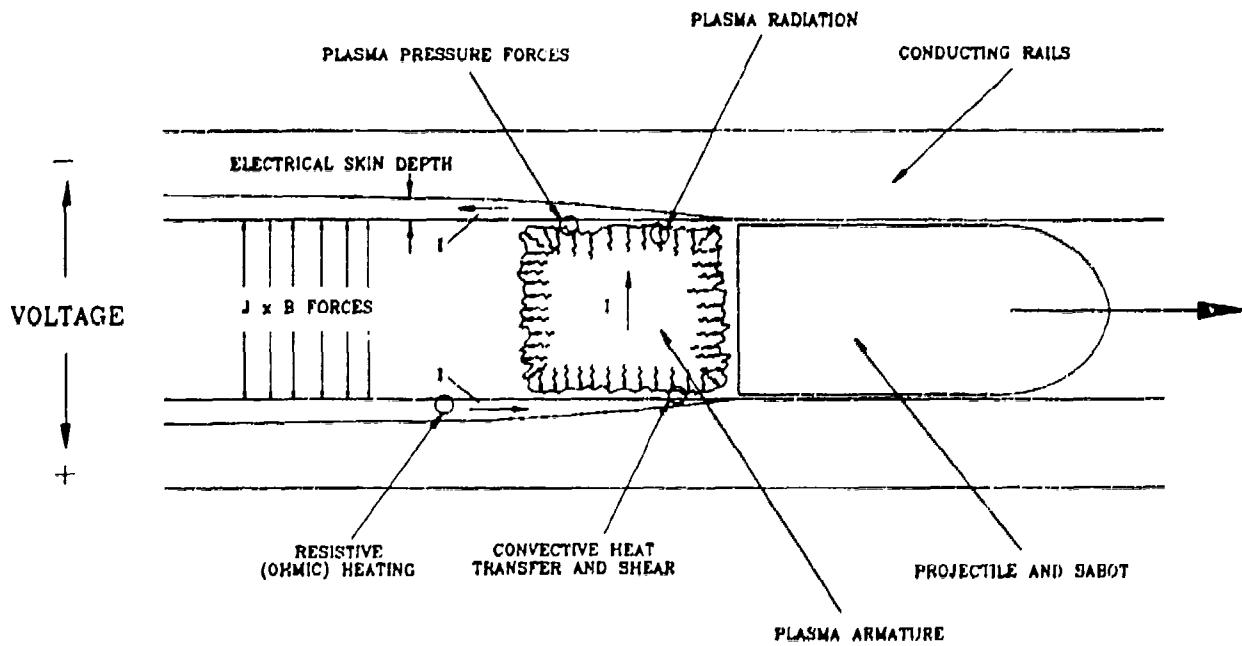


Figure 3.1 - Schematic of structural, thermal and electrical environment experienced by electromagnetic launcher bore materials.

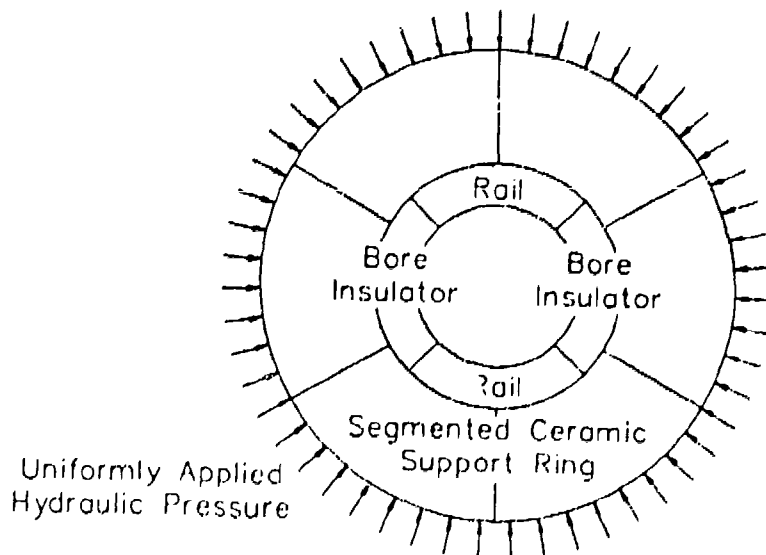
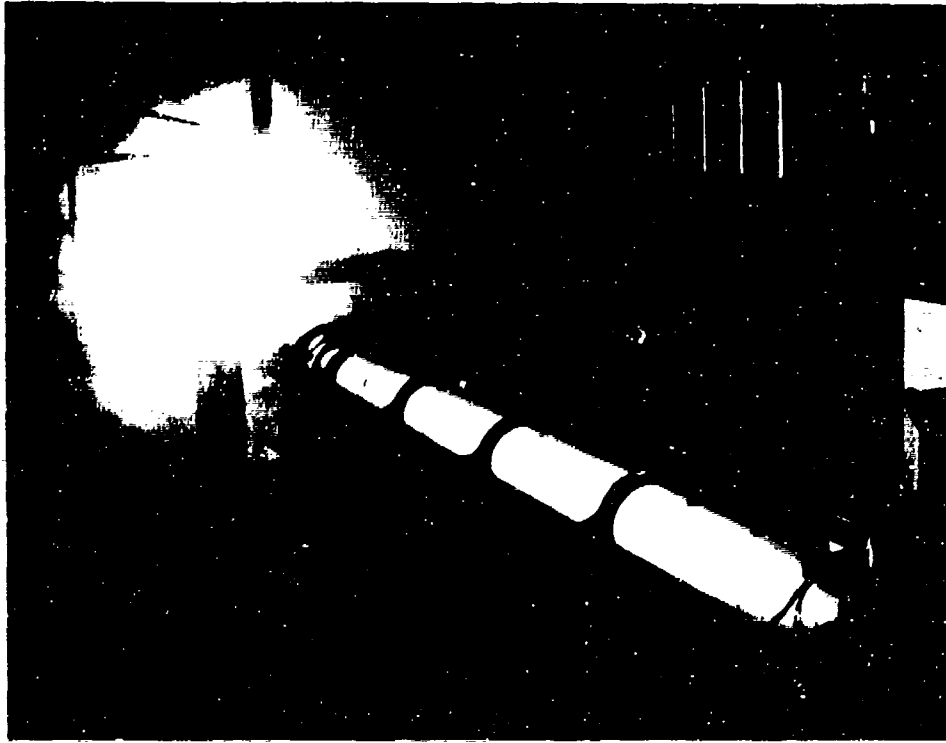


Figure 3.2 - Baseline barrel configuration used in analytical modeling studies.

TABLE 3.1 - Environmental Loads Experienced by Electromagnetic Accelerator Bore Materials

Environment	Range of Values	Time/Spatial History
<u>Structural</u> Plasma Pressure Precompression (hoop) Thermal Growth (Compressive) Local Thermal Stresses on Bore Surface Balloting/Abrasion/Erosion	30 to 60 kpsi 30 to 60 kpsi 0 to 20 kpsi 60 to 500 kpsi 5 to 10 keeeps impact	~ 0 to 2 Bore Diameters Behind Projectile Constant ~0 to 30 Minutes After Shot ~ Instantaneous With Arc During Projectile Flight
<u>Thermal</u> Plasma Radiation Bulk Joule Conductor Heating Heat Conduction Into Insulators	1 to 2 MW/cm ² 0.5 to 2.0 MJ/m 0.1 to 0.5 MJ/m	Same As Plasma Pressure Highest in Breech Region, Initially in Surface of Conductors Concentrated in Breech Region, Initially at Surface of Insulators, 0 to 60 Minutes After Shot
<u>Electrical</u> Electromagnetic Repulsion in Conductor Rail Bore Magnetic Field Rail Arc Current Rail to Rail Voltage Drop	30 to 60 kpsi 40 Tesla 2 to 5 MA 4 to 22 kV	Not Additive to Plasma Pressure, 0 at Projectile Rear Behind the Projectile Reaches Max. Value within 20 in. (0.5 m) of breech At Instant of Capacitor Discharge



Bore Diameter:	3.54 in. (90 mm)
Acceleration Length:	275.6 in. (7m)
Peak Current:	3.6 MA
Peak Bore Pressure:	60 kpsi (414 MPa)
Peak Voltage:	22 kV
Muzzle Energy	9 to 14 MJ
Inductance Gradient	> 0.38 $\mu\text{H/m}$

Figure 3.3 - ARDEC/DARPA Advanced Composite Railgun and Pertinent Operating Parameters

ANALYTICAL MODELING TO DEFINE PROPERTY REQUIREMENTS

The analytical modeling of the baseline EML design is based on a 3-level approach which includes evaluating the effect on performance of tailored material properties at a micro, macro, and subcomponent materials systems level. It considers the materials to be composite materials, which would be the most complex situation, but the model applies also to monolithic materials, since they can be viewed as composites with zero loading fractions of reinforcement. The micro-level involves estimating the anisotropic composite properties based on the constituent fiber or particulate, and matrix material components. The primary variables include fiber type, volume fraction and orientation, particulate volume fraction and type, and matrix type and microstructure. The macro-level includes multilaminate layers of these composites for the bore components (e.g. clad rails or multidirectional composite layups of bore insulators). The subcomponent or material systems level consists of configuring the macro-level components into a barrel configuration and evaluating the interplay of critical material properties (e.g. elastic modulus, etc.) on the overall barrel performance.

It is at the subcomponent level that material properties can be equated with gun performance. One measure of gun performance is bore displacement during an electrical shot. Figure 4.1 illustrates the bore deflection for two types of loading conditions (plasma and solid armature) on a barrel designed with low and high subcomponent-level stiffness. These diagrams are the result of finite-element modeling. The results support the significance of tailored and improved material properties on reducing bore deflections. The modeling also illustrates higher peak deflection values for the solid armature design resulting from the asymmetric bore loading. This is because of electromagnetic stresses acting alone; the plasma pressure being absent for the solid armature configuration.

Initial studies were also conducted around a baseline configuration to show the sensitivity of bore deflection to material stiffness. Figure 4.2 illustrates some of the results of this study. The bore insulator and rail displacements are shown for increases in modulus values above the selected baseline. The rail modulus (baselined at 20 Mpsi (138 GPa)) is not as influential as the bore and backup insulator moduli in controlling the bore displacements. This type of analysis helps in directing the study effort to the material properties and bore components that have the greatest systems payoffs.

The results presented in Figures 4.1 and 4.2 illustrate the impact of using tailored high modulus materials for the bore components and backup insulators in minimizing bore deflections. The differences between stiff and soft EML designs translate to reductions in bore deflections of 30 to 40 times.

4.1 Bore Insulators

Ceramics have almost zero plastic strain at failure (0% ductility) and fail catastrophically under load when cracks propagate from pre-existing flaws, usually at the surface. The resistance to fracture is a material property called "fracture toughness". Work was initiated to define the goal fracture toughness value for high stiffness ceramic materials being developed in the program. This work involved calculating the dynamic stress levels on the bore component free surfaces and relating these stresses to the critical flaw size that would cause fracture using the equation⁹:

$$a_{cr} = \alpha \frac{(K_{IC})^2}{\sigma^2} \quad , \quad (\text{Eq. 4.1})$$

where

a_{cr} = critical flaw size

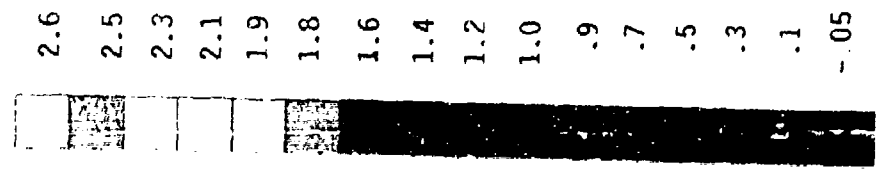
K_{IC} = plain strain fracture toughness

α = geometric term

σ = maximum tensile stress.

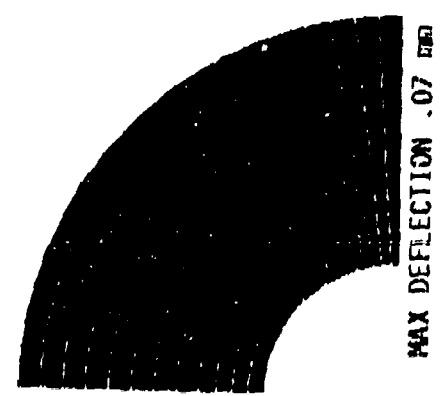
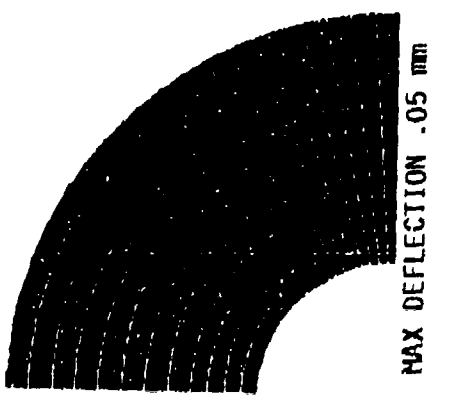
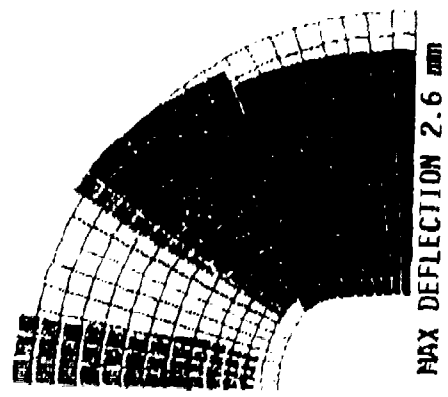
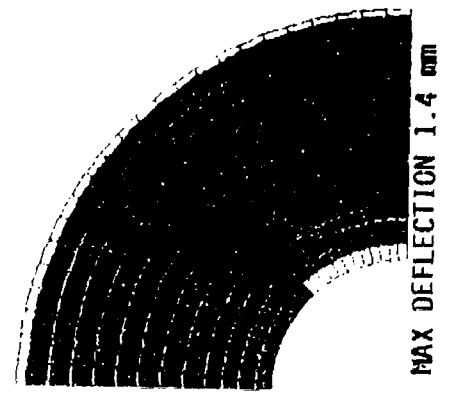
The minimum initial manufacturing/processing flaw size that is reliably detectable by inspection or proof testing then defines the required fracture toughness that will prevent ceramic failure under a given maximum operating stress. Since both the barrel configuration and linear current density (amps per centimeter of rail height) strongly influence these stress levels, both soft and stiff EML configurations were evaluated over a range of current (or pressures). The bore insulator elastic modulus was parametrically varied for each configuration. In addition, the type of armature (solid or plasma) also has major effect on the insulator stress distribution. The plasma armature results in an outward insulator movement during the electrical pulse because of the uniform plasma pressure loading. The solid armature design results in a net inward movement of the insulator during the shot due to the non-symmetric loading on the rail which pinches the bore insulators, forcing them inward.

DISPLACEMENT
(mm)



LOW MODULUS DESIGN
BORE INSULATOR (G-10): 2 Mpsi (13.8 GPa)
BACKUP INSULATOR (G-10): 2 Mpsi (13.8 GPa)

HIGH MODULUS DESIGN
BORE INSULATOR: 45 Mpsi (310 GPa)
BACK-UP INSULATOR: 41 Mpsi (283 GPa)



PLASMA ARMATURE

SOLID ARMATURE

Figure 4.1 - Finite element models of bore radial displacement for high- and low-modulus materials systems

BASELINE MODULUS PARAMETERS

- Rail: 20 Mpsi (ANSI Cooper Alloy)
- Bore Insulator: 5 Mpsi (Glass Epoxy)
- Stack-up Insulator: 40 Mpsi (Alumina AD94)

RANGE OF PARAMETERS

- 10 - 40 Mpsi
- 2 - 60 Mpsi
- 2 - 60 Mpsi

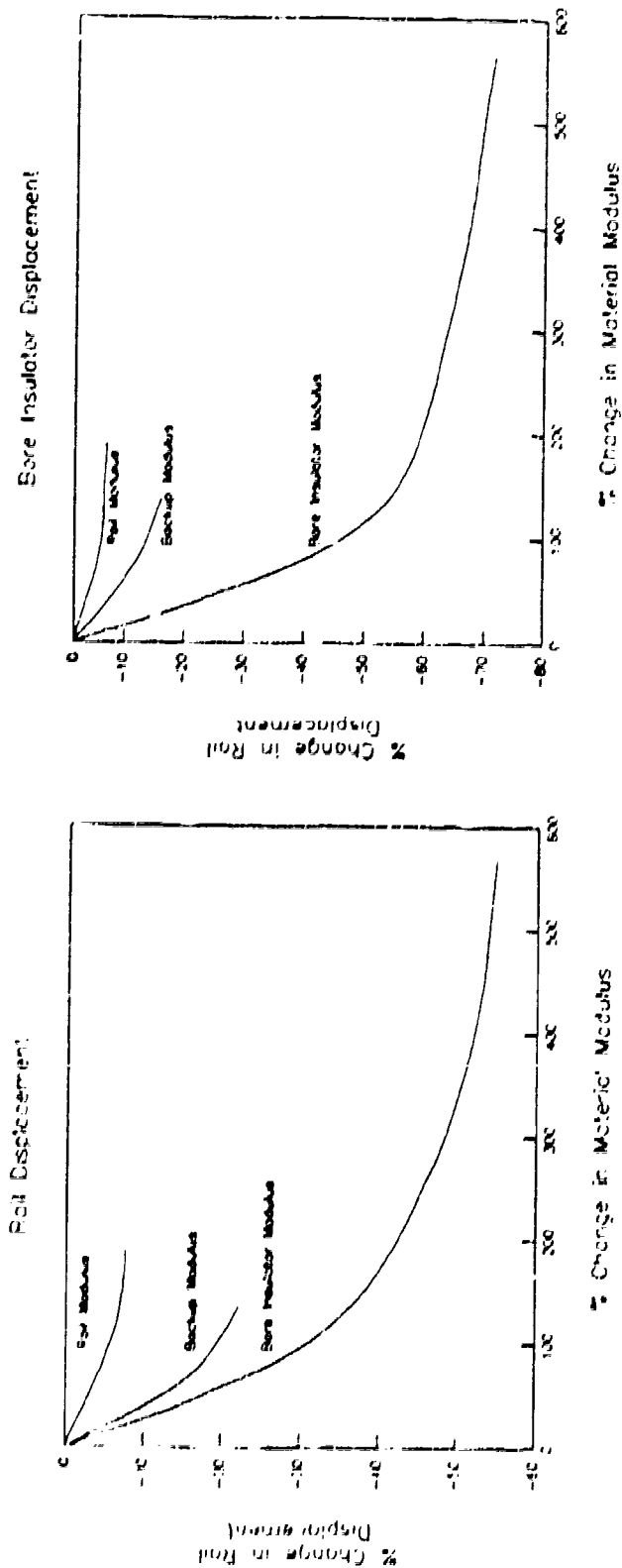


Figure 4.2 - Sensitivity of the bore component displacement to material stiffness for solid armature EMLs.

Further analysis centered on confirming the stress levels in the bore insulator during the electromagnetic shot. The previously reported results were based on two-dimensional structural analysis of the barrel system. A more detailed three-dimensional model was developed for the high modulus barrel design and evaluations were made for both plasma and solid armature loading conditions. The more detailed three-dimensional model results confirmed the two-dimensional parametric results. The detailed model also provides the axial distribution in the vicinity of the solid or plasma armature.

A representative square bore configuration was also analyzed, because this is the type of gun which would be used for screening of candidate bore materials in this program. The relevant configuration selected is that represented by the FLINT gun design at the U.S. Army Armament Research, Development and Engineering Center (ARDEC) facility, at Picatinny Arsenal, NJ (similar to the Plasma Utility Gun (PUG) at Eglin Air Force Base). This design represents both a generic square bore design and was also used in the experimental ceramic insulator screening test program (Section 6.3). We identified some modifications of the FLINT gun design to provide a higher backup insulator stiffness and modification of the geometry of the bore insulator. These modifications were necessary to reduce the backup deflection under loading and provide a better test bed for the bore rail and insulator combination. This analysis is detailed in Section 6.3.1.

The modeling and evaluation of property requirements focussed next on the applicability to various EML barrel configurations, evaluation of ceramic fracture toughness requirements and thermal effect of rail claddings. In order to evaluate the applicability of our material property requirements modeling, two round bore configurations were evaluated (these represented relevant barrel configurations being developed at the time). Prestress of barrel components can be applied in a variety of ways including both active hydraulic pressurization and passive cured-in-place residual stress application. Figure 4.3 provides a schematic of the two barrel configurations evaluated in this study. The prestress is assumed uniformly applied on the backup support ring. Two approaches have been developed in the design of the backup support ring; one using a solid ring and the other a segmented support ring. The primary difference in the concepts is the efficiency of the external prestress transfer into the rail/bore insulator interface. As shown in Figure 4.3, the segmented design results in a 3 to 1 increase in the applied prestress, thus 15 kpsi (103 MPa) externally applied provides 45 kpsi (310 MPa) on the rail/bore insulator interface. The solid support ring design approach actually results in a stress reduction of 2 to 1. However, the preload transfer is not as critical as the necessity of the backup support ring being constructed from a very high stiffness (modulus) material. Evaluations were completed for both of these barrel configurations under plasma and solid armature environments. The results show very little difference in the bore deflection magnitudes and stress levels during the railgun firing. These results provide support of the applicability of our materials property modeling to other relevant barrel configurations.

- Armature: Solid
- Rail Pressure (Outward): 45 kpsi (310 MPa)
- Rail Linear Current Density: 468 kA/cm
- Modulus:

 - Backup Ceramic: 41 Mpsi (283 GPa)
 - Conductor Rail: 19 Mpsi (138 GPa)
 - Bore Insulator: 50 Mpsi (345 GPa)
 - Hydraulic Prestress: 15 kpsi (103 GPa)

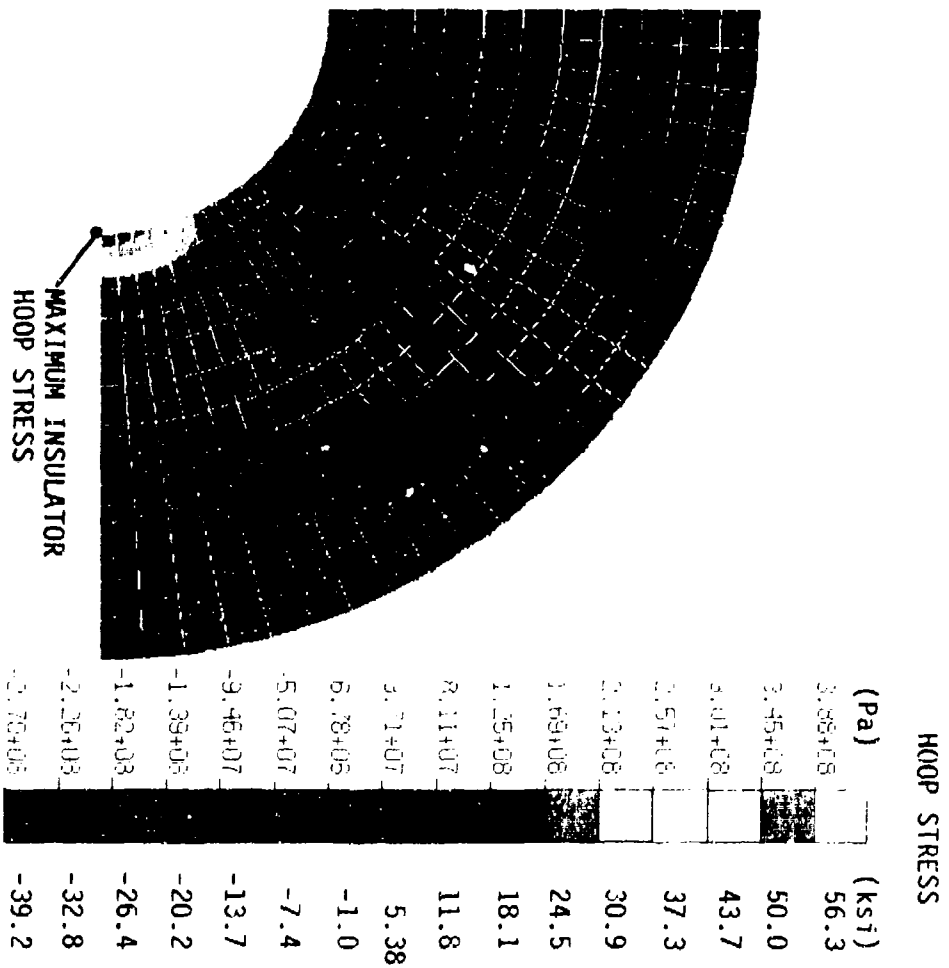
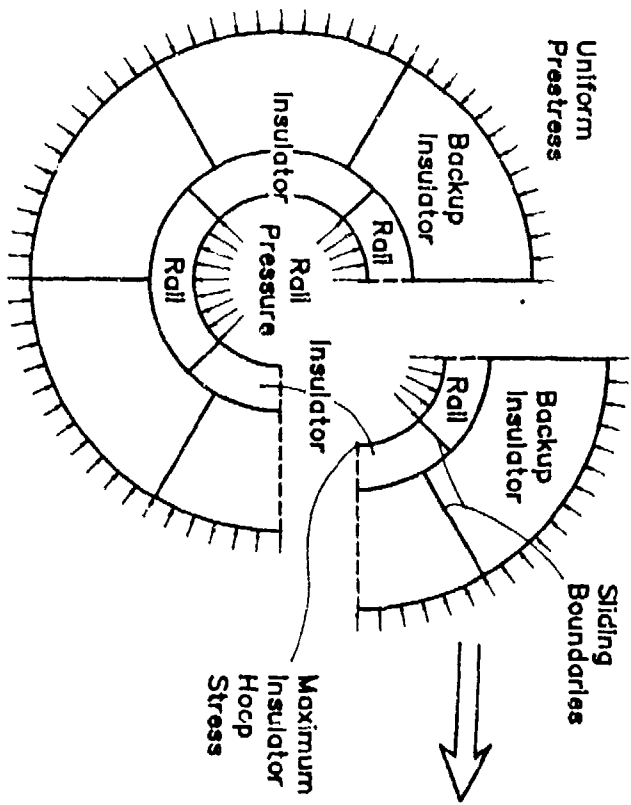


Figure 4.3 - Active prestress load transfer efficiency to the rail / bore insulator interface.

It was stated earlier that the stiff EML barrel designs translated to factors of 30 to 40 times reduction in bore deflections. Fracture toughness analysis for both stiff and the soft bore insulator materials was conducted. The required fracture toughness is defined as

$$K_{Ic} = S_f \left(\frac{1}{M} \right) \sqrt{a_{cr}} \quad , \quad (\text{Eq. 4.2})$$

where K_{Ic} = fracture toughness
 S_f = fracture strength
 $M = 1.05$ for fabrication-caused surface cracks
 a_{cr} = critical flaw size.

The minimum initial manufacturing/processing flaw size, a_{cr} , that is detectable by inspection or proof testing defines the required fracture toughness for a given operating stress.

The probability of flaw detection is a function of the thickness sensitivity, which is the flaw size divided by the part thickness. Figure 4.4 shows that a 0.010 inch (0.25 mm) flaw in a 0.5 inch (1.27 cm) thick bore insulator (2% of the section thickness) translates into a flaw detection probability of 95%.¹⁰ A 0.025 in. (0.63 mm) flaw is 5% of the section thickness, giving a flaw detection probability of 97%. Ninety-five percent is an acceptable level of detection probability, so the maximum allowable flaw size used in determining toughness requirements was 0.010 inches (0.254 mm).

Calculated maximum insulator hoop stresses and fracture toughness requirements were plotted for the high modulus backup EML barrel design case. Figure 4.5 shows the maximum insulator hoop stress as a function of the rail linear current density or rail repulsive pressure for insulator moduli of 25 Mpsi (172 GPa), 50 Mpsi (345 GPa) and 75 Mpsi (517 GPa). The rail repulsive pressure (solid armature) causes an outward deflection of the rail and an inward displacement of the bore insulator, creating a tensile hoop stress on the inner side of the bore insulator. A rail current density of 450 kA/cm was used as the upper design limit, and as Figure 4.5 shows, this translates to a maximum insulator hoop stress of 38 kpsi (266 MPa) for a modulus of 25 Mpsi (172 GPa), 52 kpsi (360 MPa) for a modulus of 50 Mpsi (345 GPa) or 64 kpsi (440 MPa) for a modulus of 75 Mpsi (517 GPa).

The maximum tensile hoop stresses on the bore insulator determine the location for the required fracture toughness calculation and for the required ceramic insulator strength determination. The maximum hoop stresses shown in Figure 4.5 were translated into required fracture toughness values for the minimum detectable manufacturing flaw size of 0.010 in. (0.254 mm). The results are plotted in Figure 4.6 for the three different bore insulator moduli.

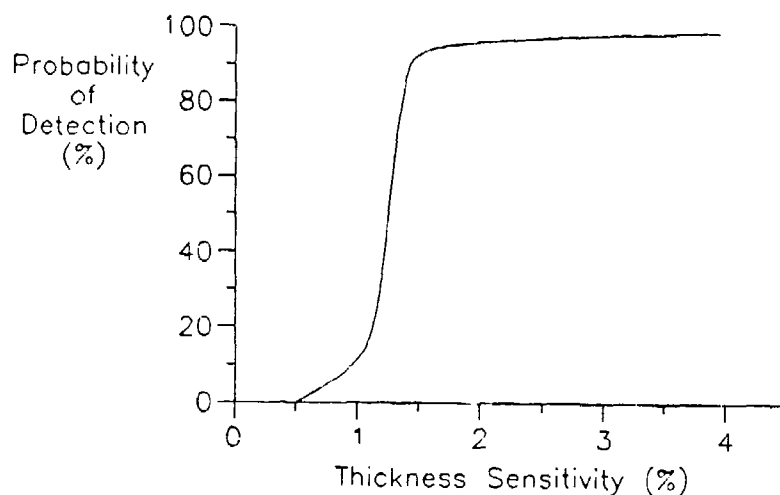


Figure 4.4 Probability of detection of a flaw as a function of thickness sensitivity (flaw size divided by section thickness).

The sensitivity to a minimum detectable crack depth size is evaluated in Figure 4.7. The required fracture toughness was plotted as a function of variation of rail linear current density and the maximum insulator tensile hoop stress for minimum detectable crack depths of 0.010 in. (0.254 mm), 0.025 in. (0.635 mm) and 0.050 in. (1.27 mm). The fracture toughness requirements decrease with the reduction of the critical flaw size that is detectable. The result of this analysis is that a fracture toughness of 5.0 kpsi·in^{1/2} (5.5 MPa·m^{1/2}) is the minimum acceptable value for a bore insulator material with a modulus of 50 Mpsi (345 GPa) and a minimum detectable flaw size of 0.010 in. (0.25 mm)

The required fracture toughness developed and shown in Figures 4.6 and 4.7 was used to establish a goal range for toughened candidate ceramic bore insulators in Figure 4.8. This encompasses the projected levels of railgun loading environments.

Figure 4.7 shows the relationship between the operating EML environments of the railgun to the required fracture toughness and critical flaw size for the solid armature case. A dimensionless analysis of the railgun was also performed to evaluate the axial loading due to a moving plasma armature. The analysis was limited to a length of 9.8 in. (25 cm) to reduce the CPU runtime to a reasonable length. The interface between the rail and the bore insulator was modeled using frictional interface elements. The soft interface between the backups and the rail/bore insulators were also modeled. A plasma pressure of 45 kpsi (310 MPa) was applied on the rail and the bore insulator between the axial locations of 0 and 2.95 in. (7.5 cm.). The backup insulator was prestressed to 15 kpsi (103 MPa). The

maximum outward radial displacements of the rail and insulator are plotted in Figure 4.9. The maximum axial stresses for the rail and bore insulator are shown as a function of the axial location in Figure 4.10. The maximum insulator tensile stresses (10 kpsi (69 MPa)) are lower for the plasma armature case compared to the solid armature.

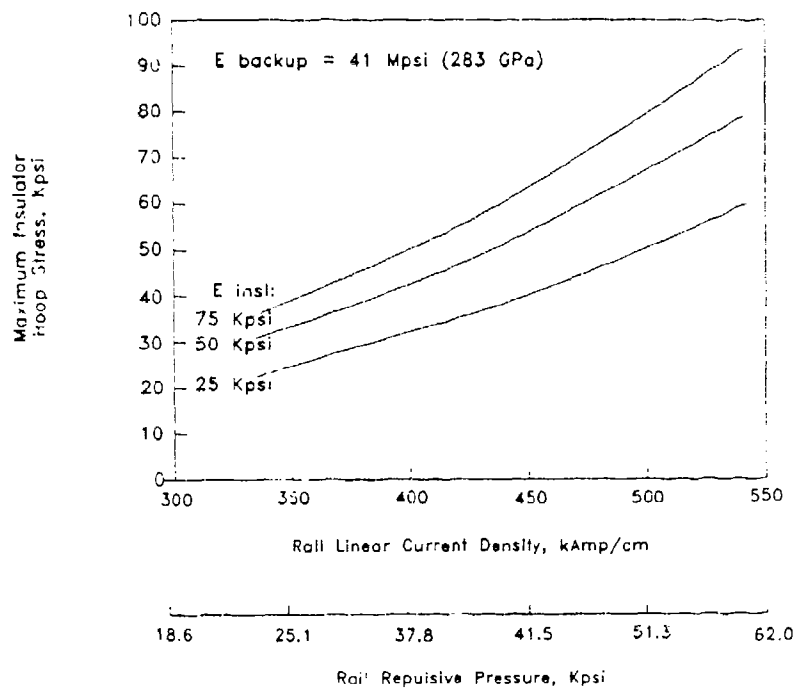


Figure 4.5 Effects of bore insulator modulus on the maximum insulator hoop stress for different current densities.

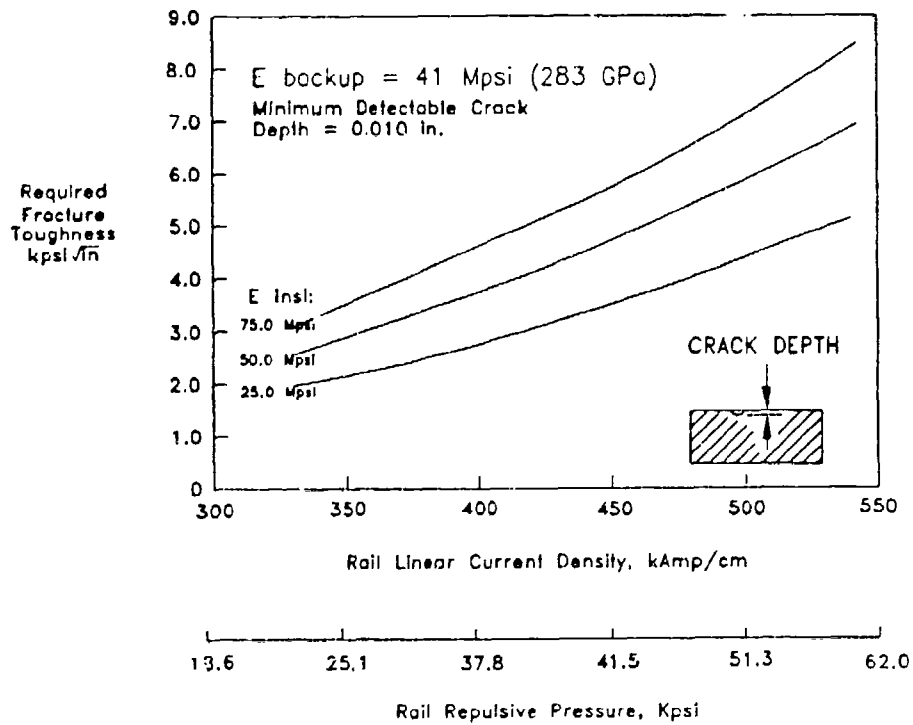


Figure 4.6 Required fracture toughness of advanced bore insulators as a function of conductor rail current density and insulator moduli.

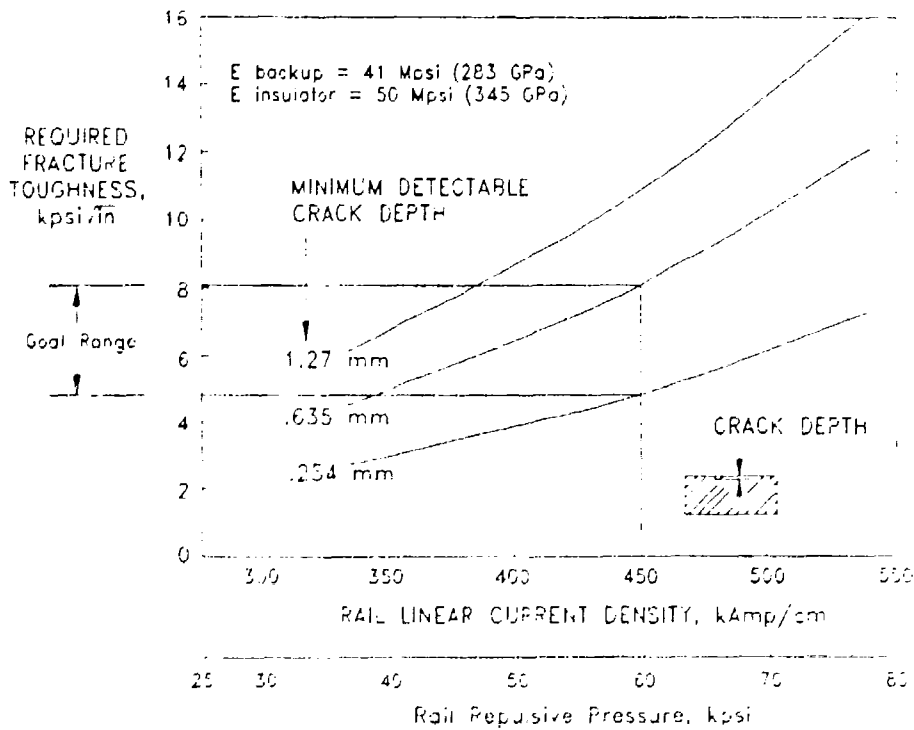


Figure 4.7 Required fracture toughness of advanced bore insulators as a function of minimum detectable crack depth and conductor rail current density.

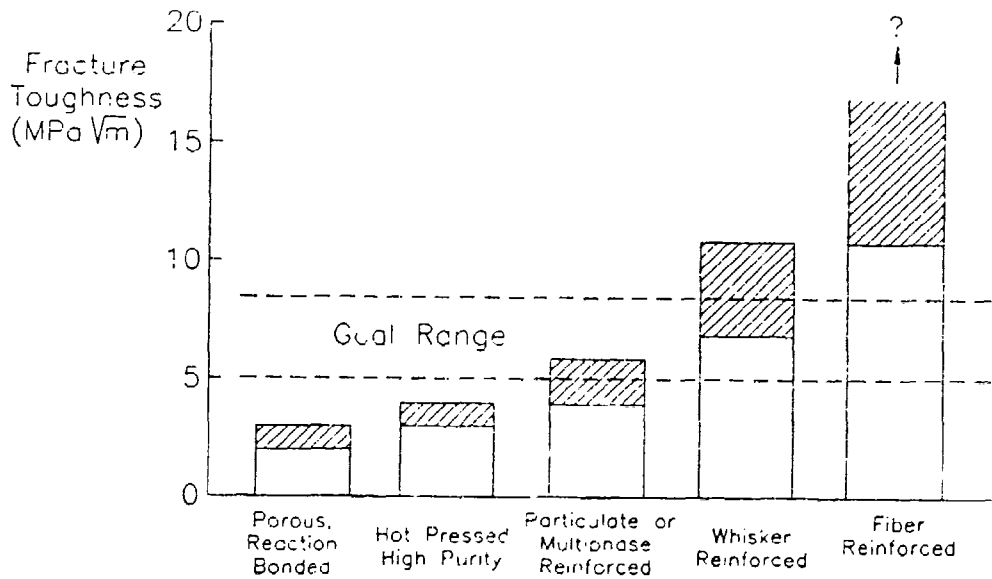


Figure 4.8 The range of achievable fracture toughness values for some ceramics and ceramic-matrix composites.

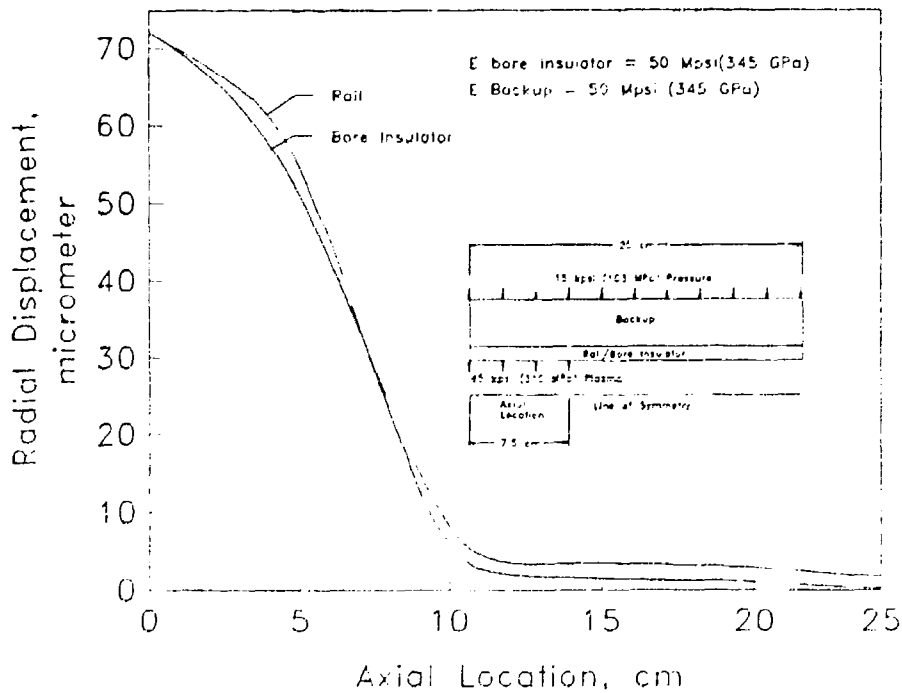


Figure 4.9 Axial variations of the rail and insulator maximum displacements due to plasma armature pressure.

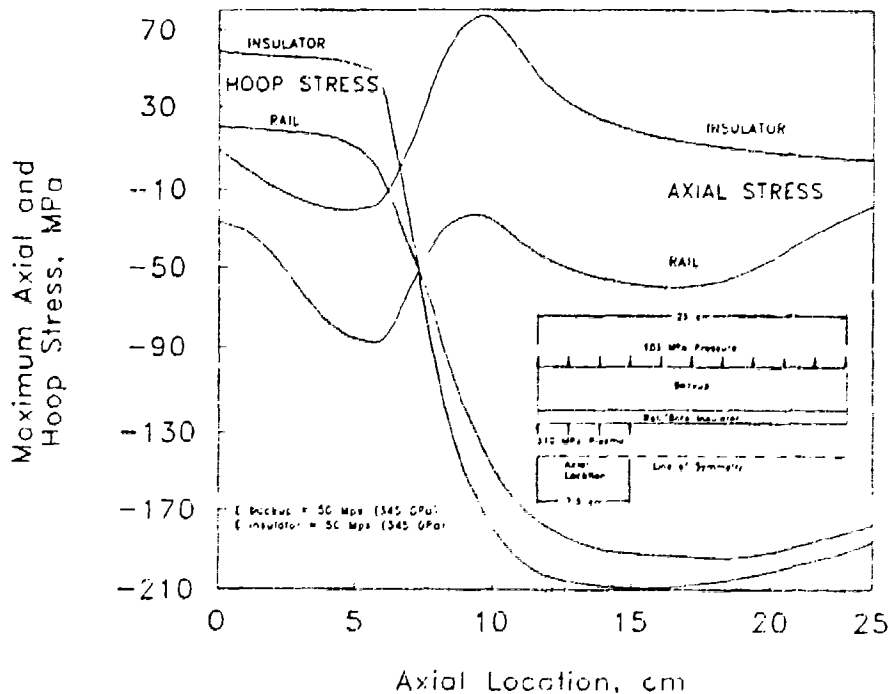


Figure 4.10 Axial variations of the maximum axial hoop stresses in the conductor rails and insulators due to plasma armature pressure.

In addition to the strength and toughness requirements which were established for candidate bore insulators, it was also necessary to assess the requirements for high voltage surface breakdown resistance. This quantity is the maximum voltage per unit length which an insulator can stand off across its surface before surface breakdown occurs and an arc traverses it. The determination of this requirement did not require any analysis: it is a simple question of the anticipated operating voltages and bore diameters that will be used in the next generation of electromagnetic launchers. This value must be retained after multiple arc exposures, since a plasma armature may degrade the insulator surface in the same manner as an arc jumping across it. Many ceramic insulators are seen to exhibit good standoff strength before they are overloaded, but their surface resistance diminishes significantly after being traversed by an arc. This is because the arc may cause chemical decomposition of the insulator material leaving conductive decomposition products. An example of this is zirconia-based ceramics. Zirconium oxide is an inherently good insulator, but if an electrical arc breaks across its surface, it causes a film of zirconium metal to form on it, reducing its resistance to subsequent voltage loading. A survey of anticipated railgun development revealed that future bore insulators will be required to stand off between 0.5 and 2 kilovolts per centimeter, depending on the configuration of the EML system. A value of 1.0 kV/cm is the most probable requirement for future gun designs. For the purposes of this development program, however, we shall choose the

upper limit of 2 kV/cm as our property goal. At least one-hundred shots should be achievable at this level without the need for cleaning or honing of the bore, so the insulator must retain this resistance after 100 arc exposures.

Based on all of the preceding analyses, the properties which will be required of a bore insulator in the next generation of electromagnetic launchers are summarized in Table 4.1.

TABLE 4.1 — Summary of Bore Insulator Property Requirements

Property		Required Value
Mechanical	Flexural Strength (Modulus of Rupture)	50 kpsi (345 MPa) (for a probability of failure of 0.1%)
	Fracture Toughness	5.0 kpsi·in ^{1/2} (5.5 MPa·m ^{1/2})
	Elastic Modulus	45 Mpsi (310 GPa)
Electrical	Surface Voltage Standoff after 100 arc pulses	2.0 kV/cm for plasma armatures 0.5 kV/cm for solid armatures
Processing	Producibility	Can be fabricated to 2.5 in. (6.4 cm) thick by 20 in. (0.5 m) long forms while retaining above properties.

4.2 Conductor Rails

A detailed thermal model was developed for the conductor rail materials to evaluate their key thermal properties such as specific heat, thermal conductivity and latent heat. The model is a coupled electrical and thermal diffusion model that can account for phase change in the material. The initial validation test cases were made for the reference barrel configuration (Figure 3.2) using two different electrical current ramp rates. Figure 4.11 illustrates that localized melting occurring in the corner region increases as the electrical ramp time decreases (as would be the case in fast moving plasma armature). The trade-off between the heat capacity (both sensible and latent) of the rail material and the effect on the current diffusion time must be properly characterized in order to effectively select the appropriate material requirements.

The results of a second sensitivity trade-off study is also shown in Figure 4.12. This shows the trade-off of rail electrical conductivity with overall gun efficiency. As the conductivity decreases, a larger fraction of energy will be deposited as Joule heat in the rail. Higher rail temperatures coupled with the increase in resistance with temperature both detract from the energy imparted to the projectile. As a result, the overall gun efficiency drops. Figure 4.12 illustrates for different starting point gun efficiencies the trade-off of efficiency with conductivity. Materials with an agglomerate rail conductivity of greater than approximately 60% I.A.C.S. are desired, at least for the simple breech fed

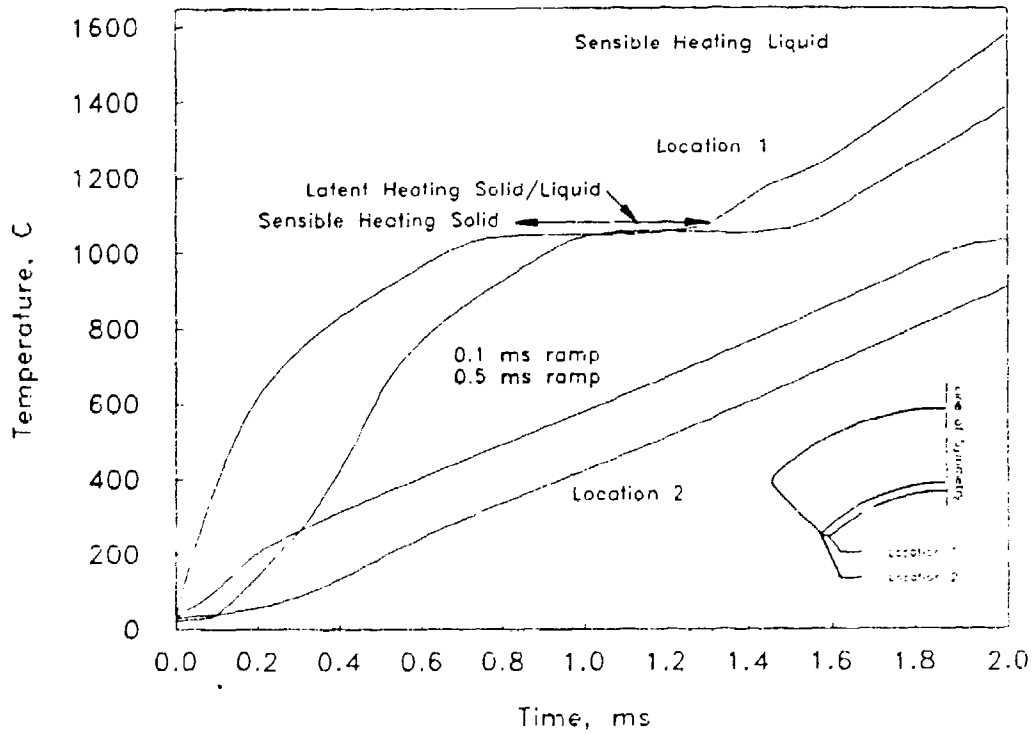


Figure 4.11 - Thermal model of rail showing localized melting on the rail corners during the electrical pulse.

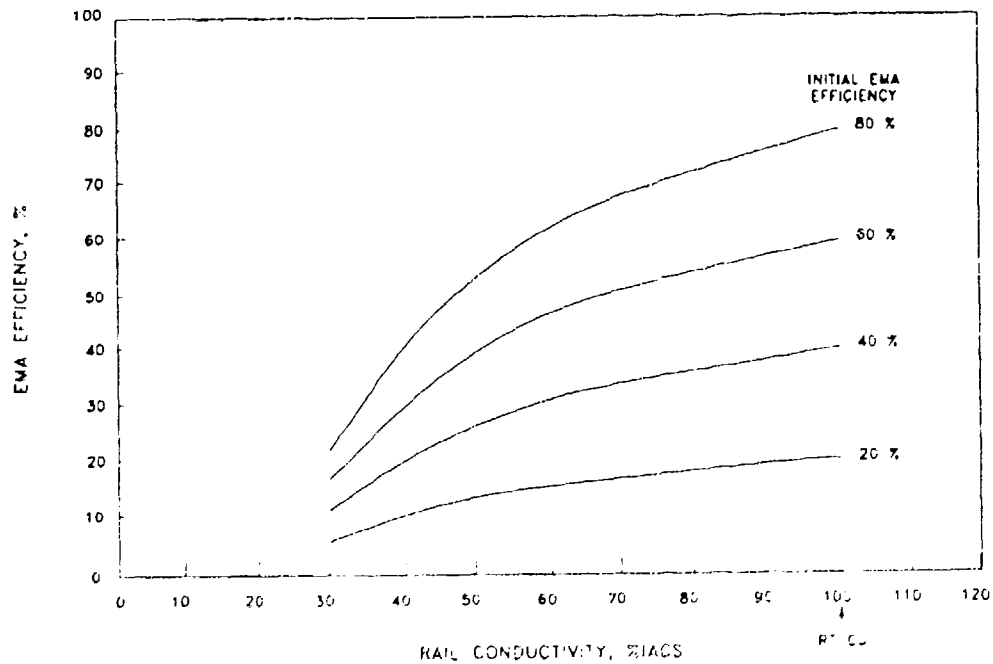


Figure 4.12 - Sensitivity trade-off of the overall EML efficiency to rail conductivity (%I.A.C.S.).

railgun which was modeled. The acronym "I.A.C.S." stands for International Annealed Copper Standard. 100% I.A.C.S. is defined as $1.7241 \mu\Omega\text{-cm}$, approximately the electrical resistivity of pure copper. Thus, 60% I.A.C.S. is 60% of the conductivity of pure copper.

A detailed thermal analysis was developed for a peak linear current density of 400 kA/cm to evaluate the effects of cladding material properties (i.e. ablation resistance and electrical conductivities) on the interface temperatures of the cladding and rail conductors. The applied current history and the initial surface current distribution are shown in Figure 4.13. High ablation resistant cladding materials such as refractory metals and graphite coatings reduce the ablation damage.^{2,11,12,13&14} However, lower electrical conductivity also increases the current penetration rate and causes a current concentration at the cladding/conductor interface. Figure 4.14 illustrates the initial results of this trade-off study. As the electrical conductivity (% I.A.C.S.) of the cladding is reduced, the potential for melting of the rail conductor at the cladding/conductor interface is increased, as shown.

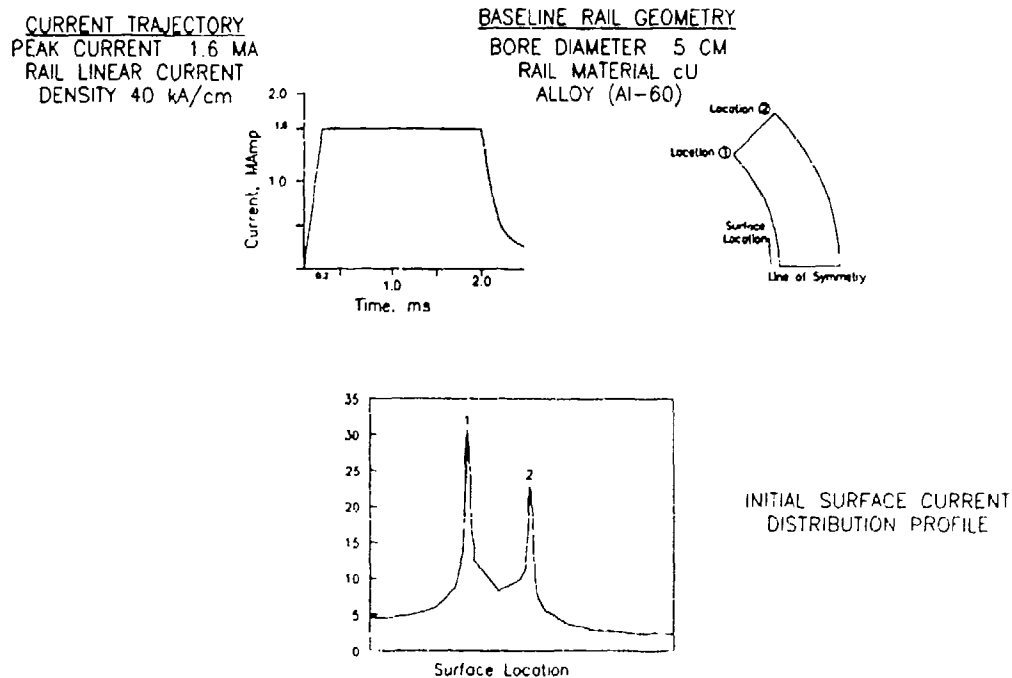


Figure 4.13 Thermal/electrical current diffusion analysis for EML rails

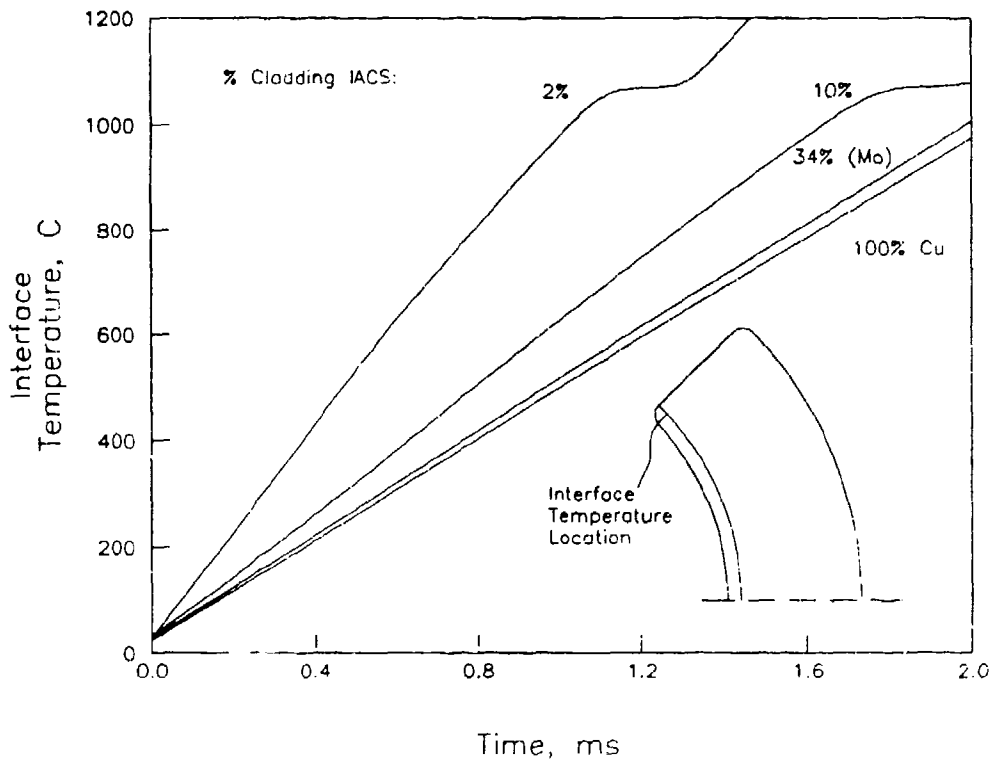


Figure 4.14 Evaluation trade-off between rail cladding thermal and electrical properties and the cladding/rail substrate temperature.

MATERIALS DESIGN, FABRICATION AND SCREENING

At the start of the program, a large number of advanced ceramics producers was contacted regarding their recommendations for systems to be investigated that might have the potential to meet the requirements listed in Table 4.1. These recommendations were combined with a review of the literature and with SPARTA's own knowledge of both advanced ceramics and of railgun needs to arrive at a number of ceramic systems and chemical compositions to be investigated and ceramic vendors to work with. Work began on the development of ceramic prototype panels to provide material for screening tests in order to select the materials that would be scaled up later in the program.

The ceramics manufacturer Cercom, Inc. of Vista, California was chosen to fabricate ceramic panels by hot-pressing. In the case of composite compositions, Cercom was also responsible for blending reinforcements such as silicon carbide whiskers with the ceramic powders, and then filling the molds with these mixtures before hot-pressing. Cercom provided valuable advice in selecting ceramic compositions and in recommending sintering and other processing aids to be added to the ceramic powder formulations.

5.1 Advanced Ceramic Insulator Design Approach

The approach that was taken to formulate advanced ceramic insulator materials in this program was to begin on the microstructural level, and using the principles of modern materials science, design a material in the same way that a mechanical engineer would design a machine. We will call this microstructural tailoring (sometimes called micro-architectural design). Shown in Table 5.1 is a summary of the possible design methods available for the microstructural tailoring of advanced ceramic composite materials to meet the mechanical and electrical requirements of high-energy railguns. We utilized these techniques to design several different ceramic materials. On the level of crystal structure, techniques of solid solution strengthening were used to combine molecules in optimum ratios. On the microstructural level, glassy phase sintering aids were used to assure high density and maximum intergranular adhesion. On the micromechanics level, whisker reinforcement was used to increase toughness. On the level of thermodynamics, oxides were selected for chemical stability to resist degradation or reduction by arc

plasmas. All of these aspects were successfully integrated into a materials system design approach with the goal of satisfying all of the property goals discussed in Chapter 4. Some of the techniques mentioned in Table 5.1 are described in more detail below.

Choice of Matrix Material - Alumina (Al_2O_3), silicon nitride (Si_3N_4) and silicon carbide (SiC) are the mostly widely used advanced ceramic structural materials utilized today and thus have a large experience base and supplier base for raw materials. Unfortunately, it has been shown that the conductivity of silicon carbide is too high to provide sufficient electrical insulation, so it cannot be considered unless heavily loaded with an additive that destroys the conductivity of the SiC , such as mullite. Another matrix material of interest is aluminum nitride (AlN) which is increasingly being used because of its high thermal conductivity. Zirconia is also gaining in importance, usually used in a stabilized or transformation toughened form or mixed with alumina. However, previous work has shown that ceramics with over about 10% zirconia decompose in the presence of a high power arc to leave a film of zirconium metal on the surface; which is unacceptable for railgun insulator use.

During this program, the matrix materials Al_2O_3 , Si_3N_4 , AlN , and ZrO_2 were investigated as potential matrix materials. However, the AlN and ZrO_2 were quickly dropped from consideration because the decomposition problem inherent with them. Late in the program, the Al_2O_3 matrix materials were down-selected based on their excellent combination of toughness, strength, and electrical properties. The Si_3N_4 matrix materials also possessed excellent mechanical properties, but their electrical properties were only marginal for railgun use.

Solid Solution Strengthening - The only solid solution strengthener considered for the matrixes of interest is chromia (Cr_2O_3) as an additive to alumina. It has been shown to be effective in moderate amounts (less than 15% by weight) in increasing the strength of alumina. The addition of the chromia to the alumina matrix did not compromise its mechanical properties (fracture toughness or strength) and tended to raise the Weibull Modulus values. The major unexpected benefit from the addition of chromia, however, was improved surface voltage standoff strength. The chromia acted to stabilize the constituents of the final alumina composition, Al_2O_3 , 8.0% ZrO_2 , 0.25% Y_2O_3 , 5.0% Cr_2O_3 , to prevent the formation of surface conductive species in the presence of high energy electric arcs.

Grain Size Refining - As mentioned in Table 5.1 this can be accomplished by three different techniques: grain boundary pinning, minimization of consolidation temperature and time, and the use of fine starting powders. For the matrixes of primary interest all three techniques can be utilized. Iteration of consolidation temperatures/pressures/times are often necessary to determine what processing conditions will deliver full density without causing excessive grain growth. Yttria (Y_2O_3) and zirconia (ZrO_2) are used for alumina, and yttria and alumina for silicon nitride as grain boundary phases that reduce grain size.

A review of the scientific literature on advanced structural ceramics revealed that a 10 micron (0.0004 in.) or smaller average grain size would be necessary to produce the mechanical properties desired for the railgun insulator ceramic. However, this small grain size would have to be reached without compromising the density of the ceramic material. In order to achieve smaller grain sizes, the processing temperatures must be reduced. This can often lead to less dense materials. Thus, a compromise between processing parameters (temperature and time), glassy grain boundary phase formers, and grain size was reached through iterative development.

Table 5.1 Microstructural Tailoring Techniques Utilized In Design of Advanced Ceramic Insulator Materials

TECHNIQUE	GOAL	COMMENTS
Matrix Composition Selection	Determine Matrix Chemical Composition With Potential to Meet Requirements When Adequately Tailored	Oxides, Nitrides and Carbides are Viable Systems
Solid Solution Strengthening	Improve Strength of Material	Too Much Can Reduce Fracture Toughness; Solubility of Additive is Important
Grain Size Refining	Reduce Grain Size to Improve Strength and Toughness	Accomplished Through Grain Boundary Pinning Materials, Minimization of Consolidation Temperature /Time, and Fine Starting Powders
Glassy Phase Sintering Aids	Reduce Consolidation Temperature Through Use of Lower Temperature Grain Boundary Phases	Glassy Compounds (Yttria, Alumina, and Zirconia Compounds) Frequently Used, Care Must be Taken Not to Decrease Toughness, Full Density Desirable
Whisker/Platelet Reinforcement	Optimize Toughness/Strength of Material Through Addition of Appropriate Reinforcement	Reinforcement Must Be Compatible With Matrix at Consolidation Temperature, Proper Amount of Bonding to Matrix is Vital
Second Phase Strengthening	Creation of Second Phase at Grain Boundaries Can Strengthen/Toughen Material	Same Glassy Grain Boundary Phases As Above
Continuous Fiber Reinforcement	High Temperature Continuous Ceramic Fibers Can Strengthen/Toughen Ceramics	Beyond the State-of-the-Art for the Sizes and Properties Needed
Transformation Toughening	Toughen the Matrix by a Phase Transformation to Put Structure in Compression	Only Used in Zirconia Based Systems

Glassy Phase Sintering Aids - Without the use of these materials, it would be necessary to consolidate alumina and silicon nitride matrix materials at such a high temperature that excessive grain growth would occur. Thus the same materials that help pin the grain boundaries (described above) also act to form a glassy grain boundary phase that initially melts and flows to fill the intergranular spaces, and then solidifies as diffusion occurs. This action serves to promote low porosity and good intergranular bonding. The materials used are called "sintering aids", but they work equally well with hot pressing ("sintering" usually refers to a pressureless process). In this program, zirconia and yttria were added to the alumina (Al_2O_3) matrix as sintering aids, and yttria and alumina were added to the silicon nitride (Si_3N_4) as sintering aids.

Whisker/Platelet Reinforcement - The term whisker, as used in this report, refers to an acicular (needle-shaped), microscopic single crystal of a high-strength, high-modulus ceramic material. Silicon carbide is the most widely used reinforcing whisker, but whiskers of aluminum oxide, titanium nitride, and boron carbide are also available. All of these materials are in the size range of 0.5 to 2 microns in diameter and 10 to 100 microns in length (25.4 microns equal 0.001 inch). Being single crystals, these materials tend to be exceedingly strong since they lack the strength-limiting defects that are normally present in bulk materials such as voids, inclusions, and grain boundaries.

Reinforcement with silicon carbide whiskers is probably the single most effective strengthening and toughening mechanism for ceramic materials. It has been demonstrated that a whisker addition of 20 v/o can nearly double the fracture toughness and quadruple the flexural strength of hot-pressed alumina materials compared to their unreinforced counterparts.¹⁵ There are five different mechanisms by which whisker reinforcement may increase the strength or toughness (or both) of a ceramic material:¹⁶

1. Load Transfer - High modulus/strength of whisker can carry load
2. Matrix Prestressing - If Coefficient of thermal expansion is greater than that of matrix, the matrix will be put into compression during cooling from consolidation temperature
3. Crack Deflection - Stress state around whisker can blunt cracks or increase work of fracture.
4. Fiber Pullout - If fiber/matrix bond is relatively weak, energy can be absorbed in fiber pullout, increasing toughness
5. Crack Bridging - Fibers may bridge cracks and raise threshold stress for further crack extension

Of these five mechanisms, fiber pull-out is most frequently credited with toughness improvement in ceramic materials. Load transfer is the primary mechanism for providing strength improvement. Both of these phenomena can occur together providing that the shear strength of the whisker/matrix interface is within a certain range. Thus the consolidation temperature/time must be compatible with the whisker in order to produce an ideal amount of whisker/matrix bonding.

Platelets can also be utilized, though they are usually not as effective as whiskers because of the whisker's geometry and mechanical properties. The electrical properties of the reinforcement material must also be taken into consideration as too much SiC added to a ceramic will unacceptably increase the material's conductivity.

During the course of the program, both whiskers and platelets were utilized. The whiskers (two different grades were investigated) were added to Al_2O_3 , Si_3N_4 and AlN matrices, and the platelets were added to AlN and the Al_2O_3 . It was quickly seen that the platelets were too large in size, and acted as crack initiators, destroying the toughness and strength of the matrix material. The whisker reinforcements worked well if kept below about 20%, producing significant increases in toughness. Above this, they would decompose under the arc exposure and lose their surface voltage holdoff strength. The whisker effects on the alumina mechanical properties were not as pronounced as on the Si_3N_4 , and because of their effect on the electrical properties, even at lower loadings, they were dropped from consideration for the alumina matrix material. The AlN and silicon nitride materials were eventually dropped because of their electrical properties. However, for certain railguns, the use of silicon nitride can probably be tolerated, and in that case, the use of SiC whisker reinforced silicon nitride would be beneficial.

Second Phase Strengthening - Ceramics can be strengthened by the addition of a material to the matrix that promotes the formation of second phases in the microstructure that act to stabilize the structure and create residual compressive loads, which raise the strength and toughness of the material. The same additive materials that promote glassy grain boundary structures and reduce grain size act as second phase strengthening agents.

Continuous Fiber Reinforcement - Much effort is underway to develop continuous fiber reinforced ceramic materials. Because of the thermal limitations of existing fibers, the choice of matrices is rather limited. Much work has been done with glass-ceramic matrices, which are processed as low temperature glasses and then turn to high temperature ceramic during the later stages of the processing. However, the current state-of-the-art for continuous fiber reinforced ceramics is far short of what is needed to develop full scale advanced ceramic insulator segments for railguns, and none were investigated in the program.

Transformation Toughening - Transformation toughening is a process where a crack front will cause a phase transformation which results in a local volume expansion, thus putting the material ahead of the crack tip into compression, and blunting the crack. Unfortunately, this mechanism only occurs in zirconia, among the matrix materials of interest and, as mentioned previously, zirconia cannot be considered a candidate material because of its poor electrical behavior in the presence of an arc. Thus, transformation toughening as a micro-architectural tailoring method was not investigated.

5.2 Fabrication of Ceramic Insulator Materials

The first panels fabricated in the program were 6 x 6 x 0.25 in. (15 x 15 x 0.64 cm) in size. The as-pressed thickness was actually 0.375 in. (0.95 cm), but they were ground down to 0.25 in. (0.64 cm) before testing to remove surface flaws. As many as eight panels of this size could be consolidated in one hot-pressing run. Later in the program, numerous eight inch (20 cm) square panels, two 1.5 x 4 x 8 inch (3.8 x 10 x 20 cm), and one 1.5 x 4 x 18 inch (3.8 x 10 x 46 cm) blocks were produced. This chapter will describe the fabrication of a variety of ceramic compositions for use as railgun insulator materials. It will also describe the preliminary mechanical testing that was performed on these panels to screen out those ceramic compositions with obviously inferior mechanical properties.

The first of five hot-pressing consolidation runs was designed to establish the process feasibility for producing high stiffness, high fracture toughness ceramic insulators and conductors. The materials shown in Table 5.2 were consolidated at 3500 psi (24.1 MPa) and 1350°C (2462°F) for 4 hr. The purpose of the initial run was to establish the feasibility of relatively low temperature processing that would be compatible with SiC whisker or platelet reinforcement. Density values of the diborides were between 65 to 75% of their theoretical density and those of the Al-based ceramics were 80 to 90%. These low densities indicated the need for higher processing temperatures.

Table 5.2 - Ceramics Consolidated in the First Hot Press Run

Matrix	Reinforcement
Conductor Ceramics	
ZrB ₂	—
TiB ₂	—
TiB ₂	SiC _w
Insulator Ceramics	
AlN	—
AlN + Y ₂ O ₃	—
Al ₂ O ₃ -Y ₂ O ₃ -ZrO ₂	—

The panels consolidated in Hot Press Run #1 were sliced up using a diamond saw to produce two strips 2.0 x 0.5 x 0.25 in. (5.1 x 1.3 x 0.64 cm) from each of the seven plates. Metallography specimens from each of the plates were prepared in order to examine the microstructure (pore structure, voids, etc.). The results from this run were used to select processing conditions (time, pressure, temperature) for the next set of runs, #2 and #3. The compositions of each panel and their final densities are listed in Table 5.3.

TABLE 5.3 - Panels Consolidated in Runs #2 and #3

Composition	Density (g/cc) Measured/ Calculated	% of Theoretical Density
Run #2		
a Si ₃ N ₄ - 10% SiC _w	3.271 / 3.290	99.4
b Si ₃ N ₄ - 10% SiC _w	3.271 / 3.290	99.4
c Si ₃ N ₄ - 8% Y ₂ O ₃ - 1% Al ₂ O ₃	3.282 / 3.30	99.5
d Si ₃ N ₄ - 8% Y ₂ O ₃ - 1% Al ₂ O ₃	3.289 / 3/30	99.7
e AlN - 0.4 Y ₂ O ₃	3.271 / 3.294	99.3
f AlN - 0.4 Y ₂ O ₃	3.274 / 3.294	99.4
g SiC - 30 v/o Mullite	3.033 / 3.188	95.1
h Si ₃ N ₄ - 30 v/o Mullite	3.077 / 3.250	94.7
Run #3		
i AlN - 0.4%Y ₂ O ₃ - 25v/o SiC _w	3.248 / 3.273	99.2
j Al ₂ O ₃ - 0.25%Y ₂ O ₃ - 8%ZrO ₂	4.076 /	
k Al ₂ O ₃ - 0.25%Y ₂ O ₃ - 8%ZrO ₂	4.061 /	
l Al ₂ O ₃ - 0.25%Y ₂ O ₃ - 8%ZrO ₂ - 5%CrO ₃	3.990 /	
m Al ₂ O ₃ - 0.25%Y ₂ O ₃ - 8%ZrO ₂ - 5%CrO ₃	3.948 /	

* All values are in weight percent unless designated by "v/o" (volume percent).

Six consolidated panels from hot pressing runs #2 and #3 were selected to be cut into modulus of rupture (MOR) bars, arc erosion test specimens, fracture toughness test specimens, rail test specimens, and metallography specimens. The cutting pattern used to make the various kinds of test coupons from the panels is shown in Figure 5.1.

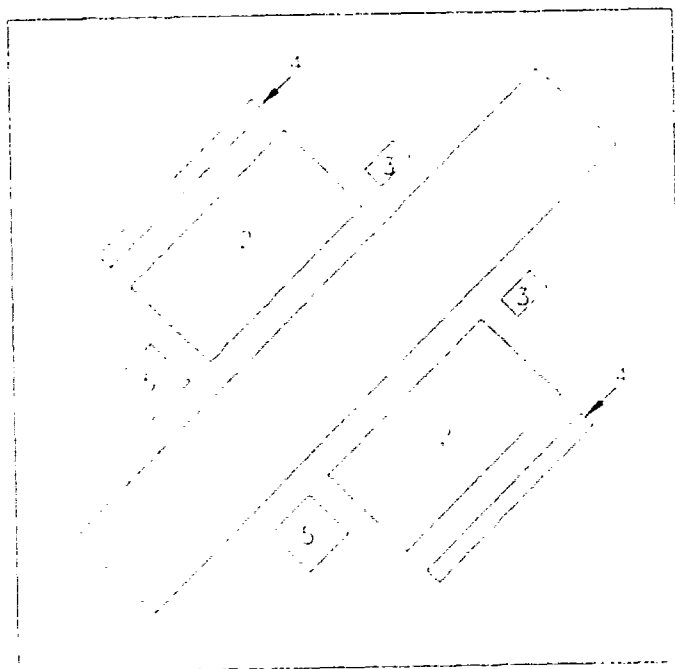


Figure 5.1 *Cutting map for consolidated 6 x 6 inch advanced ceramic panels. 1) Rail test specimen (6 x 1 x 0.25 in.). 2) Arc test specimens (2 x 1 x 0.25 in.). 3) Fracture toughness coupons (0.2175 x 0.375 x 0.250 in.) 4) MOR bars (3 x 4 x 50 mm). The MOR bars were also used for metallography after testing*

The target pressing temperature was overshoot by approximately 100 to 150C° for run #3, as evidenced by dendritic "lava" structures visible on the surface of the panels. The panels were discarded, and run #4 was pressed at a later date using all the same constituents. The average modulus of rupture values for the materials produced in run #2 are listed in Table 5.4.

The fracture toughness specimens were sent to Terratek Systems in Salt Lake City, Utah for test. The arc erosion/thermal shock test samples (two from each plate) were sent to Texas Tech University for testing (described in Section 6.2). The metallography specimens were mounted and polished to reveal the microstructure of the consolidated materials.

In July of 1988, two more sets of panels were hot pressed. The first run (#4) was a repeat of run #3 from May 1988, which overheated. Table 5.5 lists the compositions of the panels pressed in these runs and their resulting densities.

TABLE 5.4 - Modulus of Rupture Results from Run #2

Material	MOR Strength (kpsi (MPa))	
b. Si ₃ N ₄ + 10 v/o SiC _w	97.0	(669)
	104.0	(718)
d. Si ₃ N ₄ + 8w/o Y ₂ O ₃ + 1 w/o Al ₂ O ₃	109.7	(757)
	106.6	(736)
f. AlN + 0.4w/o Y ₂ O ₃	43.4	(299)
	40.0	(276)
g. SiC + 30 v/o Mullite	53.8	(371)
	56.2	(388)
h. Si ₃ N ₄ + 30 v/o Mullite	63.0	(435)
	55.2	(381)
i. AlN + 25 v/o SiC _w + 0.4 Y ₂ O ₃	67.6	(466)
	65.8	(454)

TABLE 5.5 - Panels Consolidated in Runs #4 and #5

Composition	Density (g/cc) Measured/ Calculated	% of Theoretical Density
<u>Run #4</u>		
Al ₂ O ₃ - 0.25 Y ₂ O ₃ - 8 ZrO ₂	4.090 / 4.127	99.1
Al ₂ O ₃ - 0.25 Y ₂ O ₃ - 8 ZrO ₂ - 5Cr ₂ O ₃	4.127 / 4.127	100.0
Al ₂ O ₃ - 0.25 Y ₂ O ₃ - 8 ZrO ₂ / 30v/oSiC _w	3.765 / 3.815	98.7
Al ₂ O ₃ - 0.25 Y ₂ O ₃ - 8 ZrO ₂ / 25v/o SiC platelets	3.799 / 3.865	98.3
AlN - 0.25 Y ₂ O ₃ - 25 Si ₃ N ₄	— / —	approx. 76%
<u>Run #5</u>		
AlN - 6 Y ₂ O ₃	3.265 / 3.30	102
AlN - 6 Y ₂ O ₃ - 25 Si ₃ N ₄	3.351 / 3.27	102.5
AlN - 0.4 Y ₂ O ₃ / 25v/o SiC _w	3.249 / 3.273	99.3

The processing temperature used in hot press run #4 was too low to consolidate the AlN - 0.25 Y₂O₃ - 25 Si₃N₄ material so it was repressed in Run #5 with a higher percentage of yttria (6% versus 0.25%). This greatly improved the densification. Two of the density values for materials consolidated in Run #5 are slightly greater than 100% calculated density. This is because it was not possible to make an accurate prediction of theoretical density due to lack of data on these compositions. Modulus of rupture strengths were measured for the panels from runs 4 and 5 and are presented in Table 5.6. The relatively high quality of the panels is reflected by the narrow spread in MOR values, given that they were cut from opposite corners of the relatively large panels.

TABLE 5.6 - Modulus of Rupture Results from Hot-Pressing Runs #4 & 5

Material	MOR Strength kpsi (MPa)
SiC - 30 v/o Mullite	53.8 (371)
	56.2 (387)
AlN - 0.4 Y ₂ O ₃	43.4 (299)
	40.0 (276)
Si ₃ N ₄ - 8 Y ₂ O ₃ - 1 Al ₂ O ₃	109.7 (756)
	106.6 (735)
AlN - 0.4 Y ₂ O ₃ - 25 v/o SiC _w	67.6 (466)
	65.8 (454)
Si ₃ N ₄ - 30 v/o Mullite	63.0 (434)
	55.2 (381)
Si ₃ N ₄ -8Y ₂ O ₃ -1Al ₂ O ₃ -10 v/o SiC _w	97.0 (669)
	104.0 (717)
Al ₂ O ₃ -0.25Y ₂ O ₃ -8ZrO ₂	89.4 (616)
	96.3 (664)
Al ₂ O ₃ -0.25Y ₂ O ₃ -8ZrO ₂ -5Cr ₂ O ₃	97.3 (671)
	90.0 (621)
Al ₂ O ₃ -0.25Y ₂ O ₃ -8ZrO ₂ -30v/oSiC _w	74.8 (516)
	79.9 (551)
Al ₂ O ₃ -0.25Y ₂ O ₃ -8ZrO ₂ -25v/oSiC _p	36.7 (253)
	39.0 (269)
AlN-6Y ₂ O ₃ -25Si ₃ N ₄	56.1 (387)
	19.8 (343)
Si ₃ N ₄ -8Y ₂ O ₃ -1Al ₂ O ₃ -5SiC _w	123.5 (852)
	124.3 (857)
Si ₃ N ₄ -8Y ₂ O ₃ -1Al ₂ O ₃ -15SiC _w	113.4 (782)
	116.5 (803)

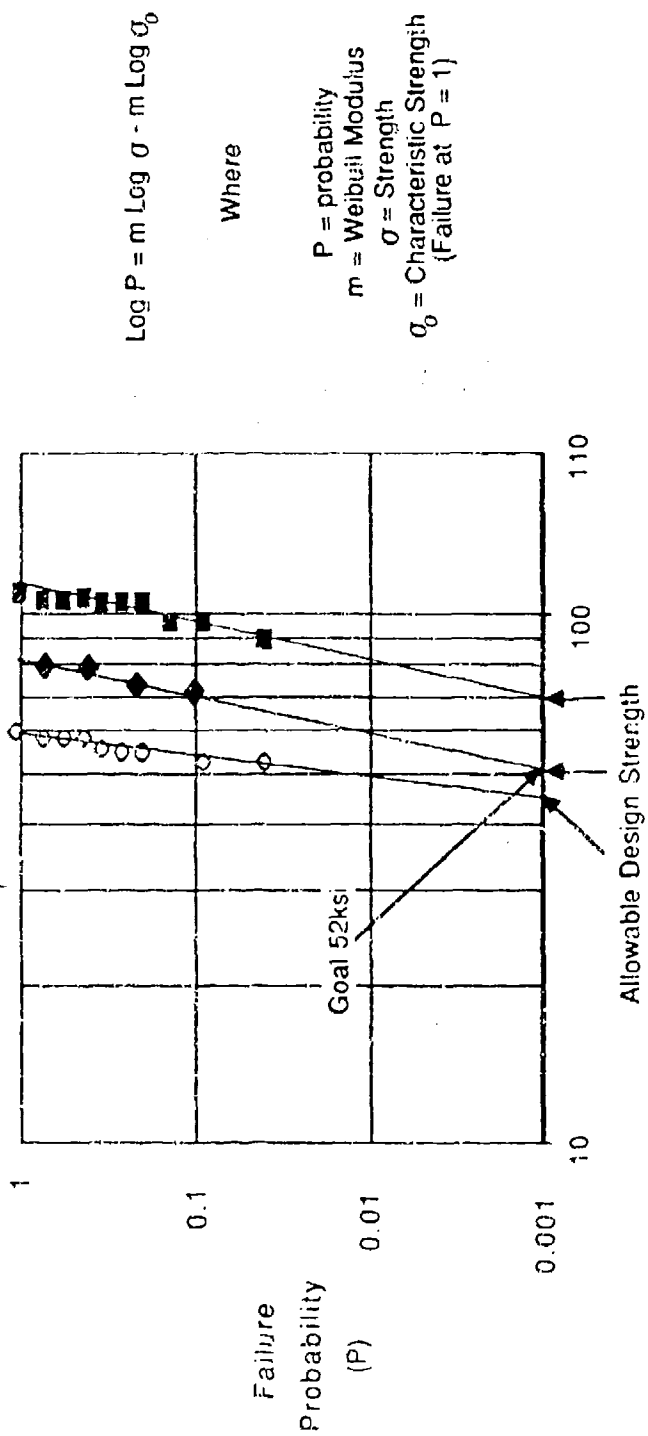
* All compositions given in weight percent unless otherwise stated

As the values in this table show, the Si_3N_4 and Al_2O_3 based materials have the highest modulus of rupture (MOR) values. The AlN based materials, with or without reinforcement, are lower in strength. The only material that does not follow this trend is the SiC platelet reinforced Al_2O_3 material in which the recently developed platelets were so large that they acted as stress risers and led to failure at low levels of flexure.

Three of these materials were selected for the fabrication of additional MOR test bars. This was in order to provide enough values to determine their Weibull modulus. The values measured are reported in Table 5.7 and plotted in the standard Weibull statistics form in Figure 5.2. It is generally accepted that a minimum of 12 test bars is necessary for a valid Weibull modulus determination. However, insufficient material was available for this number, thus, the Weibull curves shown are for comparison only. It is seen that both the silicon nitride and silicon carbide whisker reinforced aluminum nitride materials meet the goal 50 kpsi (345 MPa) strength for a failure probability level of 0.001 (i.e. 99.9% reliability).

TABLE 5.7 - Modulus of Rupture Values Used for Weibull Modulus Determination

Material	MOR Strength kpsi (MPa)
Si ₃ N ₄ -8Y ₂ O ₃ -1Al ₂ O ₃	109 (752)
	96 (662)
	105 (724)
	110 (758)
	90 (621)
	109 (752)
	97 (669)
	106 (731)
	<u>107 (738)</u>
	Average: 103.5(714)
AlN-0.4Y ₂ O ₃	385 (55.9)
	398 (57.7)
	361 (52.3)
	414 (60.1)
	363 (52.6)
	400 (58.0)
	376 (54.5)
	375 (54.4)
	398 (57.7)
	<u>398 (57.7)</u>
Average: 387 (56.1)	
AlN-0.4Y ₂ O ₃ -25v/oSiC _w	508 (73.7)
	550 (79.7)
	489 (70.9)
	<u>543 (78.7)</u>
	Average: 523 (75.8)



MOR Strength (ksi)

Symbol	Material	Weibull Modulus	Design Allowable MOR Strength kpsi (MPa) 99.9%
◇	AIN - 0.4%Y ₂ O ₃	22.3	48.8 (336)
◆	AIN - 0.4%Y ₂ O ₃ - 25%SiC _w	14.5	60.7 (419)
■	Si ₃ N ₄ - 8%Y ₂ O ₃ - Al ₂ O ₃	13.0	83.6 (576)

Figure 5.2 Determination of candidate ceramic allowable design stresses utilizing Weibull statistics.

As seen in Figure 5.2 the allowable design strengths are indicated by the point where the Weibull modulus slopes cross the Probability of Failure line at 0.001 (99.9% reliability). These design allowable strengths of 43 kpsi (296 MPa), 51 kpsi (352 MPa), and 69 kpsi (476 MPa) are respectively 77, 67, and 67% of the average values taken from Table 5.7. Thus, the three materials tested whose Weibull slopes were all above 13 have a relatively narrow distribution of flexure strengths in the volume of materials evaluated, indicating good control of raw materials and process parameters. Their design allowable strengths are more than two thirds of their average strengths. For some advanced ceramics, the values can be as low as one third to one half.

Figure 5.3 is a plot of the Weibull equation reconfigured from Figure 5.2 to show the effect of Weibull Modulus on the ratio of Design Strength to Average Strength for three different values of Probability of Failure, 0.1, 0.001, and 0.000001. As can be seen, there is tremendous payoff in raising the Weibull Modulus to a value of about 15. The curves flatten out somewhat above that point. Low grade ceramics typically have Weibull values from 3 to 8. Thus, in going to a high quality structural ceramic with a Weibull value of 13 to 15 or higher, a tremendous increase in design strength can be realized. For example, take a ceramic with an average MOR strength of 80 kpsi (552 MPa) and use the probability of failure ratio of 0.001. The design strength would vary from 21.6 kpsi (149 MPa) for a Weibull Modulus of 5 to a design strength of 52.8 kpsi (364 MPa) for a Weibull Modulus of 15; an increase of 144% in design strength brought about from the increase in Weibull Modulus. This explains why it is important to measure the Weibull Modulus for the developmental ceramic insulator materials.

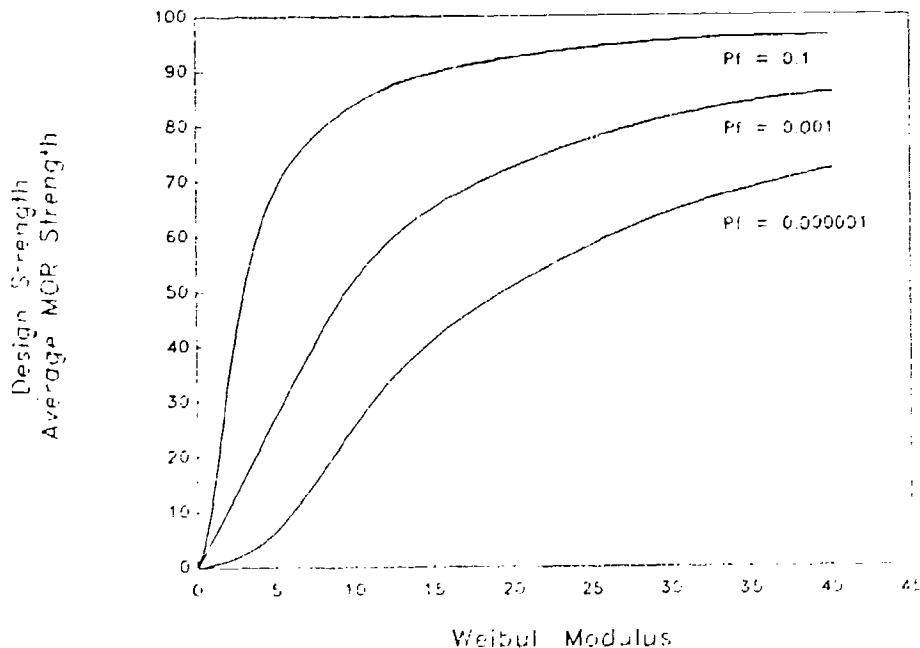


Figure 5.3 The effect of Weibull Modulus on the ratio of design strength to average MOR strength for different values of probability of failure.

Valid fracture toughness results on six advanced ceramic materials from runs 4 and 5 were determined from specimens tested at TerraTek Systems Inc. in Salt Lake City, Utah using a Chevron notch short beam test specimen. Figure 5.4 shows the configuration of the Chevron Notch short beam coupon, a SENB fracture toughness coupon (described later), and a standard MOR test bar.^{17,18} The Chevron Notch short beam fracture toughness test is conducted by inserting a mercury-filled stainless steel bladder into the notch and pressurizing the mercury until the specimen fractures. The pressure versus displacement traces are plotted and the fracture toughness determined by the maximum load. The slopes of the curves are examined to determine the validity of the test. Some of the specimens tested did not produce "valid" fracture toughness values because of the residual stresses in the material caused by reinforcements (whiskers or platelets). These specimens were cut from 0.25 in. (6.35 mm) thick plates and were the only sized Chevron notch short beam fracture toughness test specimen that can be used. If larger sizes could have been used, valid results on additional materials would have been possible.

Shown in Table 5.8 are the results of the valid fracture toughness tests conducted in this series. The AlN material exhibited by far the lowest fracture toughness. The unreinforced alumina materials were both above 3.5 kpsi•in^{1/2} (3.9 MPa•m^{1/2}), very good for unreinforced alumina. Upon adding the whiskers or platelets to the alumina, the toughness increased to above 5.0 kpsi•in^{1/2} (5.55 MPa•m^{1/2}). This coincides with the lower band of the fracture toughness goal that was determined in Chapter 4. The goal represents the value needed to survive the environment of an electromagnetic railgun bore without fracture. The unreinforced silicon nitride material had a fracture toughness of 4.26 kpsi•in^{1/2} (4.7 MPa•m^{1/2}), slightly above what is to be expected from unreinforced silicon nitride. Tests of the reinforced silicon nitride had to be repeated with a different type of test specimen configuration in order to obtain valid results.

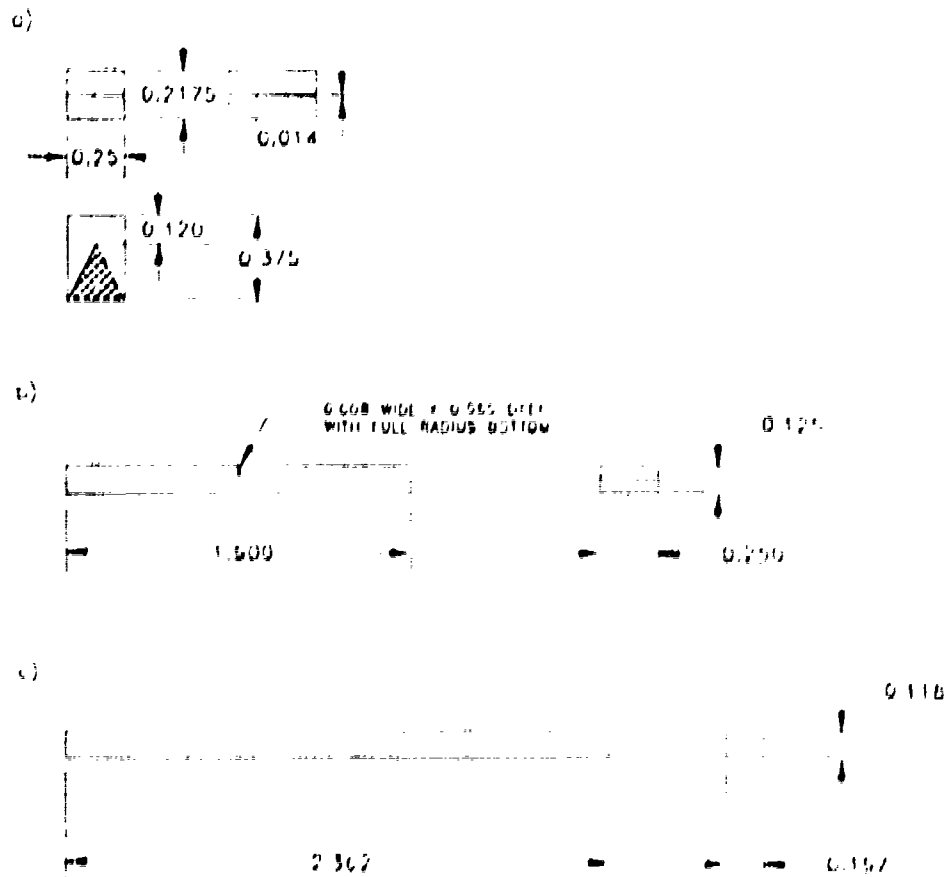


Figure 5.4 Designs of three types of mechanical test specimens used in this program: a) Chevron Notch short beam fracture toughness test specimen; b) Single Edge Notched Beam (SENB) fracture toughness test specimen; c) Modulus of Rupture (MOR) flexural strength test specimen. (All dimensions in inches)

Because of the number of invalid tests resulting from the small Chevron Notch short beam test specimen it was decided to perform additional tests of the advanced ceramic insulator materials using a SENB (single edge notched beam) test specimen. This is a widely used configuration for the toughness testing of ceramic materials.¹² Samples of all the advanced ceramic materials to be tested were machined into three test specimens each of the SENB design. The SENB test specimen is more forgiving of the internal residual stress state caused by the presence of whiskers or platelets in the material and will give valid results even for 0.25 in. (6.35 mm) thick specimens. The test bar is 0.125 x 0.250 x 1.500 in. (3.18 x 6.35 x 38.1 mm) in size with a notch ground into one face, as shown in Figure 5.3b. The bars were cut from the plates with the 0.25 in. (6.35 mm) dimension centered in the through-the-thickness direction of the plate. The SENB bars were tested on

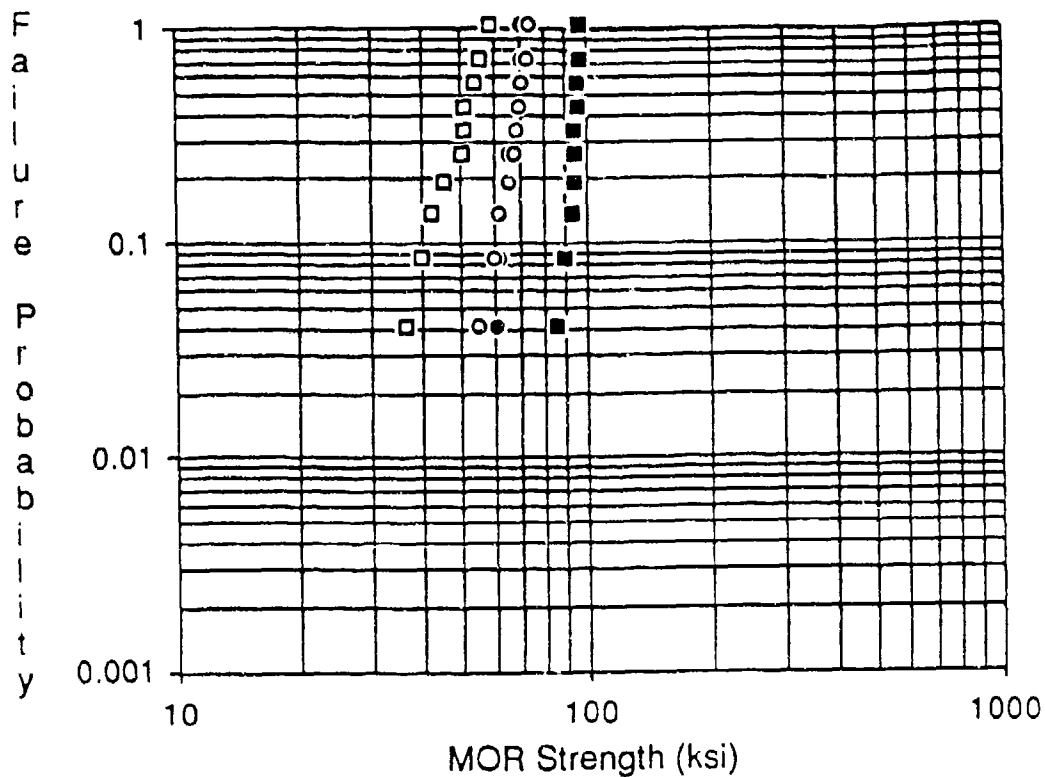
TABLE 5.8 - Results of Chevron Notch Short Beam Fracture Toughness Tests

Material	Fracture Toughness	
	kpsi·in ^{1/2}	(MPa·m ^{1/2})
AlN-0.4Y ₂ O ₃	2.64	(2.90)
Si ₃ N ₄ -8Y ₂ O ₃ -1Al ₂ O ₃	4.26	(4.68)
Al ₂ O ₃ -0.25Y ₂ O ₃ -8ZrO ₂	3.54	(3.89)
Al ₂ O ₃ -0.25Y ₂ O ₃ -8ZrO ₂ -5Cr ₂ O ₃	3.55	(3.90)
Al ₂ O ₃ -0.25Y ₂ O ₃ -8ZrO ₂ -5Cr ₂ O ₃	3.73	(4.10)
Al ₂ O ₃ -0.25Y ₂ O ₃ -8ZrO ₂ -30SiC _w	5.16	(5.67)
Al ₂ O ₃ -0.25Y ₂ O ₃ -8ZrO ₂ -25SiC _w	5.05	(5.55)

the same fixture as the modulus of rupture test specimens (four point bend fixture). Fracture toughness values were calculated from the known notch geometry and the maximum load.

Modulus of rupture and fracture toughness test specimens for the four different advanced ceramic insulator materials that were made into rails for the modified FLINT barrel (Section 6.3) were fabricated. The fracture toughness specimens were made with the two different designs, SENB (single edge notched beam) type and Chevron notch short beam type. The two different test specimen types were used because, as previously mentioned, it was determined that the size of Chevron notch short beam type fracture toughness test specimen that was possible (because of the 0.25 in. (6.4 mm) thickness of the as pressed ceramic plates) does not give "valid" results for some types of whisker or particulate loaded ceramics. Thus it was necessary to test specimens of both types to establish a correlation with previously tested materials.

Shown in Figure 5.5 is a listing of the results from the modulus of rupture (MOR) test specimens for the four materials that were to be initially tested in the modified FLINT barrel. The Weibull modulus curves for these materials are shown in Figure 5.5. It can be seen that the addition of the 5% Cr₂O₃ to the Al₂O₃-0.25Y₂O₃-8ZrO₂ has very little effect on the average strength, but did significantly raise the Weibull modulus (18 versus 10.9) and thus the 99.9% probability strength, 48.4 kpsi (338 MPa) versus 39.5 kpsi (276 MPa). The addition of the 30% SiC whisker to the matrix resulted in an 40.4% increase in average MOR strength, 93.1 kpsi (650 MPa) versus 66.3 kpsi (463 MPa); a 84.4% increase in 99.9% probability strength, 72.9 kpsi (509 MPa) versus 39.5 kpsi (276 MPa); and an increase in Weibull modulus (22.9 versus 10.9). The mullite-Si₃N₄ material (N083) had relatively low strengths and a low Weibull modulus.



Symbol	ID	Composition	Weibull Modulus	Design Allowable MOR Strength kpsi (MPa)	
				99.0%	99.9%
●	N080	$\text{Al}_2\text{O}_3\text{-}8\text{ZrO}_2\text{-}5\text{Cr}_2\text{O}_3\text{-}0.25\text{Y}_2\text{O}_3$	18.0	55.0 (384)	48.4 (338)
○	N081	$\text{Al}_2\text{O}_3\text{-}8\text{ZrO}_2\text{-}0.25\text{Y}_2\text{O}_3$	10.9	48.9 (342)	39.5 (276)
■	N082	$\text{Al}_2\text{O}_3\text{-}8\text{ZrO}_2\text{-}0.25\text{Y}_2\text{O}_3\text{-}30\text{v/o SiC}_w$	22.9	80.6 (563)	72.9 (509)
□	N083	$\text{Si}_3\text{N}_4\text{-}30\text{v/o Mullite-}10\text{v/o SiC}_w$	6.4	28.7 (201)	20.0 (140)

Figure 5.5 Weibull curves and calculated data for the four different advanced ceramic insulator materials used for testing in the modified FLINT gun barrel.

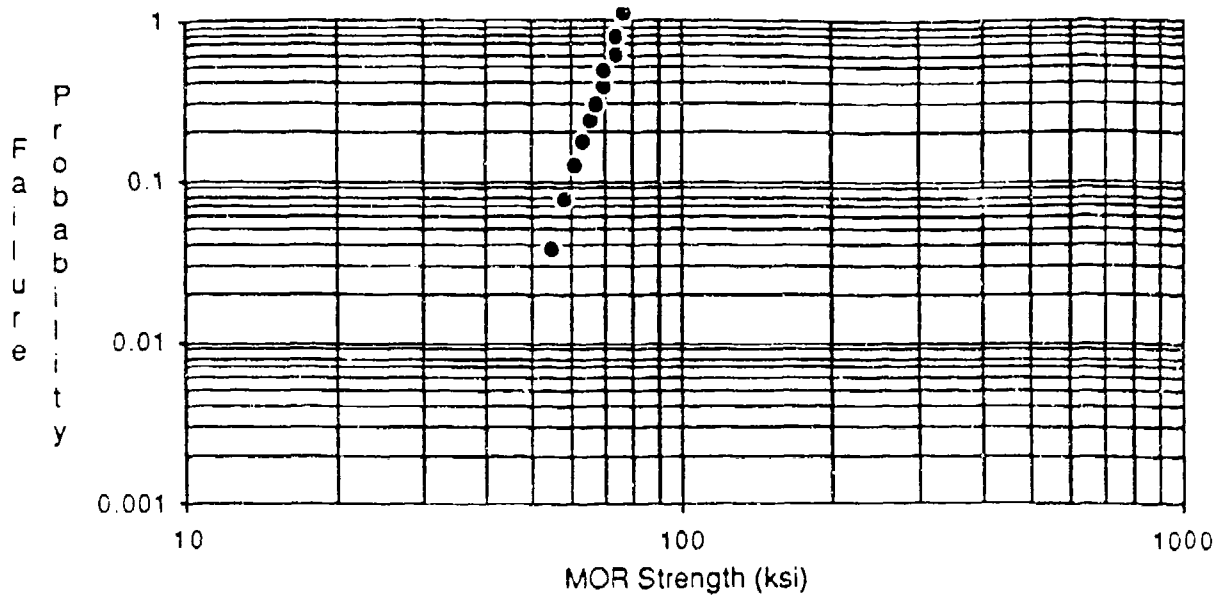
Modulus of rupture (four point bend) tests were conducted for ten different materials that were hot isostatically pressed (HIPped) after their initial uniaxial hot pressing. HIPping can be used to improve the strength and fracture toughness of hot-pressed ceramics through the closing of pores and voids. The MOR values from these specimens are compared with the values received from specimens cut from the panels before they were HIPped in Table 5.9. The HIP treatment had the greatest effect on the four whisker loaded materials. The strengths increased 10 to 20% after HIPping, evidently due to the healing of defects or porosity around the SiC whiskers by the HIP treatment. The platelet loaded material (484-4) experienced a decrease in MOR strength (37.9 to 29.6 kpsi (261 to 204 MPa)) after HIPping. The large SiC platelets evidently became even more effective

crack initiators after the HIP cycle, resulting in further reduction of the MOR strength. The other solid solution type ceramic materials all had only small changes in their MOR values due to HIPping. These changes can be explained by scatter in data inherent in ceramics. This result substantiates the quality of the as-hot-pressed panels.

Shown in Figure 5.6 is a Weibull curve for the advanced ceramic insulator $\text{AlN-0.4Y}_2\text{O}_3\text{-25 v/o SiC}_w$ (495-4H). This plate was made in a different pressing than the other $\text{AlN-0.4Y}_2\text{O}_3\text{-25 v/o SiC}_w$ plate (442-5). It had a higher average MOR strength, 66.6 kpsi (465 MPa) versus 56.8 kpsi (392 MPa), than the plate made earlier. This illustrates the range of properties and lot to lot variation that can be expected in advanced developmental ceramics.

Table 5.9 MOR Results for hot-pressed ceramic insulator materials with and without HIP processing.

Material	Condition	Code #	MOR Value MPa (Kpsi)	Material	Condition	Code #	MOR Value MPa (Kpsi)
Al ₂ O ₃ 0.25Y ₂ O ₃ -8ZrO ₂ -30w/o SiC(w)	Before HIP	483-3-MR-A	671 (97.3)	Al ₂ O ₃ 0.25Y ₂ O ₃ -8ZrO ₂ -30w/o SiC(w)	Before HIP	484-3-MR-A	516 (74.8)
		483-3-MR-B	621 (90.0)			484-3-MR-B	551 (79.2)
		Average:	546 (93.7)			Average:	534 (77.4)
	After HIP	483-3H-1	504 (72.1)	Al ₂ O ₃ 0.25Y ₂ O ₃ -8ZrO ₂ -30w/o SiC(w)	After HIP	484-3H-1	627 (89.8)
		483-3H-2	508 (72.7)			484-3H-2	567 (81.2)
		483-3H-3	494 (70.7)			484-3H-3	590 (84.4)
		483-3H-4	501 (71.7)			484-3H-4	586 (83.9)
	Average:	502 (71.6)	Average:	593 (84.8)			
	Before HIP	440-3-MR-A	678 (97.0)	Al ₂ O ₃ 0.25Y ₂ O ₃ -8ZrO ₂ -25w/o SiC(p)	Before HIP	484-4-MR-A	253 (36.7)
		440-3-MR-B	727 (104.0)			484-4-MR-B	269 (39.0)
Average:		703 (100.5)	Average:			261 (37.9)	
After HIP	440-3H-1	784 (112.2)	Al ₂ O ₃ 0.25Y ₂ O ₃ -8ZrO ₂ -25w/o SiC(p)	After HIP	484-4H-2	205 (29.4)	
	440-3H-2	742 (106.2)			484-4H-3	200 (28.6)	
	440-3H-3	773 (110.6)			484-4H-4	215 (30.7)	
	440-3H-4	784 (112.2)			Average:	203 (29.6)	
Average:	771 (110.3)	Average:	385 (55.9)				
Before HIP	440-6-MR-A	756 (109.7)	AlN-0.4w/o Y ₂ O ₃	Before HIP	442-4-MR-C	398 (57.7)	
	440-6-MR-B	745 (106.6)			442-4-MR-D	392 (56.8)	
	Average:	756 (108.2)			Average:	404 (57.8)	
	440-6H-1	742 (106.2)			442-4H-1	412 (58.9)	
	440-6H-2	710 (101.6)			442-4H-2	402 (57.6)	
440-6H-3	718 (102.8)	442-4H-3	402 (57.6)				
440-6H-4	743 (106.3)	442-4H-4	402 (57.6)				
Average:	728 (104.2)	Average:	405 (58.0)				
Before HIP	440-1-MR-A	440 (63.0)	AlN-0.4Y ₂ O ₃ -25w/o SiC(w)	Before HIP	442-5-MR-A	466 (67.6)	
	440-1-MR-B	396 (55.2)			442-5-MR-B	454 (65.8)	
	Average:	413 (59.1)			Average:	460 (66.7)	
After HIP	440-1H-1	415 (59.4)	AlN-0.4Y ₂ O ₃ -25w/o SiC(w)	After HIP	442-5H-1	522 (74.7)	
	440-1H-2	350 (50.1)					
	440-1H-4	416 (59.5)					
Average:	394 (56.3)	Average:	616 (89.4)				
Al ₂ O ₃ 0.4Y ₂ O ₃ -25w/o SiC(w)	Before HIP	435-4H-1	535 (76.5)	Al ₂ O ₃ 0.25Y ₂ O ₃ -8ZrO ₂	Before HIP	483-2-MR-A	616 (89.4)
		435-4H-2	427 (61.1)			483-2-MR-B	664 (95.3)
		435-4H-3	469 (67.1)			Average:	640 (92.9)
	435-4H-4	518 (74.1)	After HIP	483-2H-1	572 (81.8)		
	435-4H-5	484 (69.2)		483-2H-2	574 (82.1)		
	435-4H-6	439 (62.8)		483-2H-3	593 (83.5)		
	435-4H-7	484 (69.3)		483-2H-4	564 (80.7)		
	435-4H-8	515 (73.7)	Average:	573 (82.0)			
	435-4H-9	439 (62.8)					
	435-4H-10	405 (57.9)					
435-4H-11	381 (54.8)						
Average:	455 (65.6)						



Symbol	ID	Composition	Weibull Modulus	Design Allowable MOR Strength kpsi (MPa)	
				99.0%	99.9%
●	495-4H	AIN-0.4 Y ₂ O ₃ -25 v/oSiC _w	9.5	47.0 (328)	36.9 (258)

Figure 5.6 Weibull curve for advanced ceramic insulator AIN - 0.4 Y₂O₃ - 25 v/o SiC_w

The round of MOR testing tabulated in Table 5.9 marked the end of the first phase of panel fabrication and screening studies. The next phase of this work comprised the fabrication of larger panels, 8 x 8 in. (20 x 20 cm) in size. The range of compositions studied was narrowed somewhat by eliminating AlN-based ceramics, which had performed poorly in the mechanical and electrical screening tests. All of the ceramics investigated from this point on were either alumina-based or silicon nitride-based. The panels consolidated during the January to September 1989 time frame from these materials are listed in Table 5.10. The first hot pressing run occurred in mid-January 1989 on Series I of the silicon nitride matrix materials. All of the consolidated panels exhibited some degree of cracking. Replacement panels were pressed (at vendor expense) using excess backup raw material that had been mixed prior to the hot press run. In order to eliminate the cracking, the panels were ground flat after cold pressing (while they were in the "green" state) and the pressing load was not applied until the panel was at a higher temperature than previously used in order to increase the plasticity of the material and prevent cracking. Table 5.11 lists the processing conditions used in the hot-pressing of these panels. It must be kept in mind that these advanced ceramic insulating materials are being fabricated as

8 x 8 in. (20 x 20 cm) plates. Much data found in the literature for advanced ceramics is derived from 2 to 4 in. (5 to 10 cm) diameter discs. It requires less attention to processing details to achieve good results in these smaller sizes; the larger plates represent a much more rigorous optimization of process parameters.

Cutting maps were developed for the 8.0 in. (20 cm) square panels in order to cut the required number of test specimens from each plate. Two different types of cutting maps were utilized: type I (quantity = 23) which was the standard to produce all types of test specimens from and type II (quantity = 2) to produce property variation test specimens. Schematics of the two types of cutting maps are shown in Figures 5.7 and 5.8 along with descriptions of the various test specimens. These cutting plans allow for enough MOR bars to be cut from each panel in order to establish a Weibull modulus value for each material. The type II panels were designed to measure the amount of property variation (topology of rupture and fracture toughness) across typical panels. Two type II panels, one air-enforced and one reinforced with whiskers, were fabricated. The mechanical and physical testing of all type II panels will be described in Chapter 6.

Because of the availability of two different whiskers (different in terms of diameter, apparent chemistry and crystal habit), and the different strength/toughness values reported by other investigators using these different whiskers, it was decided to compare the SiC whiskers made by American Matrix Inc. (AMI) of Knoxville, TN, with those made by Advanced Composite Material Company (ACMC) of Greer, SC. The whisker/matrix with the best combination of fracture toughness, modulus of rupture strength and voltage holdoff strength would eventually be chosen in order to optimize performance as bore insulators for railguns. The SiC whisker reinforced panels made per the program had contained AMI whiskers.

Duplicate panels were included for some of the more promising materials to confirm performance levels and to provide additional data for property variation.

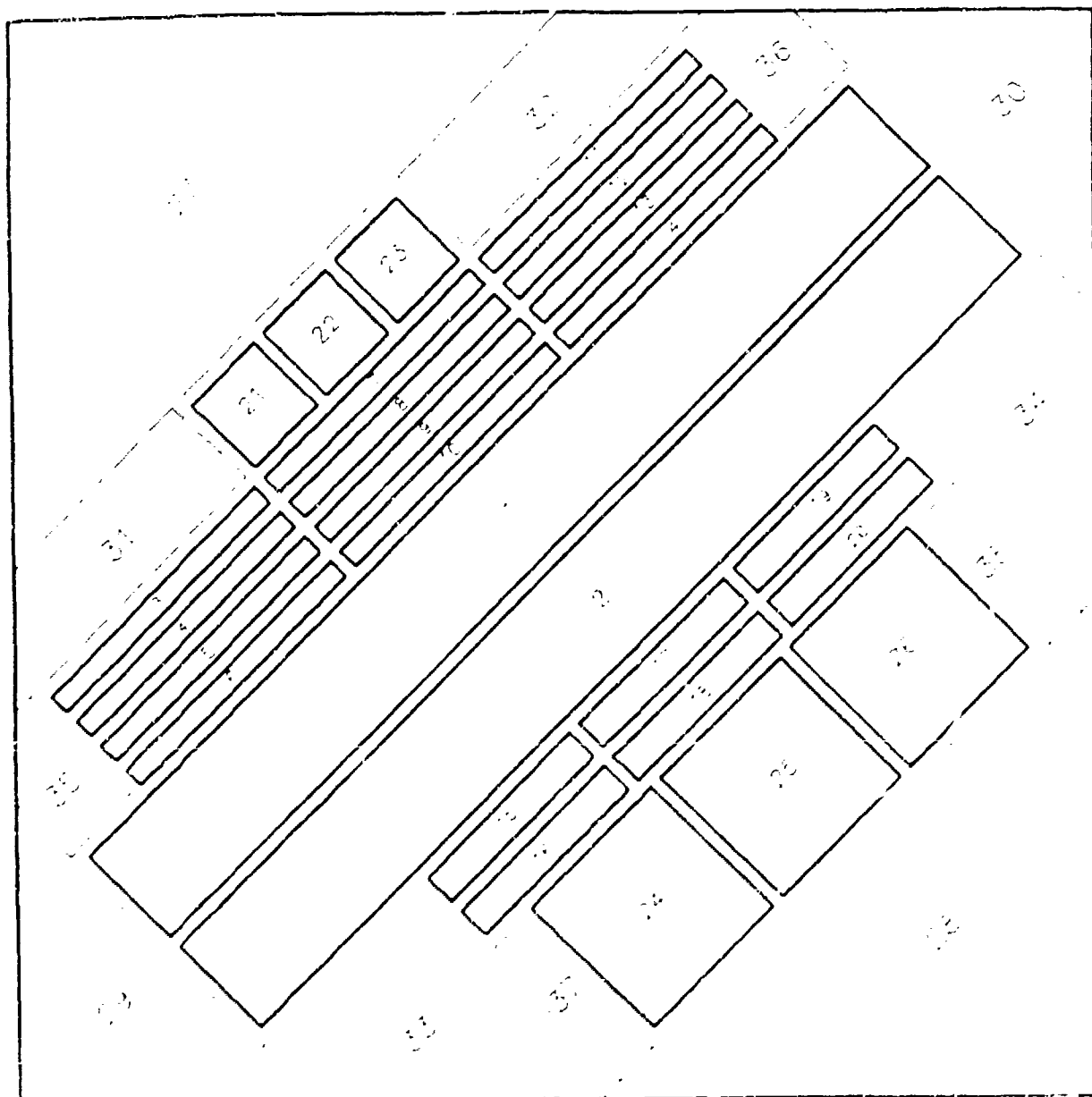
The Si₃N₄ material is reaction bonded during the hot pressing. The process involves the reaction of silicon (Si) metal powder along with aluminum (Al₂O₃), zirconium (ZrO₂) and silicon carbide (SiC) whisker into forms where they are heated in a nitrogen atmosphere around a matrix and convert the Si metal to Si₃N₄. The reaction bonded joints are produced in the "green" state and are very weak. They were not fired to assure flatness and then loaded into the hot pressing final conditions to complete the reaction.

TABLE 5.10 - 8x8 In. (20x20 cm) Ceramic Panels Fabricated January to September 1989

Compo- sition No.	Panel ID	Composition	Purpose
Alumina - 8% Zirconia / Chromia			
1.	4-253-4	$Al_2O_3-8.0ZrO_2-0.25Y_2O_3$	Measure the effect of chromia additions on mech. prop's of alumina- 8% zirconia
2	4-253-3	$Al_2O_3-8.0ZrO_2-0.25Y_2O_3-2.0Cr_2O_3$	
3	4-253-1	$Al_2O_3-8.0ZrO_2-0.25Y_2O_3-5.0Cr_2O_3$	
3.	4-253-5	$Al_2O_3-8.0ZrO_2-0.25Y_2O_3-5.0Cr_2O_3$	
4.	4-253-2	$Al_2O_3-8.0ZrO_2-0.25Y_2O_3-8.0Cr_2O_3$	
4.	4-253-6	$Al_2O_3-8.0ZrO_2-0.25Y_2O_3-8.0Cr_2O_3$	
Alumina - 8% Zirconia / SiC _w			
5.	4-255-1	$Al_2O_3-8.0ZrO_2-0.25Y_2O_3/30\%SiC_w$	Compare effects of whisker vs chromia additions on Alumina-Zirconia
5	4-255-4	$Al_2O_3-8.0ZrO_2-0.25Y_2O_3/30\%SiC_w$	
6	4-255-2	$Al_2O_3-8.0ZrO_2-0.25Y_2O_3-5Cr_2O_3/25\%SiC_w$	
6	4-255-3	$Al_2O_3-8.0ZrO_2-0.25Y_2O_3-5Cr_2O_3/25\%SiC_w$	
Alumina - 15% Zirconia / SiC _w			
7	269-1	$Al_2O_3-15.0ZrO_2-15\%SiC_w$ (ACMO SiC _w)	Compare whiskers from two different sources, and measure effect of varying loading fractions for Alumina - 15% Zirconia
8	270-7	$Al_2O_3-15.0ZrO_2-25\%SiC_w$ (ACMO SiC _w)	
9	AMI908-1	$Al_2O_3-15.0ZrO_2-15\%SiC_w$ (AMI SiC _w)	
9	AMI908-3	$Al_2O_3-15.0ZrO_2-15\%SiC_w$ (AMI SiC _w)	
Alumina - 5% Zirconia - 5% Chromia - SiC _w			
10	4-329-5	$Al_2O_3-5ZrO_2-0.25Y_2O_3-5Cr_2O_3$	Measure the effect of various whisker loading fractions on the mech. prop's of Alumina - 5% Zirconia - 5% Chromia
11	4-329-3	$Al_2O_3-5ZrO_2-0.25Y_2O_3-5Cr_2O_3-15\%SiC_w$	
11	4-329-4	$Al_2O_3-5ZrO_2-0.25Y_2O_3-5Cr_2O_3-15\%SiC_w$	
12	4-329-1	$Al_2O_3-5ZrO_2-0.25Y_2O_3-5Cr_2O_3-25\%SiC_w$	
12	4-329-2	$Al_2O_3-5ZrO_2-0.25Y_2O_3-5Cr_2O_3-25\%SiC_w$	
Silicon Nitride - 2% Yttria - SiC _w			
13	4-268-3	$Si_3N_4-2.0Y_2O_3-0.25Al_2O_3$	Effect of whisker additions on silicon nitride - 2% Yttria - (HF washed whiskers)
14	4-268-4	$Si_3N_4-2.0Y_2O_3-0.25Al_2O_3-5\%SiC_w$	
15	4-268-5	$Si_3N_4-2.0Y_2O_3-0.25Al_2O_3-10\%SiC_w$ (HF)	
16	4-268-7	$Si_3N_4-2.0Y_2O_3-0.25Al_2O_3-10\%SiC_w$	
17	4-268-6	$Si_3N_4-2.0Y_2O_3-0.25Al_2O_3-15\%SiC_w$	
Silicon Nitride - 8% Yttria - SiC _w			
18	4-268-5	$Si_3N_4-8.0Y_2O_3-1.0Al_2O_3$	Measure the effect of varying whisker additions on the mech. prop's of silicon nitride - 8% Yttria
18	4-347-2	$Si_3N_4-8.0Y_2O_3-1.0Al_2O_3$	
19	4-268-4	$Si_3N_4-8.0Y_2O_3-1.0Al_2O_3-5\%SiC_w$	
20	4-268-3	$Si_3N_4-8.0Y_2O_3-1.0Al_2O_3-10\%SiC_w$	
21	4-268-1	$Si_3N_4-8.0Y_2O_3-1.0Al_2O_3-15\%SiC_w$	
21	4-268-2	$Si_3N_4-8.0Y_2O_3-1.0Al_2O_3-15\%SiC_w$ (HF)	
22	4-268-7	$Si_3N_4-8.0Y_2O_3-1.0Al_2O_3-20\%SiC_w$	
22	4-268-8	$Si_3N_4-8.0Y_2O_3-1.0Al_2O_3-20\%SiC_w$	
23	4-268-9	$Si_3N_4-8.0Y_2O_3-1.0Al_2O_3-25\%SiC_w$	
23	4-268-10	$Si_3N_4-8.0Y_2O_3-1.0Al_2O_3-25\%SiC_w$	

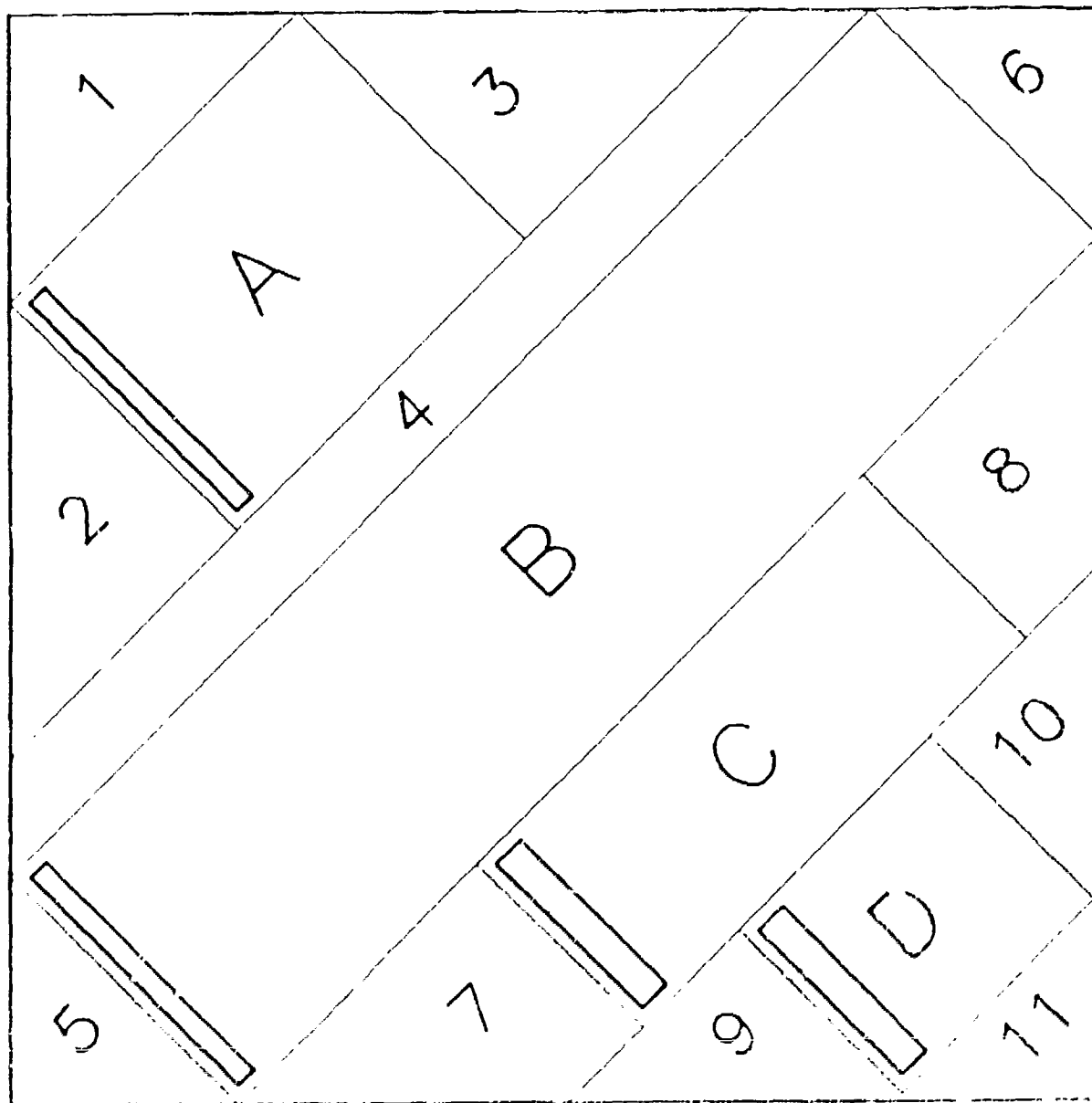
TABLE 5.11 - Processing Conditions Used to Hot-Press 8x8 in. (20x20 cm) Panels

Composition No.	Panel ID	Pressing Date	Max. Temp (°C)	Time at Max. Temp (min.)	Max Pressure (psi)	Time at Max. Pressure (min)	Heating Rate (°C/min)	Total Cycle Time (hr/min)
Alumina - 8% Zirconia / Chromia								
1.	4-253-4	3-4-89	1570	95	3000	125	4	9/45
2	4-253-3	3-4-89	1570	95	3000	125	4	9/45
3.	4-253-1	3-4-89	1570	95	3000	125	4	9/45
3.	4-253-5	3-4-89	1570	95	3000	125	4	9/45
4.	4-253-2	3-4-89	1570	95	3000	125	4	9/45
4.	4-253-6	3-4-89	1570	95	3000	125	4	9/45
Alumina - 8% Zirconia / SiC _x								
5.	4-255-1	3-7-89	1700	20	3500	230	2	10/20
5	4-255-1	3-7-89	1700	20	3500	230	2	10/20
6.	4-255-2	3-7-89	1700	20	3500	230	2	10/20
6	4-255-2	3-7-89	1700	20	3500	230	2	10/20
Alumina - 15% Zirconia / SiC _x								
7.	269-1							
8	270-7							
9	AMI008-1	Proprietary to American Matrix Inc						
9	AMI008-3	Proprietary to American Matrix Inc						
Alumina - 5% Zirconia - 5% Chromia / SiC _x								
10	4-329-5	7-27-89	1740	190	5300	180	3	13/25
11	4-329-3	7-27-89	1740	190	5300	180	3	13/25
11	4-329-4	7-27-89	1740	190	5300	180	3	13/25
12	4-329-1	7-27-89	1740	190	5300	180	3	13/25
12	4-329-2	7-27-89	1740	190	5300	180	3	13/25
Silicon Nitride - 2% Yttria / SiC _x								
13	4-268-3	4-1-89	1775	180	3500	270	2	10/5
14	4-268-4	4-1-89	1775	180	3500	270	2	10/5
15	4-268-5	4-1-89	1775	180	3500	270	2	10/5
16	4-268-7	4-1-89	1775	180	3500	270	2	10/5
17	4-268-1	4-1-89	1775	180	3500	270	2	10/5
Silicon Nitride - 8% Yttria / SiC _x								
18	4-265-5	1-27-89	1770	180	3500	350	2	11/5
19	4-265-2	1-27-89	1765	180	2900	285	2	13/20
19	4-265-4	1-27-89	1770	180	3500	350	2	11/5
20	4-265-3	1-27-89	1770	180	3500	350	2	11/5
21	4-265-6	1-17-89	1765	120	3500	150	2	10/5
21	4-265-1	1-27-89	1770	180	3500	350	2	11/5
22	4-265-7	1-27-89	1770	180	3500	350	2	11/5
22	4-265-2	1-27-89	1770	180	3500	350	2	11/5
22	4-265-3	1-27-89	1770	180	3500	350	2	11/5
22	4-265-4	1-27-89	1770	180	3500	350	2	11/5
22	4-265-5	1-27-89	1770	180	3500	350	2	11/5
22	4-265-6	1-27-89	1770	180	3500	350	2	11/5
22	4-265-7	1-27-89	1770	180	3500	350	2	11/5



Number	Description	Size in inches (in plane)
1-3	Ballpin Balls	8.000 x 0.649
4-14	Mold Bars	0.158 x 2.559
15-20	SI TB Bars	0.250 x 1.500
21-23	Optical Metallography	0.65 x 0.65
24-26	Arc Test Specimens	1.59 x 1.59
7-11	Remnants	misc.

Figure 5.7 Ceiling map (reproduced from [1]).



Group	Description	Size in Inches (in plane)
A	MOR Bars (quantity = 12)	2.996 x 2.754
B	MOR Bars (as many as possible)	9.5 x 2.759
C	SENB Bars (quantity = 12)	4.056 x 1.760
D	SENB Bars (quantity = 6)	2.000 x 1.790
1-11	Remnants	misc.

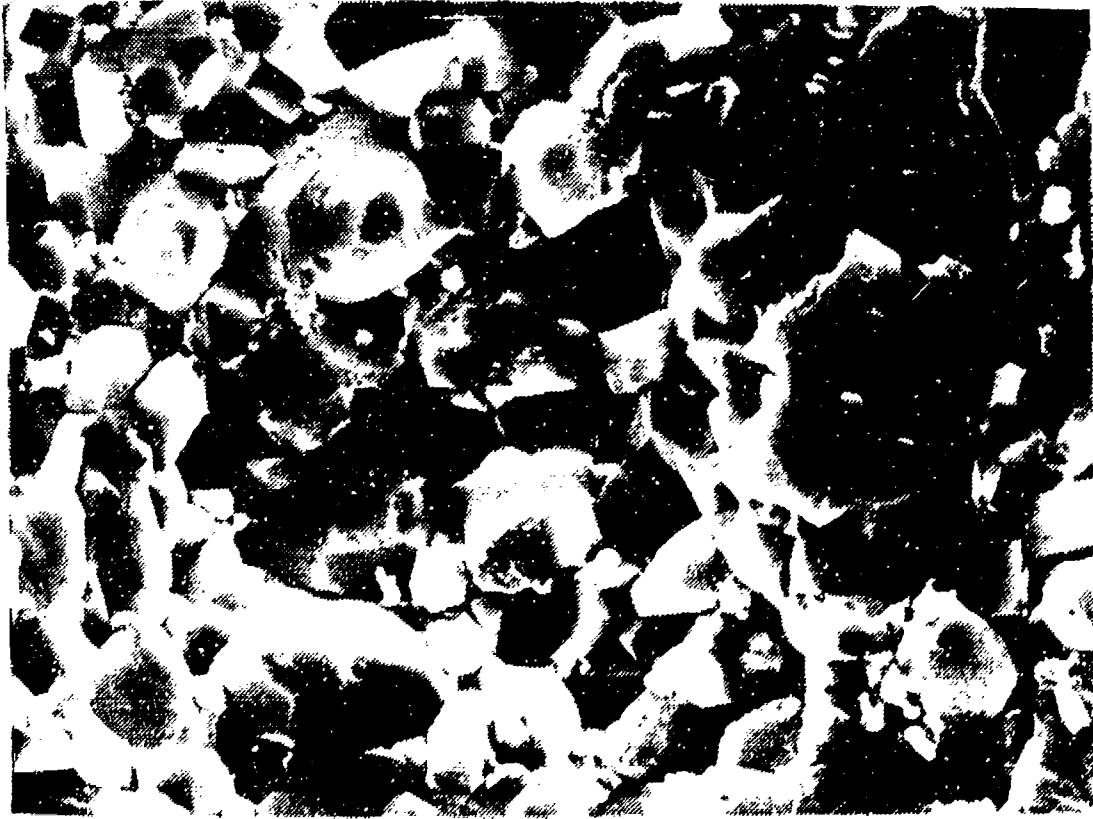
Figure 5b Cutting map for ceramic plates, type 2

Shown in Figures 5.9 and 5.10 are representative micrographs of the two compositions that were selected to be scaled up in size during the next portion of the program. They are alumina-zirconia-chromia and SiC whisker reinforced silicon nitride. The explanation for their good combination of flexural strength and fracture toughness is explained by their microstructures as detailed in the figures. The mechanical and electrical properties of these materials are examined in detail in Chapter 6.

The last materials fabricated in this program were three blocks scaled-up in size. The purpose of this was to see whether the mechanical properties observed in the 8 x 8 x 0.375 in. (20 x 20 x 0.635 cm) panels could be reproduced in a form with dimensions comparable to those which would be used in a full-scale railgun insulator segment. The compositions of these blocks, measuring 4 x 19.5 in. (10.2 x 20.4 x 3.8 cm) in size for 4-365-2 and 4-366-2, and 1.5 x 4 x 19.7 inches (3.8 x 10 x 50 cm) for 4-392-1 are shown in Table 5.12 along with measurements of their density. The blocks evidenced no cracking and had a good surface finish. After hot press consolidation followed by HIPping the blocks were ground to a thickness of 1.25 in. (3.18 cm) in order to remove any surface imperfections created during the fabrication procedure. Density measurements were similar to those measured on thinner panels consolidated previously in the program indicating that the blocks had achieved full density. The blocks were machined into mechanical, electrical, and metallographic test specimens. The test results on these materials are presented in Chapter 6.

TABLE 5.12 . Compositions and Densities of Two Scaled-Up Thickness Blocks of Advanced Ceramic Composite Insulators For Electromagnetic Launchers

ID	Composition (wt %)	Measured Density (g/cc)	% Theoretical Density
4-365-2	Al ₂ O ₃ , 5.0ZrO ₂ , 0.25Y ₂ O ₃ , - 5.0Cr ₂ O ₃	4.126	99.4
4-366-2	Si ₃ N ₄ , 8.0Y ₂ O ₃ , 1.0Al ₂ O ₃ , - 15.0SiC _w	3.265	99.6
4-392-1	Al ₂ O ₃ , 5.0ZrO ₂ , 0.25Y ₂ O ₃ , - 5.0Cr ₂ O ₃	4.134	99.6



10 microns

Features:

- Fine Grained (10 microns)
- Fully Dense (100%)
- Mixed-Mode, High Energy Fracture
- Uniform Distribution of Chromia (Revealed by X-Ray EDS Mapping)

Implications of Features:

- Good Process Control
- Good Combination of Strength and Fracture Toughness
- Superior Electrical Properties (Due to Chromia Dispersion)

Figure 5.9 Photomicrograph of typical microstructure of Al₂O₃ 80.7%, 5.0Cr₂O₃, 0.25Y₂O₃, advanced ceramic insulator material and explanation and implications of features. (1500X)



10 microns

Features:

- Fine Grained (~5 microns)
- Fully Dense (~100%)
- Uniform Distribution of Whiskers
- Minimal Whisker/Matrix Bonding
- Second Phases at Grain Boundaries

Implications of Features:

- Good Process Control
- Whiskers Can Pull Out and Blunt Cracks, Improving Toughness.
- SiC Whiskers Don't Touch, Improving Electrical Properties
- High Strength

Figure 5.10 Photomicrograph of typical microstructure of $50\text{Al}_2\text{O}_3$, 6BY_2 , $1.0\text{Al}_2\text{O}_3$, $15\% \text{SiC}$, advanced ceramic insulator material and explanation and implications of features. (1500X)

This page is intentionally left blank

TESTING OF MATERIALS

The testing of the advanced ceramic insulating materials and the conductor materials took place at four major locations:

- SPARTA Inc. materials research laboratories located in Del Mar, California and San Diego, California; metallography, density measurements, modulus of rupture testing, and scanning electron microscopy (SEM)
- University of California at Los Angeles (UCLA), Los Angeles, California; Materials Science and Engineering Department, group headed by Dr. Jenn Ming Yang, density measurements, fracture toughness measurements, elemental analysis by EDAX, optical metallography, and scanning electron microscopy
- Texas Tech University (TTU), Lubbock, Texas; Department of Electrical Engineering, group headed by Dr. Kris Kristiansen; stationary arc testing of insulators and conductors (single pulse and repeated)
- U.S. Army Armament Research, Development and Engineering Center (ARDEC), Picatinny Arsenal, New Jersey, group headed by Greg Colombo, railgun testing in HINTIME system.

The modulus of rupture (MOR), fracture toughness, density, arc test, and metallographic samples were cut from the advanced ceramic insulator panels at BOMAS Machine Specialties, Inc. in Somerville, Massachusetts. This company has had a large amount of experience in the preparation of mechanical test specimens from ceramic materials. The quality of data from mechanical tests of ceramics is very dependent upon the quality of the test specimens. BOMAS was able to produce specimens with a minimum of surface defects, allowing screening tests to be accurately conducted with a minimum number of specimens (2 MOR specimens and six fracture toughness specimens per panel).

The two University groups (UCLA and TTU) were chosen because of their specific knowledge and experience base in the area of advanced ceramics and high current arc testing respectively. Both groups included a group of graduate students under the direction of an

experienced Professor to carry out the tests and aid SPARTA in interpreting the data. The FLINT EML system at ARDEC was chosen because of its initial availability and ease of changeout for test of insulator side wall specimens.

6.1 Mechanical Testing

Modulus of rupture (MOR) and fracture toughness (SENB type) specimens cut from the 8 x 8 x 0.375 in. (20 x 20 x 0.95 cm) hot-pressed ceramic plates listed in Table 5.9 were subjected to mechanical testing. The data from these tests is summarized in Table 6.1. The Weibull modulus values shown in this table (indicative of spread in property values) are very high, among the highest we have ever measured in any ceramic materials. This indicates good blending of powders and full consolidation of the panels.

The strength values (averages of 12 tests for each material) for the alumina-based materials were moderately high, but the SiC whisker reinforced alumina materials were lower in strength. The fracture toughness values (averages of six tests per panel) were very high, 7.2 kpsi·in^{1/2} (7.9 MPa·m^{1/2}), with the whisker reinforced materials the highest of all the panels. The trends seem to indicate that chromia contents above 10% lower the MOR strength, but do not decrease the Weibull modulus. The fracture toughness values do not seem to follow any trend with chromia content.

Mechanical property tests for the nine silicon nitride matrix panels revealed especially high strength, consistency, and toughness. A summary of the data is included in Table 6.1. As can be seen, very high average strength 91 to 114 kpsi (628 to 783 MPa) values were obtained, as well as high fracture toughness values (all above 8.2 kpsi·in^{1/2} (9 MPa·m^{1/2})). These nine plates were made in three different pressings. Panels 258-5 and 258-6 received better powder and whisker blending and thus had significantly higher Weibull modulus values than the panels in pressing 265. The same careful blending and mixing operations were then repeated in pressing 340, with even better MOR results.

Mechanical property test data of specimens from the two specially fabricated alumina panels with 35% silicon carbide whiskers are included in Table 6.1. Exceptionally high toughness values of over 9.1 kpsi (10 MPa·m^{1/2}) were measured, however, the modulus of rupture values (71 kpsi [500 MPa]) were lower than expected. It is thought that the processing parameters were not ideal because the plates that were made were much larger than those made previously (by other groups) with this composition and several iterative hot pressing runs would be needed to arrive at the correct pressing parameters. Two silicon carbide whisker reinforced alumina panels using 15 and 25% whiskers were consolidated using whiskers from a different source than before, Advanced Composite Materials Corporation (ACMC). The new ACMC whiskers were 0.5 to 0.8 microns in diameter (compared to the previously used American Matrix 1.2 to 1.5 micron diameter whiskers), are primarily alpha phase in structure (compared with the AMI beta phase whiskers), and have received more attention by the ceramic matrix composite community. They are only one quarter to one half as strong as the previously used whisker, however. The ACMC

TABLE 6.1 - Mechanical Test Results from 8 x 8 in. (20 x 20 cm) Ceramic Panels

Composition No.	Panel ID	Composition	Average MOR Strength kpsi (MPa)	Weibull Modulus	Average Fracture Toughness kpsi·in ^{1/2} (MPa·m ^{1/2})
Alumina - 8% Zirconia / Chromia					
1.	4-253-4	Al ₂ O ₃ -8.0ZrO ₂ -0.25Y ₂ O ₃	91.8 (633)	25.0	5.81 (6.38)
2	4-253-3	Al ₂ O ₃ -8.0ZrO ₂ -0.25Y ₂ O ₃ - 2.0Cr ₂ O ₃	93.1 (642)	16.9	5.21 (5.72)
3.	4-253-1	Al ₂ O ₃ -8.0ZrO ₂ -0.25Y ₂ O ₃ - 5.0Cr ₂ O ₃	94.37 (651)	22.5	5.08 (5.58)
3.	4-253-5	Al ₂ O ₃ -8.0ZrO ₂ -0.25Y ₂ O ₃ - 5.0Cr ₂ O ₃	85.56 (590)	24.1	5.72 (6.29)
4.	4-253-6	Al ₂ O ₃ -8.0ZrO ₂ -0.25Y ₂ O ₃ - 8.0Cr ₂ O ₃	80.45 (555)	20.5	5.83 (6.41)
Alumina - 8% Zirconia / SiC _w					
5.	4-255-1	Al ₂ O ₃ -8.0ZrO ₂ -0.25Y ₂ O ₃ / 30%SiC _w	64.95 (448)	13.0	6.94 (7.63)
6.	4-255-2	Al ₂ O ₃ -8.0ZrO ₂ -0.25Y ₂ O ₃ -5Cr ₂ O ₃ / 25%SiC _w	50.51 (348)	15.0	7.15 (7.86)
Alumina - 15% Zirconia / SiC _w					
7.	269-1	Al ₂ O ₃ - 15.0 ZrO ₂ / 15%SiC _w (ACMC SiC _w)	83.2 (574)	9.7	6.5 (7.1)
8.	270 7	Al ₂ O ₃ - 15.0 ZrO ₂ / 25%SiC _w (ACMC SiC _w)	85.4 (589)	10.2	6.6 (7.3)
9.	AM1008-1	Al ₂ O ₃ - 15.0 ZrO ₂ / 35%SiC _w (AMI SiC _w)	72.5 (500)	14.5	9.0 (9.9)
9	AMI008-3	Al ₂ O ₃ - 15.0 ZrO ₂ / 35%SiC _w (AMI SiC _w)	74.5 (514)	25.2	9.3 (10.2)
Alumina - 5% Zirconia - 5% Chromia / SiC _w					
10.	4-329-5	Al ₂ O ₃ -5ZrO ₂ -0.25Y ₂ O ₃ -5Cr ₂ O ₃ /	89.0 (614)	25.8	6.2 (6.8)
10.	4-329-5H	Al ₂ O ₃ -5ZrO ₂ -0.25Y ₂ O ₃ -5Cr ₂ O ₃ /	88.5 (610)	23.6	6.2 (6.8)
11.	4-329-3	Al ₂ O ₃ -5ZrO ₂ -0.25Y ₂ O ₃ -5Cr ₂ O ₃ /15%SiC _w	56.3 (388)	12.6	5.4 (5.9)
11	4-329-4	Al ₂ O ₃ -5ZrO ₂ -0.25Y ₂ O ₃ -5Cr ₂ O ₃ /15%SiC _w	54.7 (377)	17.0	5.4 (5.9)
11	4-329-4H	Al ₂ O ₃ -5ZrO ₂ -0.25Y ₂ O ₃ -5Cr ₂ O ₃ /15%SiC _w	49.5 (341)	16.0	6.1 (6.7)
12.	4-329-1	Al ₂ O ₃ -5ZrO ₂ -0.25Y ₂ O ₃ -5Cr ₂ O ₃ /25%SiC _w	74.4 (513)	18.1	5.2 (5.7)
12	4-329-1H	Al ₂ O ₃ -5ZrO ₂ -0.25Y ₂ O ₃ -5Cr ₂ O ₃ /25%SiC _w	63.9 (441)	8.8	6.2 (6.8)
12	4-329 2	Al ₂ O ₃ -5ZrO ₂ -0.25Y ₂ O ₃ -5Cr ₂ O ₃ /25%SiC _w	69.1 (476)	11.6	5.7 (6.3)
Silicon Nitride - 8% Yttria / SiC _w					
18	4-265-5	Si ₃ N ₄ -8.0Y ₂ O ₃ -1.0Al ₂ O ₃	91.5 (631)	10.0	5.3 (5.8)
18	4-340-2	Si ₃ N ₄ -8.0Y ₂ O ₃ -1.0Al ₂ O ₃	127.8 (881)	20.6	8.4 (9.2)
19	4-265-4	Si ₃ N ₄ -8.0Y ₂ O ₃ -1.0Al ₂ O ₃ - 5%SiC _w	92.4 (637)	8.7	9.4 (10.3)
20	4-265-3	Si ₃ N ₄ -8.0Y ₂ O ₃ -1.0Al ₂ O ₃ - 10%SiC _w	102.9 (709)	8.8	9.7 (10.7)
20	4-258-6	Si ₃ N ₄ -8.0Y ₂ O ₃ -1.0Al ₂ O ₃ - 10%SiC _w	113.6 (783)	49.3	8.6 (9.4)
21	4-265-1	Si ₃ N ₄ -8.0Y ₂ O ₃ -1.0Al ₂ O ₃ - 10%SiC _w	91.1 (628)	9.1	8.6 (9.5)
22	4-265-2	Si ₃ N ₄ -8.0Y ₂ O ₃ -1.0Al ₂ O ₃ - 15%SiC _w	93.5 (666)	8.1	8.1 (8.9)
22	4-258-5	Si ₃ N ₄ -8.0Y ₂ O ₃ -1.0Al ₂ O ₃ - 15%SiC _w	112.8 (778)	35.1	8.6 (9.5)
22	4-340-3	Si ₃ N ₄ -8.0Y ₂ O ₃ -1.0Al ₂ O ₃ - 15%SiC _w	119.6 (829)	25.2	8.3 (9.1)
13	4-268-3	Si ₃ N ₄ -2.0Y ₂ O ₃ -0.25Al ₂ O ₃	101.4 (700)	7.1	8.4 (9.2)

* Materials with an H after the panel ID number have been HIPped after hot pressing

whiskers also have lower electrical conductivity. The panels were made in order to compare properties with panels made by other laboratories from these whiskers and to see the effect of the different conductivity whiskers on the electrical performance of the panels.

Shown in Figure 6.1 are the results of the mechanical property tests conducted on the specimens cut from the panels. Their Weibull curves, along with design allowable strengths, are also included. The flexural strengths and fracture toughness values measured for the 15% silicon carbide whisker loaded material agreed well with those advertised by APMC (Advanced Composite Materials Corporation), the company that makes the whiskers and blends the powders for sale to consolidation companies. The properties of the 25% whisker loaded material were about 15% below the values expected, however. This decrease was caused by the presence of the combination of a number of over-sized whiskers and iron-chromium impurities which acted as failure initiation sites.

The high toughness values exhibited by both materials were a result of the good distribution of whiskers and a proper level of whisker/matrix bonding which allowed the whiskers to deflect and blunt cracks, thereby increasing toughness. The defects noted above did affect the toughness of the 25% loaded material, however, as its toughness should have been closer to $8.1 \text{ kpsi}\cdot\text{in}^{1/2}$ ($8.8 \text{ MPa}\cdot\text{m}^{1/2}$), instead of the 6.5 (7.1) value measured.

Shown in Figure 6.2 is an optical micrograph of a polished cross-section of the 25% loaded material (4-270-7) revealing the presence of selected over-sized whiskers. Shown in Figure 6.3 is a typical scanning electron microscope view of the fracture surface of the same material revealing the fiber pull-out at the fracture surface which resulted in good fracture toughness.

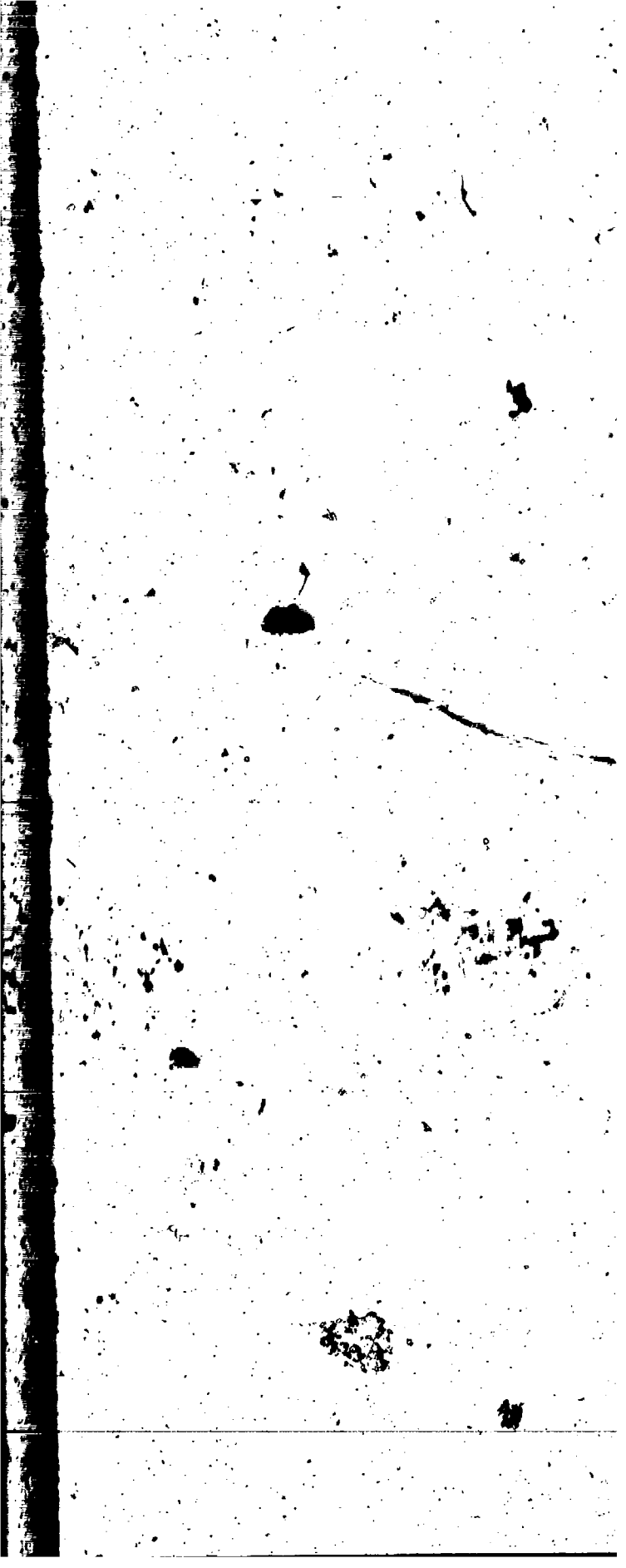




Figure 6.2 Typical optical microstructure of 25% SiC whisker (ACMC) reinforced alumina material (1000X)

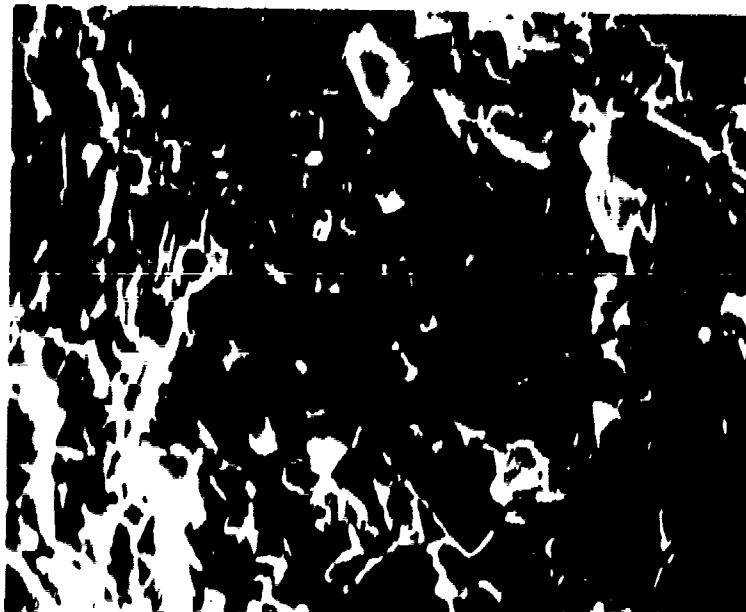


Figure 6.3 Typical fracture surface of 25% silicon carbide whisker (ACMC) reinforced alumina material revealing whisker pull out (5000X)

Panels AMI008-1 and -3 of the 35% SiC whisker loaded composition were purchased as-consolidated from AMI. Very high toughness values (approximately $9.3 \text{ kpsi}\cdot\text{in}^{1/2}$ ($10 \text{ MPa}\cdot\text{m}^{1/2}$)) were measured, the highest observed in alumina-based insulators during this program. The strength values (about 73 kpsi [500 MPa]), however, were somewhat low. Scanning electron microscopy examination of the failure surfaces of modulus of rupture bars was conducted. The material exhibited small grain size (less than 5 microns) which leads to good strength and toughness. The whiskers in one specimen (AMI-008-3) were well distributed, but the other specimen (AMI-008-1) exhibited clumps of whiskers which led to its lower Weibull modulus (15 vs. 25 for the -3 specimen). In both specimens there was a mixture of pulled out whiskers and bonded whiskers at the fracture surfaces. This indicates that the pressing conditions used too high a temperature or too long a period of time, resulting in slightly too much whisker-matrix interaction. This reduced the strength of the material as cracks did not run around the whiskers but went through them. Thus, with optimized mixing and consolidation parameters, better properties could have resulted.

Overall, the silicon nitride - 8% yttria panels showed the best mechanical properties of any of the compositions studied. These panels are listed at the bottom of Table 6.1. The mechanical properties measured for these panels were outstanding. The results from panel 4-258-6 are especially noteworthy. This panel showed an average MOR strength of 113.6 kpsi (783 MPa), a fracture toughness of $8.6 \text{ kpsi}\cdot\text{in}^{1/2}$ ($9.4 \text{ MPa}\cdot\text{m}^{1/2}$), and a Weibull modulus of 40.3. This combination of properties is among the best ever reported in the scientific literature for a ceramic material. It was important to understand what microstructural features led to the strength, toughness, and Weibull properties measured in all the silicon nitride-based materials. The microstructures of the silicon nitride materials were studied both by optical metallography and by SEM observation of fracture surfaces. The key microstructural observations include:

- Very small grain size, less than 5 microns. This leads to reduced flaw size, narrow distribution of existing flaws, high strength, high toughness and reliability
- Uniform distribution of whiskers. This results in isotropic in-plane properties. Whiskers blunt and deflect cracks which raises the toughness of the material.
- No detectable porosity, resulting in high strength.
- Whiskers have been broken out at the surface, leaving troughs behind. This indicates that the whiskers are not tightly bonded to the matrix. This permits cracks to be blunted and to lose energy as they reach whiskers, increasing toughness through fiber pull out.
- The use of second phase toughening (through the addition of the yttria and alumina) results in full density and high strength through the formation of a glassy grain boundary phase that cannot be seen at the magnification of the micrograph.

This combination of small grain size, good distribution of whiskers, high density, proper amount of whisker/matrix bonding, and glassy grain boundary phase led to the outstanding strength, toughness, and property spread (Weibull modulus) properties of the silicon nitride matrix advanced ceramic insulator materials. These microstructural characteristics were planned through a combination of proper: chemistry of the matrix, whisker and whisker loading, and processing conditions to arrive at the desired mechanical properties. This process is called "microstructural tailoring", and it enabled the development of the high-quality material which was produced.

A direct comparison between the as-hot pressed and hot pressed and HIPped properties was carried out in the alumina - 5% zirconia - 5% chromia series. It was thought that HIPping might be necessary in order to produce the full-scale ceramic composite insulators for electromagnetic launchers. Thus these tests were used to measure the properties obtained from materials processed in the same fashion which might be used for larger scale railgun insulators.

The test specimens were measured and examined optically to detect any gross flaws due to grinding prior to testing. Testing of the modulus of rupture (MOR) bars and fracture toughness specimens (SENB type) from each panel were completed and are summarized in Table 6.1. As always, an adequate number of MOR bars (12) was tested from each panel to establish a valid Weibull modulus for each material. The fracture surfaces of selected MOR bars was examined with a scanning electron microscope (SEM) to characterize the microstructure of the insulator materials and determine if the improved processing parameters utilized during the preparation of the panels was reflected in the microstructure. The density of the panels was also measured.

The results listed in Table 6.2 show that the tested panels compare very favorably with prior results. The tested panels demonstrated that:

- Improvements in properties can be obtained from slight chemistry changes and improvements in mixing/blending techniques
- The mechanical properties obtained on prior panels could be duplicated (or improved) on panels made using different lots of starting materials and different hot pressing runs.

Both of these goals were met and thus next step in the program, scale-up to sizes suitable for use in larger scale guns, was begun.

It can be seen the HIPping resulted in slight strength decreases (and toughness increases) for the whisker containing alumina materials but did not change the properties of the alumina material with only chromia added. The whisker containing alumina specimens were inferior to the alumina-chromia (with no whisker) material originally, and thus the alumina/chromia/whisker system was dropped from the development cycle. This decision was supported by the rather poor electrical performance of the SiC whisker reinforced alumina material as described in Section 6.2.

Fabrication of mechanical, electrical and metallographic test specimens from the first two scaled-up thickness blocks of advanced ceramic composite insulator materials was begun after the testing of the 8 x 8 in. (20 x 20 cm) panels was completed. Because the properties of advanced ceramics are so process-sensitive, this scale-up was necessary to ensure that the good results seen in the 0.25 inch (0.64 cm) thick panels could be repeated in pieces of material that were closer in size to real railgun insulators. The compositions of the consolidated blocks, measuring 4 x 8 x 1.5 in. (10.2 x 20.4 x 3.8 cm) in size, are shown in Table 6.2 along with measurements of their density. Also included are the density values for an additional block of even larger size that is discussed later.

TABLE 6.2 - Compositions and Densities of Scaled-Up Blocks of Advanced Ceramic Composite Insulators For Electromagnetic Launchers

Panel ID	Size (inches)	Composition (wt. %)	Density (g/cc)	% of Theoretical Density
4-365-2	1.5x4x8	Al ₂ O ₃ -5.0ZrO ₂ -0.25Y ₂ O ₃ - 5.0Cr ₂ O ₃	4.126	99.4
4-366-2	1.5x4x8	Si ₃ N ₄ -8.0Y ₂ O ₃ - 1.0Al ₂ O ₃ - 15.0SiC _w	3.265	99.6
4-392-1	1.5x4x18	Al ₂ O ₃ -5.0ZrO ₂ -0.25Y ₂ O ₃ - 5.0Cr ₂ O ₃	4.134	99.6

Twelve different Modulus of Rupture (MOR) bars and four fracture toughness specimens were cut from each block. This number of MOR bars was sufficient for a valid determination of Weibull modulus. The average MOR strengths for the thicker panels were 4.4% lower (89.0 kpsi (614 MPa) vs. 85.1 kpsi (587 MPa)) and 2.4% lower (127.8 kpsi (881 MPa) vs. 124.7kpsi (860 MPa)) for the alumina and silicon nitride matrix materials respectively than for the thinner, previously consolidated panels. This reduction is acceptable for use as the bore insulator in advanced, full scale, electromagnetic launchers. The fracture toughness values for the thicker panels were 4.4% lower (6.8 vs. 6.5 MPa·m^{1/2}) and 9.8% lower (9.2 vs. 8.3 MPa·m^{1/2}) than for the thinner Al₂O₃ and Si₃N₄ panels. Again, this reduction is acceptable in terms of the goal properties outlined in Chapter 4.

Based on the successful result of the scale-up just described, a second scale-up to a 1.5 x 4 x 18 inch (3.8 x 10.2 x 46 cm) size block was carried out with the alumina-chromia composition. The reasons for the selection of this material for the final scale-up will be explained in detail in the next section, 6.2. This final size (1.5 x 4 x 18 in.) is representative of the insulator segment size needed for 90 or 120 mm bore state-of-the-art EMLs. Shown in Figure 6.4 is the cutting map utilized for the sectioning of the block. The MOR and fracture toughness test results are shown in Table 6.3 and compared to the best results

from previous thin panels. The comparison of properties in the long and short axis directions of the full-sized alumina block demonstrates that the material is isotropic, with no significant differences between the two orientations.

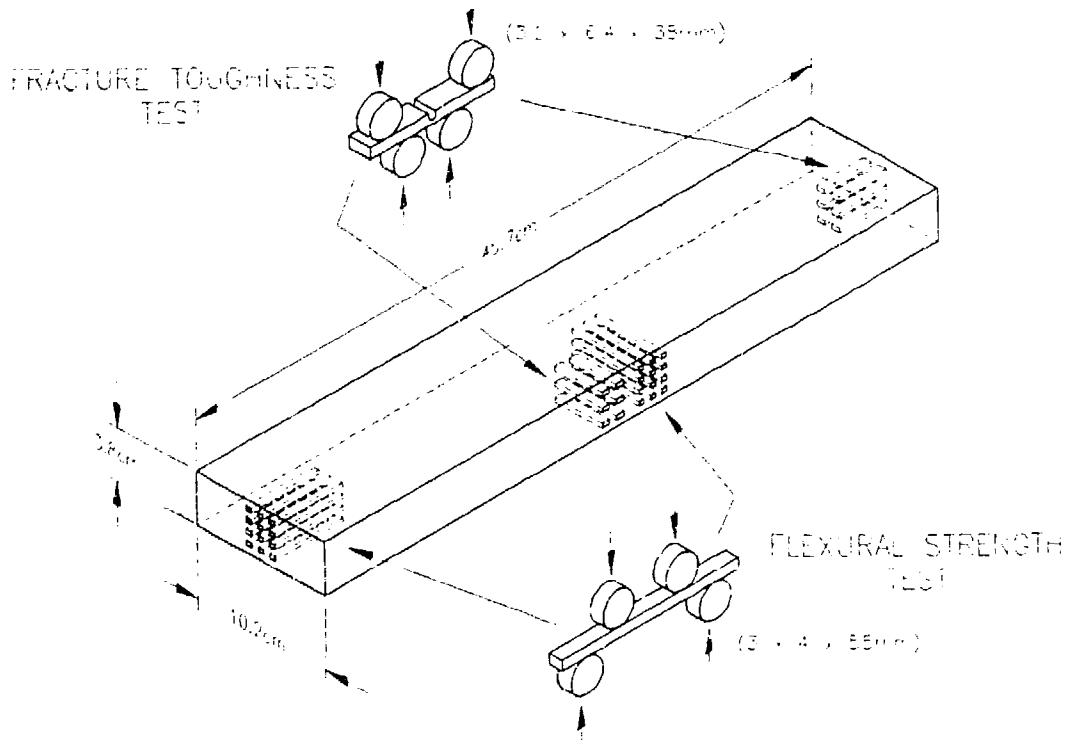


Figure 6.4 Cutting map for mechanical test specimens from full-sized 1.5 x 4 x 18 in. (3.8 x 10.2 x 45.7 cm) alumina-zirconia-chromia insulator block.

Selected mechanical test specimens that had been cut from the full sized, advanced ceramic composite insulator test block and tested were examined utilizing scanning electron microscopy (SEM). The SEM analysis revealed a very uniform microstructure consisting of small grains and an even distribution of chromia within the structure. No evidence of porosity was found. This microstructural description is the same as that seen in the 0.25 in. (0.635 cm) thick previously consolidated panels. Shown in Figure 6.5 is a typical micrograph of the full scale block, depicting the uniform, small grain size with no evidence of porosity.

**TABLE 6.3 - Results of Modulus of Rupture and Fracture
Toughness Tests on Scaled-Up Advanced Ceramic Insulator Materials**

Comp- osition No.	Panel ID	Size (in.)	Average MOR Strength kpsi (MPa)	Weibull Modulus	Average Fracture Toughness kpsi·in ^{1/2} (MPa·m ^{1/2})
		Alumina-based			
10.	4-329-5	8 x 8 x 0.25	89.0 (614)	23.6	6.2 (6.8)
10.	4-365-2	1.5 x 4 x 8	85.1 (587)	25.2	5.9 (6.5)
10.	4-392-1	1.5 x 4 x 18 (Long Axis Properties)	82.5 (569)	20.1	5.8 (6.4)
10.	4-392-1	1.5 x 4 x 18 (Short Axis Properties)	82.7 (570)	19.8	5.8 (6.4)
		Silicon Nitride-based			
22.	4-340-2	8 x 8 x 0.25	127.8 (881)	20.6	8.4 (9.2)
22.	4-366-2	1.5 x 4 x 8	124.7 (860)	17.8	7.6 (8.3)



10 microns

Figure 6.5 *Representative micrograph of alumina-chromia block consolidated to demonstrate retainment of mechanical properties in full scale pieces. Evidence of mixed mode failure is shown by sharp grains (intergranular) and arrows indicating areas of transgranular failure (and thus high toughness), (3,500X)*

6.2 Electrical Testing

Three types of high-voltage, high-current electrical tests were used to evaluate the materials studied in this program. Conductor materials were subjected to stationary electrode arc erosion tests, and rotating armature arc erosion tests. Insulator materials were subjected to a surface discharge switch (SDS) arc erosion tests. The testing of insulator materials comprised the largest part of the electrical testing done during the program.

6.2.1 Candidate Ceramic Insulator Materials

All of the electrical testing of insulator materials was performed by the Pulsed Power Laboratory of the Electrical Engineering Department of Texas Tech University (TTU) in Lubbock Texas under subcontract to SPARTA. The Texas Tech surface discharge switch (SDS III) testing device uses two electrodes placed on the surface of the tested insulator block one inch (2.54 cm) apart.^{20,21} The SDS III is connected to a capacitor bank, and is contained within a chamber which can be operated in a vacuum or under controlled atmosphere. A schematic diagram of the testing system is shown in Figure 6.6, and drawings of the capacitor bank and the surface discharge switch itself are shown in Figure 6.7. Photographs of the testing system are presented in Figures 6.8 and 6.9. The electrodes are driven up in voltage and discharged at about 25 kV. This is cycled until the surface of the insulator will no longer hold off a predetermined amount of voltage or until a certain number of pulses have been fired at about 1 Hz.

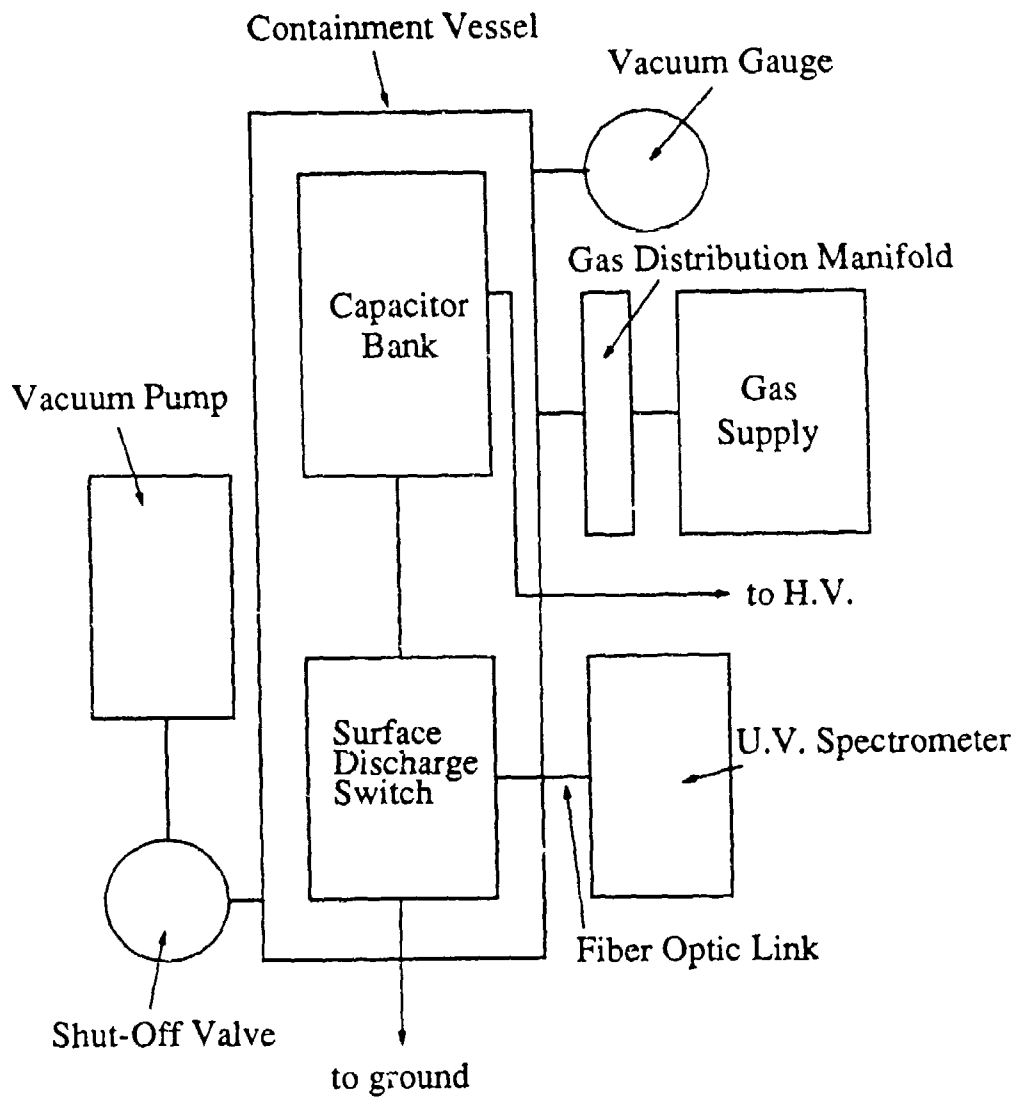


Figure 6.6 Schematic diagram of the SDS III test facility at Texas Tech University.

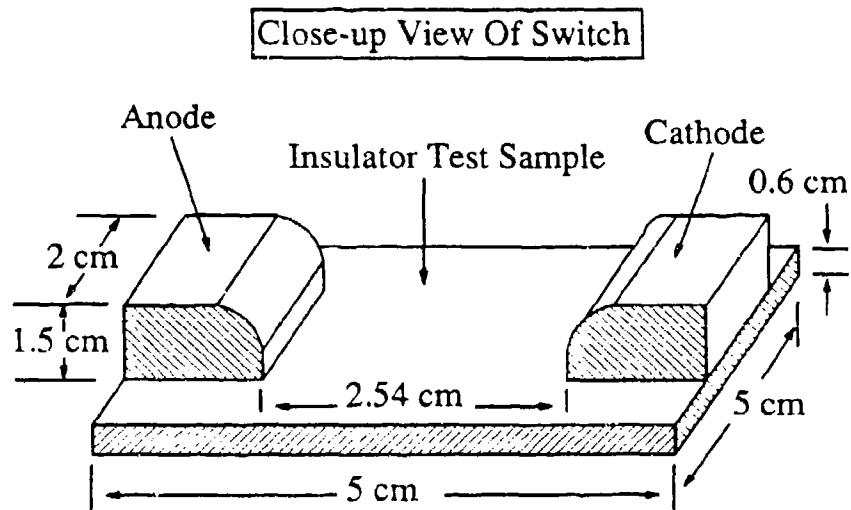
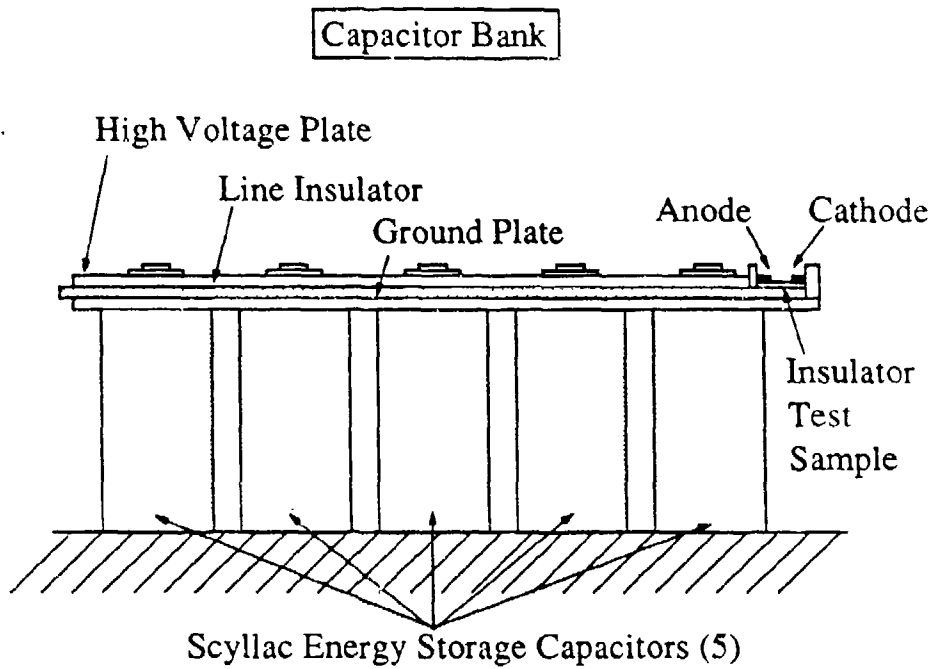


Figure 6.7 Drawings of the capacitor bank and the surface discharge switch used for testing insulator materials.

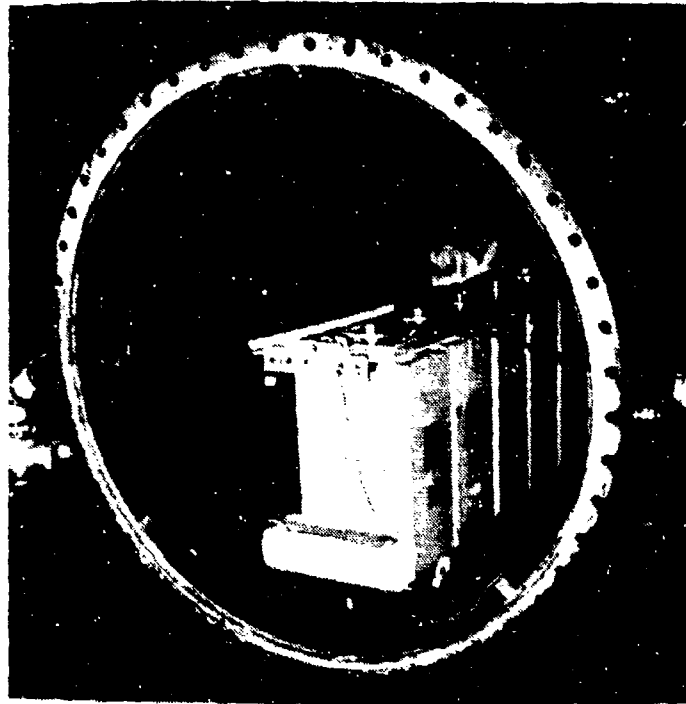


Figure 6.8 *Rep-rated (1 Hz) standing arc exposure test facility (SDS III) for advanced insulators at Texas Tech University.*

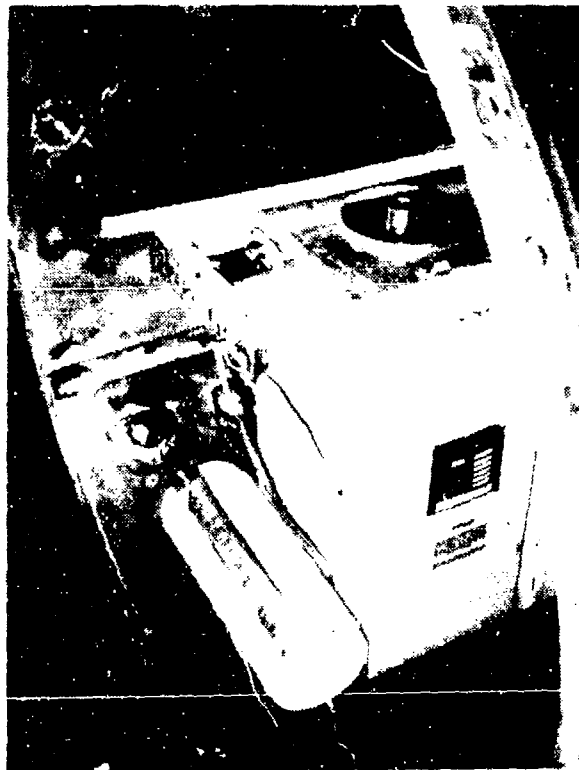


Figure 6.9 *Closeup photograph of test section revealing test block with electrodes clamped on its surface.*

The first insulator arc erosion tests were conducted on the NEMA "G" series of electrical insulation grade fiberglass-reinforced polymer composites. Figure 6.10 illustrates the results of these tests conducted on G-7, G-9, and G-10. In all these tests the initial discharge current was 300 kA (simulating expected railgun environments) at 1 pps (pulses per second). The performance of these materials provides a baseline against which to compare the advanced ceramics that were studied in this program. These NEMA "G" grade materials are already in widespread use as railgun bore insulators, as described previously in Section 1.1.

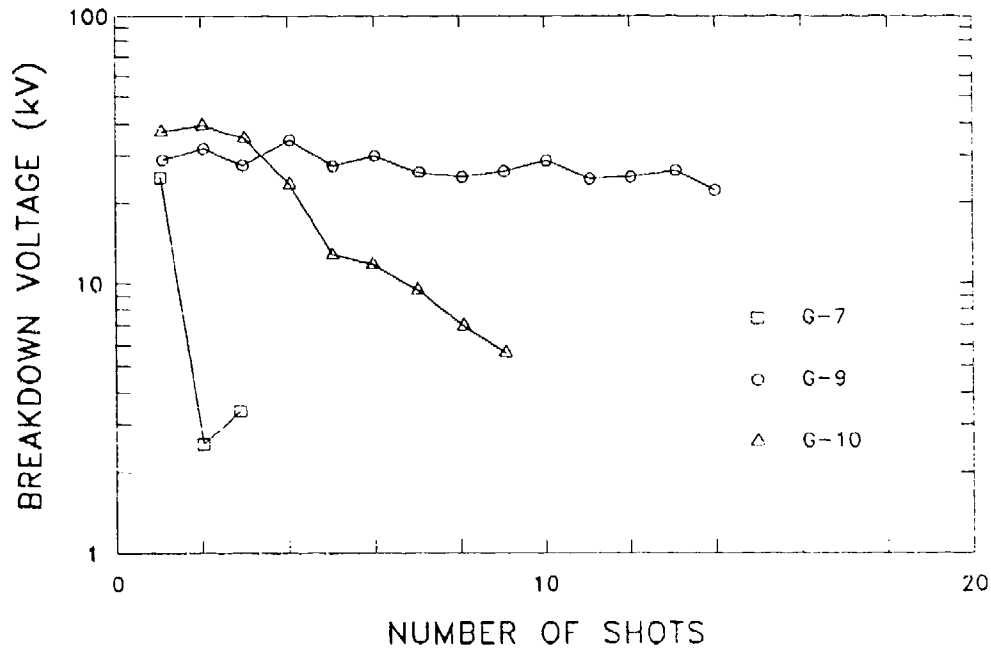


Figure 6.10 Surface breakdown voltage as a function of number of discharges for tested railgun bore insulator materials. Current level of approximately 300kA with pulse repetition rate of 1 Hz.

It can be seen that the G-9 and G-10 materials behaved exactly as expected. The cleanly ablating G-9 material dropped only slightly in breakdown voltage over the 14 pulses to which it was exposed. Much of the effect seen was probably due to thermal effects caused by the 1 Hz pulsing. The breakdown voltage was about 30 kV/in. (12 kV/cm). The G-10 material dropped from 36 kV to 5.2 kV after 9 pulses due to formation of conductive residue on its surface.

Shown in Table 6.4 are the results from the tests conducted on the first six ceramic insulator materials examined in this test series. Some of these materials were purchased in consolidated form from outside vendors, and others hot-pressed by SPARTA at Cercom. As the table shows, five of the materials held off only one discharge, and were

unable to stand-off the voltage for a second shot. The sixth material, Al_2O_3 - 25% SiC_w , held off the full test sequence of pulses (over 100). The whisker reinforced alumina material was tested with both molybdenum and Cu-W electrodes with similar results.

TABLE 6.4 — Summary of Arc Erosion Tests on First Six Ceramic Insulator Materials

Insulator and Electrode Material Used	Composition	Lifetime	Initial Break-down Voltage (kV) and Arc Length	Initial Break-down Current (kA)	Average Rep-rate (pps)	Mass Loss: Insulators (g)	Mass Loss: Electrodes (g)
TZ3Y (Ceramtec) (mol%)	Proprietary	1	26.36 1.0 in. (2.54 cm)	293.9	N.A.	0.01	0.01
AlN (Cercom) (mol%)	AlN	1	26.20 1.0 in. (2.54 cm)	292.1	N.A.	0.01	0.01
TZ (Cercom) (mol%)	ZrO ₂ -5MgO	1	26.56 1.0 in. (2.54 cm)	296.1	N.A.	0.00	0.00
FSZ (Nobra) (mol%)	ZrO ₂ -5MgO	1	27.52 1.0 in. (2.54 cm)	306.8	N.A.	0.01	0.02
S ₂ (Cercom) (mol%)	S ₂ N ₂ S ₂ O ₇ 1Al ₂ O ₃	1	28.16 0.99 in. (2.29 cm)	313.9	N.A.	0.01	0.01
Al ₂ O ₃ -SiO ₂ (Cercom) (mol%)	Al ₂ O ₃ -0.25Y ₂ O ₃ 6ZrO ₂ -3SiO ₂	75	20.80 1.25 in. (3.18 cm)	231.9	0.65	0.17	0.02
Al ₂ O ₃ -SiO ₂ (Cercom) (mol%)	Al ₂ O ₃ -0.25Y ₂ O ₃ 6ZrO ₂ -3SiO ₂	115	20.45 1.26 in. (3.18 cm)	229.4	0.65	0.14	0.05

Lifetime defined as the number of shots required to reduce the holdover voltage to 70% of the initial breakdown voltage.

Shown in Figures 6.11 through 6.14 are representative microstructures of: transformation-toughened zirconia (TTZ by Coors Ceramics), partially-stabilized zirconia (PSZ by Niler Inc.), and zirconia-alumina (TZ3Y by Ceramtec Inc.) all after one pulse, and Al_2O_3 - 25% SiC_x after 166 pulses. All of the micrographs were taken at 200X. As the micrographs show, there is a fine network of cracks on the first three materials after a single pulse. These networks are identical in appearance to those seen on the exposed surfaces of advanced ceramics tested by SPARTA in a railgun at the Army Ballistic Research Laboratory in Aberdeen, Maryland.²⁷ This substantiates the observation that the arc exposure test fixture at TTU is a good simulation of railgun arc exposure damage. Figure 6.14 shows the optical microstructure of the surface of the Al_2O_3 - 25% SiC_x material after 166 pulses. No crack network is seen at 200X, although SEM might have revealed one.

The first three materials were unable to hold off the voltage for a second pulse. The poor stand off voltage resistance is a result of formation of a thin conductive layer of zirconium metal on the surface due to decomposition of the zirconia in the ceramic. Because of the poor electrical performance of the zirconia-based ceramics, these materials were dropped from consideration in the program. Zirconia ceramics are among the strongest and toughest available, so it was with some reluctance that they were abandoned. It was very clear, however, that they could not withstand arc exposure and retain their surface voltage standoff capability.



Figure 6.11 Photomicrograph of the exposed surface of transformation toughened zirconia (TTZ by Coors Ceramics) after one pulse, 200X

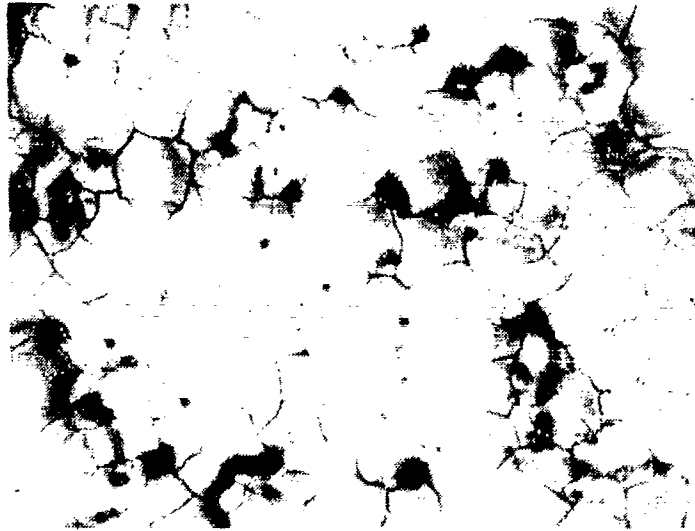


Figure 6.12 *Photomicrograph of the exposed surface of partially-stabilized zirconia (PSZ by Nilcra, Inc.) after one pulse. 200X*



Figure 6.13 *Photomicrograph of the exposed surface of alumina-zirconia (TZ3Y by Ceramtec, Inc.) after one pulse. 200X*

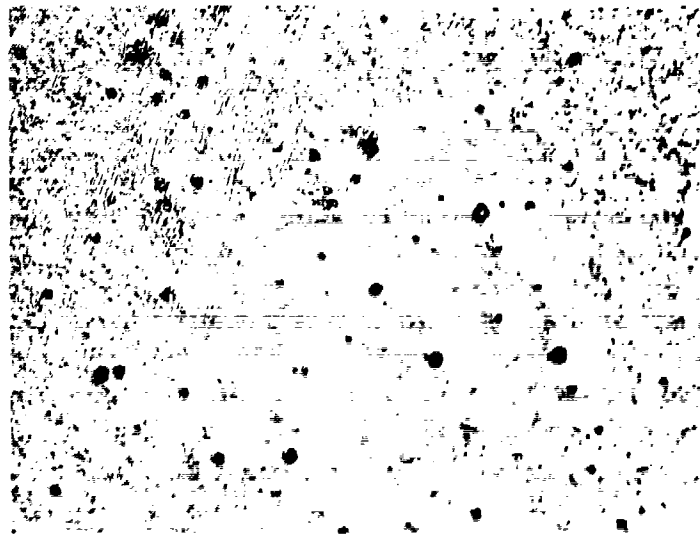


Figure 6.14 Photomicrograph of the exposed surface of alumina / 25% SiC_w after 166 pulses. 200X

The next series of materials that were evaluated in the SDS III apparatus were cut from the 6 x 6 x 0.25 inch (15 x 15 x 0.64 cm) ceramic panels hot-pressed for SPARTA by Cercom, Inc. (Tables 5.3 and 5.4). These consisted of two silicon nitride-based compositions, and two aluminum nitride-based compositions. All of these materials behaved poorly, failing to hold off the more than 70% of the initial applied voltage after the first arc pulse. A summary of these results are presented in Table 6.5.

TABLE 6.5 — Insulator Surface Breakdown Data

Material	Lifetime	Initial Breakdown Voltage (kV)	Initial Breakdown Current (kA)
Si ₃ N ₄ - 10v/o SiC _w	1	17.28	192.7
Si ₃ N ₄ - 8 Y ₂ O ₃ - 1 Al ₂ O ₃	1	24.32	271.2
AlN-0.4 Y ₂ O ₃ - 25v/o SiC _w	1	24.96	278.3
AlN - 0.4 Y ₂ O ₃	1	34.56	385.3

The values of the AlN matrix materials (with or without the silicon carbide whiskers) were very poor, and it was seen by Auger analysis that the arc had decomposed the AlN, forming aluminum metal on the surface and drastically lowering (or short circuiting) the breakdown voltage. These results caused the AlN based ceramic materials to be dropped from further consideration in the program.

At this point in the electrical testing of the advanced ceramic insulator materials, it was decided that the rather arbitrary level of 70% of initial applied voltage cut-off was too severe. It was felt that the silicon nitride results, for example, might have had an initial drop-off greater than 30% in breakdown voltage, but still be above the 2kV/cm value for railgun operation on subsequent pulses. Thus, later SDS III tests were taken to a greater number of pulses and maps were made of the breakdown voltage versus pulse number for every pulse.

A fifth composition in this same series, silicon nitride - 30% mullite, was also tested, but it resisted arcing to such a great extent that it surpassed the peak voltage capability of the testing system after the third pulse. The results of this test are shown in Table 6.6. This was the only specimen tested in the entire program that showed progressively increasing arcing resistance after each pulse. Unfortunately, the material's mechanical performance was not equally outstanding. With an average MOR strength value of only 63 kpsi (434 MPa) and a low Weibull modulus, the material was eliminated from further consideration. A sixth material that was tested, silicon carbide - 30% mullite, exhibited quite the opposite behavior from the silicon nitride, and was too conductive to be measured.

TABLE 6.6 — Initial Test Results of Surface Breakdown for Si_3N_4 - 30% Mullite

Shot #	Breakdown Voltage (kV)
1	32.5
2	34.0
3	37.5

The four materials consolidated during Hot Press Run #4 were tested next. Shown in Figure 6.15 are the results from these four tests along with values from a second specimen of Si_3N_4 - 30 %/o mullite material from hot press run #2 and the Al_2O_3 - 25% SiC_w material that had been tested previously. Plots are displayed which show the breakdown voltage recorded for each arc across a given insulator for a least 100 shots per test. As the figure demonstrates, all six materials retained voltage standoffs above 2 kV/cm even after 100 pulses. Much of the observed drop in voltage standoff capability is due to thermal effects, as the specimens heat up due to the arcing across them. After allowing the specimen to cool, the standoff voltages often return to levels very close to their original values.

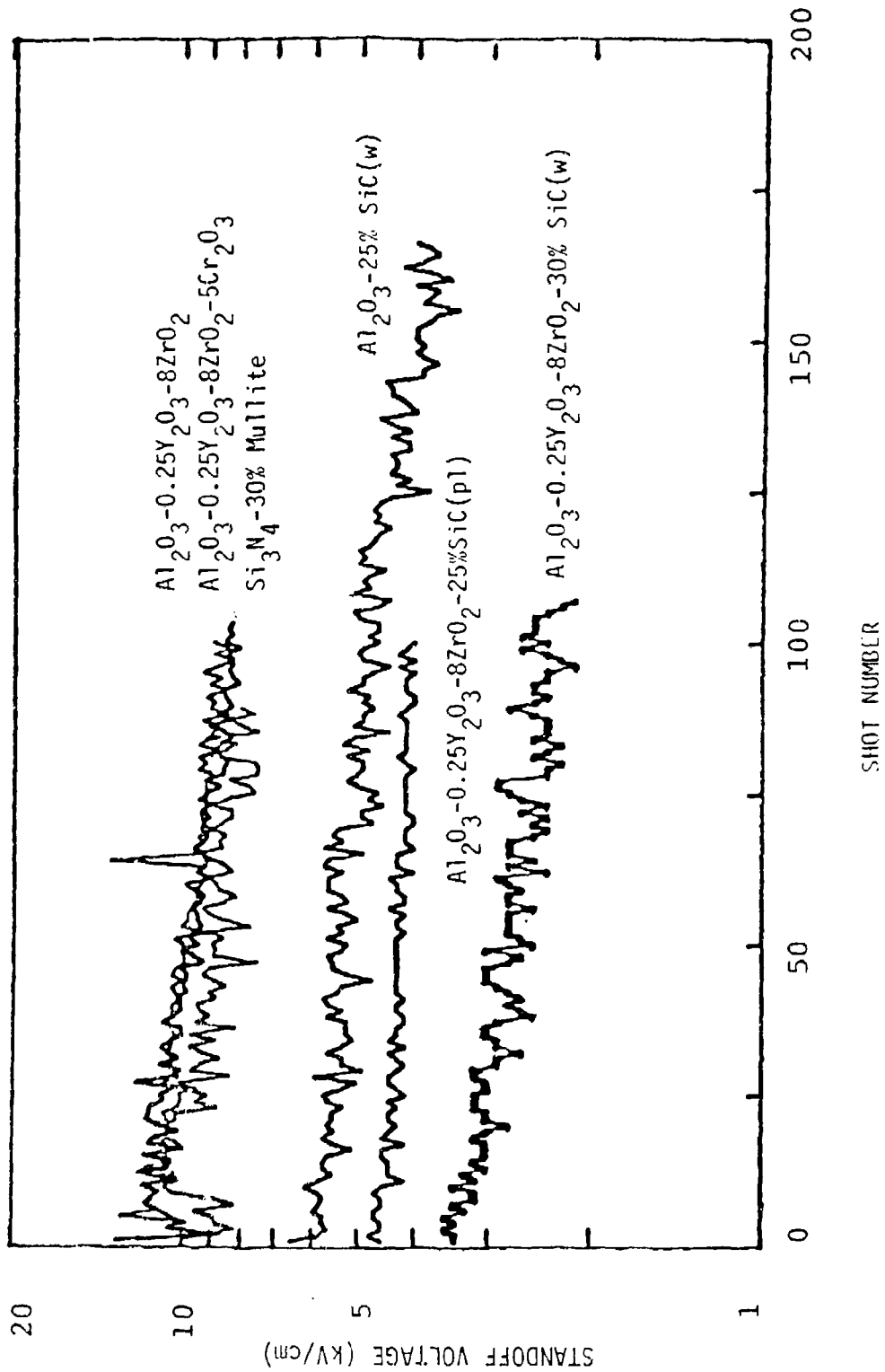


Figure 6.15 The response of ceramic insulator materials to repeated arc exposures. Surface standoff voltage is plotted for each arc pulse in a series of 100 for six different materials.

Shown in Figures 6.16 through 6.20 are typical surface microstructures of the ceramic materials with codes 483-2, 483-3, 484-4, 484-3, and 440-1 after exposure to more than 100 arc pulses in the SDS III facility. As Figure 6.16 shows, the $\text{Al}_2\text{O}_3 + 0.25 \text{Y}_2\text{O}_3 + 8 \text{ZrO}_2$ (483-2) experienced the greatest amount of thermal shock microcracking of the four alumina based specimens. The addition of 5% Cr_2O_3 (483-3) to the materials (Figure 6.17) did not appreciably reduce the amount of microcracking. The addition of 25% volume SiC platelets (484-4) to the material (Figure 6.18) resulted in a smaller crack network but the appearance of a large number of nodules on the surface, presumably silicon metal from decomposed SiC. When the SiC was added in the smaller form of whiskers (484-3), no crack network could be resolved at 400X (Figure 6.19) but metallic nodules were still present on the surface. However, these metallic nodules do not link up and the materials still retain standoff voltage of about 2.5 kV/cm after more than 100 pulses. Figure 6.16 illustrates that the alumina materials reinforced with 25% SiC_w , 25% SiC (platelets) and 30% SiC_w are somewhat lower in standoff voltage than the Al_2O_3 based ceramics without SiC included. This is most likely due to the presence of the metallic nodules on the surface which act as enhanced breakdown sites, however, the standoff voltage is still considerable.

The microstructure of the Si_3N_4 - 30v/o mullite material (440-1) is shown in Figure 6.20. No microcracking is seen at the 400X magnification, although numerous silicon metal nodules are present. Despite the presence of the silicon metal nodules, the standoff voltage is still above 8 kV/cm even after more than 100 pulses. The effect of mullite on the retention of high voltage standoff on Si_3N_4 based ceramics is a new and surprising observation. As shown in Figure 6.15 both grades of unreinforced Si_3N_4 rapidly dropped in voltage standoff to values below 1 kV/cm. The low MOR strength and Weibull Modulus of this composition makes the material unsuitable for railgun applications, but this discovery may, nevertheless, prove to be of value in other areas.

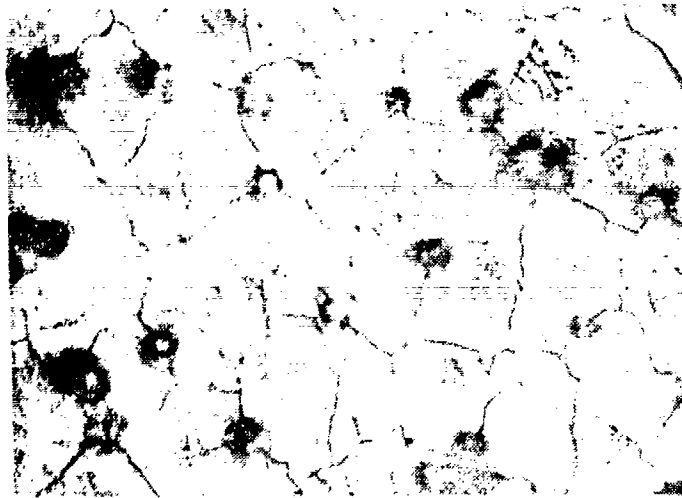


Figure 6.16 *Micrograph of $\text{Al}_2\text{O}_3\text{-}0.25 \text{ Y}_2\text{O}_3\text{-}8 \text{ ZrO}_2$ (483-2) After Exposure to Greater Than 100 Pulses in Arc Test Facility. Microcrack network and limited spalling is seen. 400X*

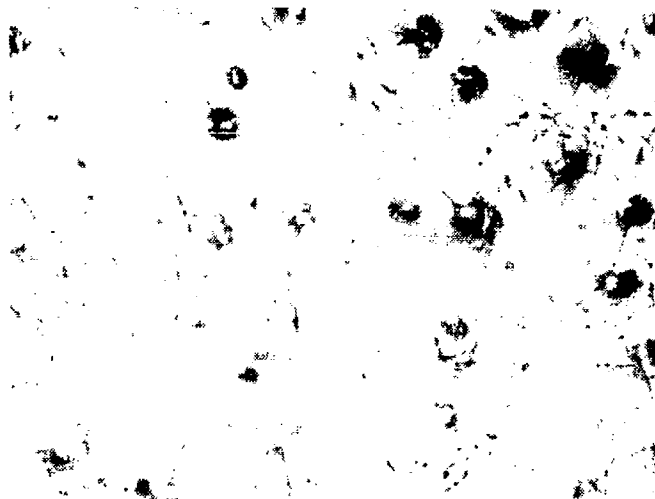


Figure 6.17 *Micrograph of $\text{Al}_2\text{O}_3\text{-}8\text{ZrO}_2\text{-}0.25\text{Y}_2\text{O}_3\text{-}5\text{Cr}_2\text{O}_3$ (483-2) after exposure to greater than 100 pulses in arc test facility. Microcrack network and limited spalling is seen. 400X*

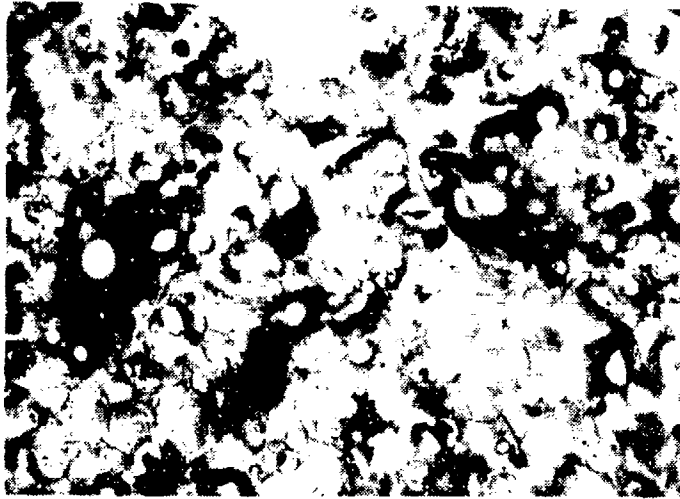


Figure 6.18 *Micrograph of $\text{Al}_2\text{O}_3\text{-}0.25\text{Y}_2\text{O}_3\text{-}8\text{ZrO}_2\text{-}25\text{v/o SiC}$ (platelets) (484-4) after exposure to greater than 100 pulses in arc test facility. Microcrack network and metallic nodules (Si) are seen. 400X*

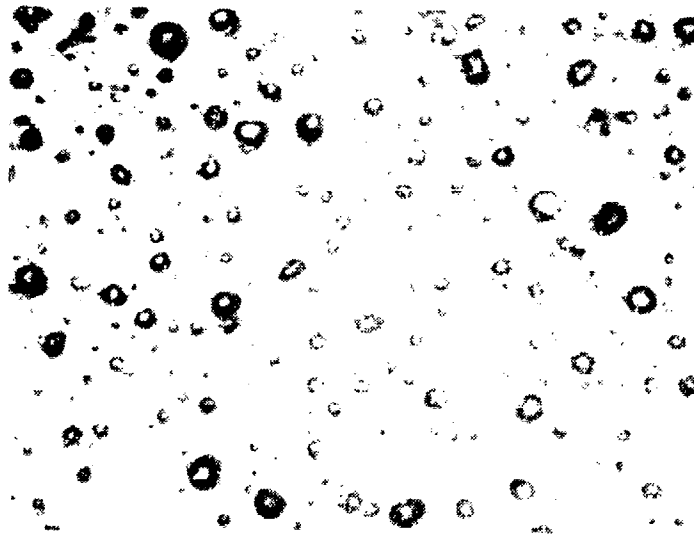


Figure 6.19 *Micrograph of $\text{Al}_2\text{O}_3\text{-}0.25\text{Y}_2\text{O}_3\text{-}8\text{ZrO}_2\text{-}30\text{ v/o SiC}_w$ (484-3) after exposure to greater than 100 pulses in arc test facility. No microcrack network is seen, but metallic nodules (Si) are present 400X*

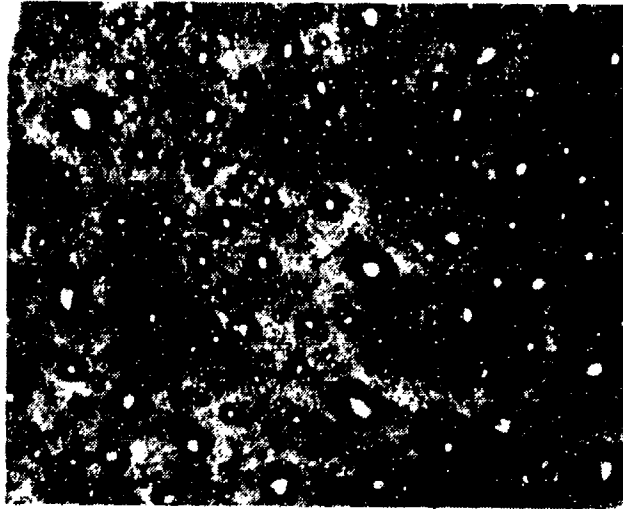


Figure 6.20 *Micrograph of Si_3N_4 -30v/o mullite after exposure to greater than 100 pulses in arc test facility. No microcrack network is seen but silicon metal nodules are present. 400X*

The most important series of insulator breakdown tests were those that were conducted on specimens cut from the developmental 8 x 8 in. (20.3 x 20.3 cm) panels. These panels were the highest quality panels made during the program with the culmination of the improvements in ceramic powder blending and processing parameter (time, temperature and pressure) development. This was especially true of the chromia containing alumina materials, which earlier in the program (as shown in Figure 6.15) evidenced electrical breakdown behavior similar to alumina without any chromia addition. The earlier panels (cut from the 6 x 6 in. (15.2 x 15.2 cm) panels) were subjected to EDAX elemental mapping which showed the chromia was present as large scattered clumps in the alumina. Optimized blending operations resulted in EDAX chromia maps that were completely uniform with the chromia in solid solution in the alumina matrix. This improved blending resulted in improved electrical characteristics. The results from twelve different materials cut from the developmental 8 x 8 in. (20.3 x 20.3 cm) panels are presented in Figures 6.21 through 6.24.

The most striking point that is apparent from comparing these graphs is that the silicon nitride-based materials are almost an order of magnitude lower in breakdown voltage than the alumina-based materials (notice the different scales used on the voltage axis in the plots). The poor performance of the Si_3N_4 is due to the formation of nodules of metallic silicon on the surface of the material during the passage of the first arc. The second salient feature of the comparison is that the presence of silicon carbide whiskers significantly degrades the holdoff resistance of the alumina. It appears, then, that it will

not be possible to take advantage of the significant toughening effect conferred by these whiskers. The semiconducting nature of the SiC greatly reduces the voltage standoff capability of the ceramic composite material. This series of arc exposure tests led us to conclude, therefore, that no materials containing either silicon nitride or silicon carbide could be used as bore insulators because of their poor surface voltage standoff.

As discussed previously, the value of standoff voltage necessary for operation of present or near-term railguns is in the 0.5 to 2 kV/cm range. For some types of solid armature guns the required standoff voltage may drop to 500 Volts, even for large guns (90 mm bore diameter). Thus the required voltage standoff may be as low as 150 V/cm, and materials based on Si_3N_4 may be acceptable as bore insulators and certainly as backup insulators for these types of guns.

A summary of the voltage breakdown behavior of the major advanced ceramic insulator materials is summarized in Figure 6.25. The major conclusion to be derived from the electrical arc testing is that the chromia containing alumina materials possessed the best voltage standoff resistance of any of the materials (except for the mechanically inferior mullite materials). As can be seen the chromia containing alumina material has, on the average, a two to three kV/cm better breakdown voltage than the alumina material without the chromia. In addition, the presence of the silicon carbide whiskers in the alumina material further reduces the breakdown voltage another two to three kV/cm. The silicon nitride material (reinforced with silicon carbide whiskers) was taken to over 350 shots, and still possessed approximately 1 kV/cm surface breakdown voltage breakdown strength. Based on these observations, coupled with the results of the mechanical tests, the chromia containing alumina material was chosen as the composition to be scaled up to the final 1.5 x 4 x 18 in. (3.81 x 10.16 x 45.72 cm) size block.

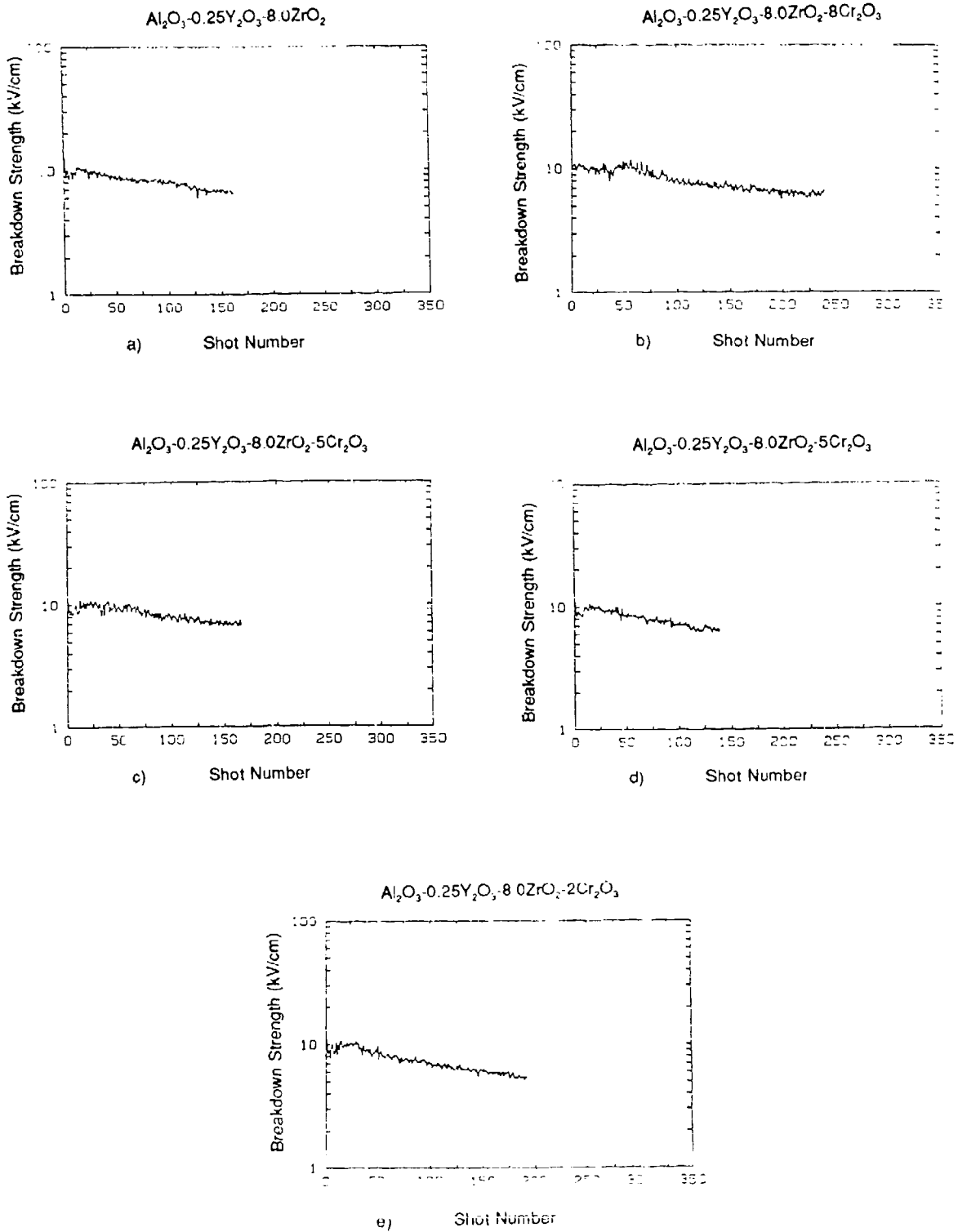


Figure 6.21 Voltage holdoff degradation performance of alumina-chromia materials, a) 4-253-4, b) 4-253-6, c) 4-253-1, d) 4-253-5, e) 4-253-3

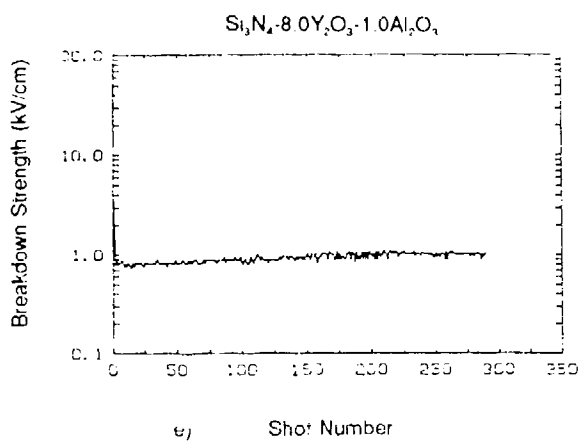
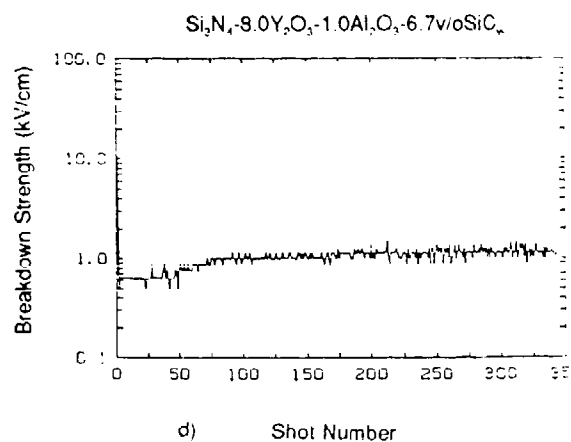
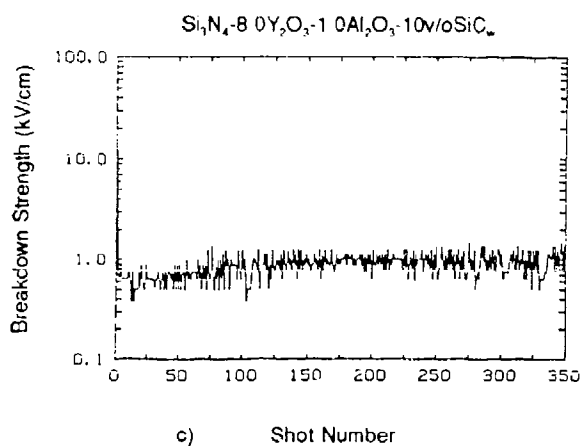
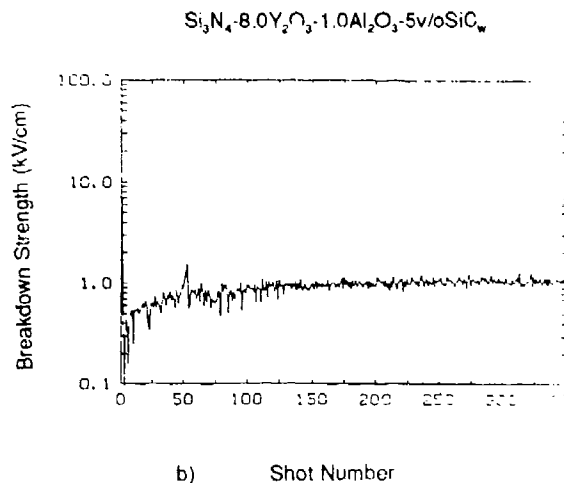
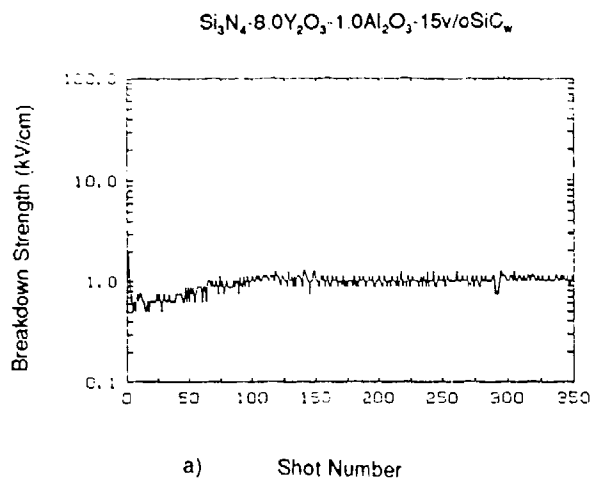


Figure 6.22 Voltage holdoff degradation performance of silicon nitride / SiC_w materials 4-265-3, b) 4-265-4, c) 4-258-6, d) 4-265-1, e) 4-265-5

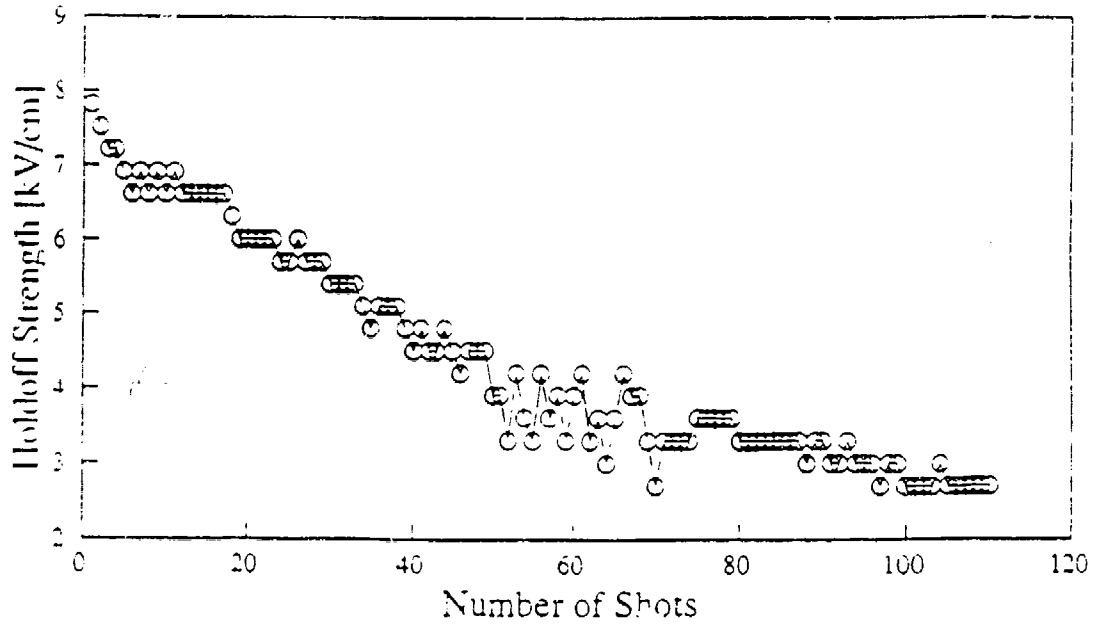


Figure 6.23 Voltage holdoff strength versus number of pulses for Al_2O_3 - 15ZrO_2 - $35\%\text{SiC}_w$ (AMI008-1)

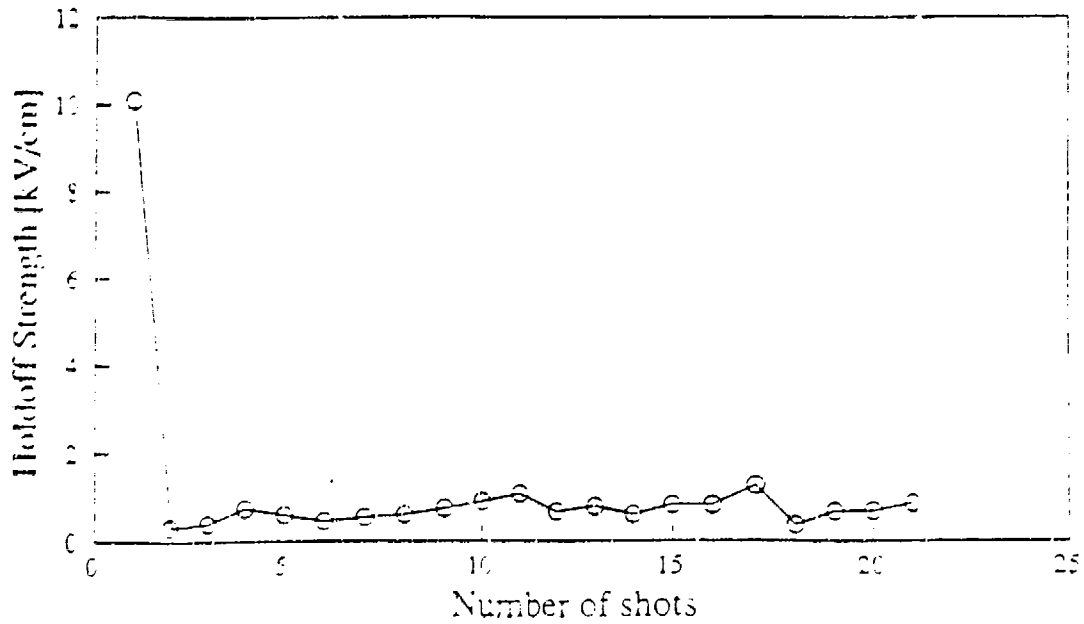


Figure 6.24 Voltage holdoff strength versus number of pulses for Si_3N_4 - $8\text{Y}_2\text{O}_3$ - $1\text{Al}_2\text{O}_3$ - $35\%\text{SiC}_w$ (S-340-2)

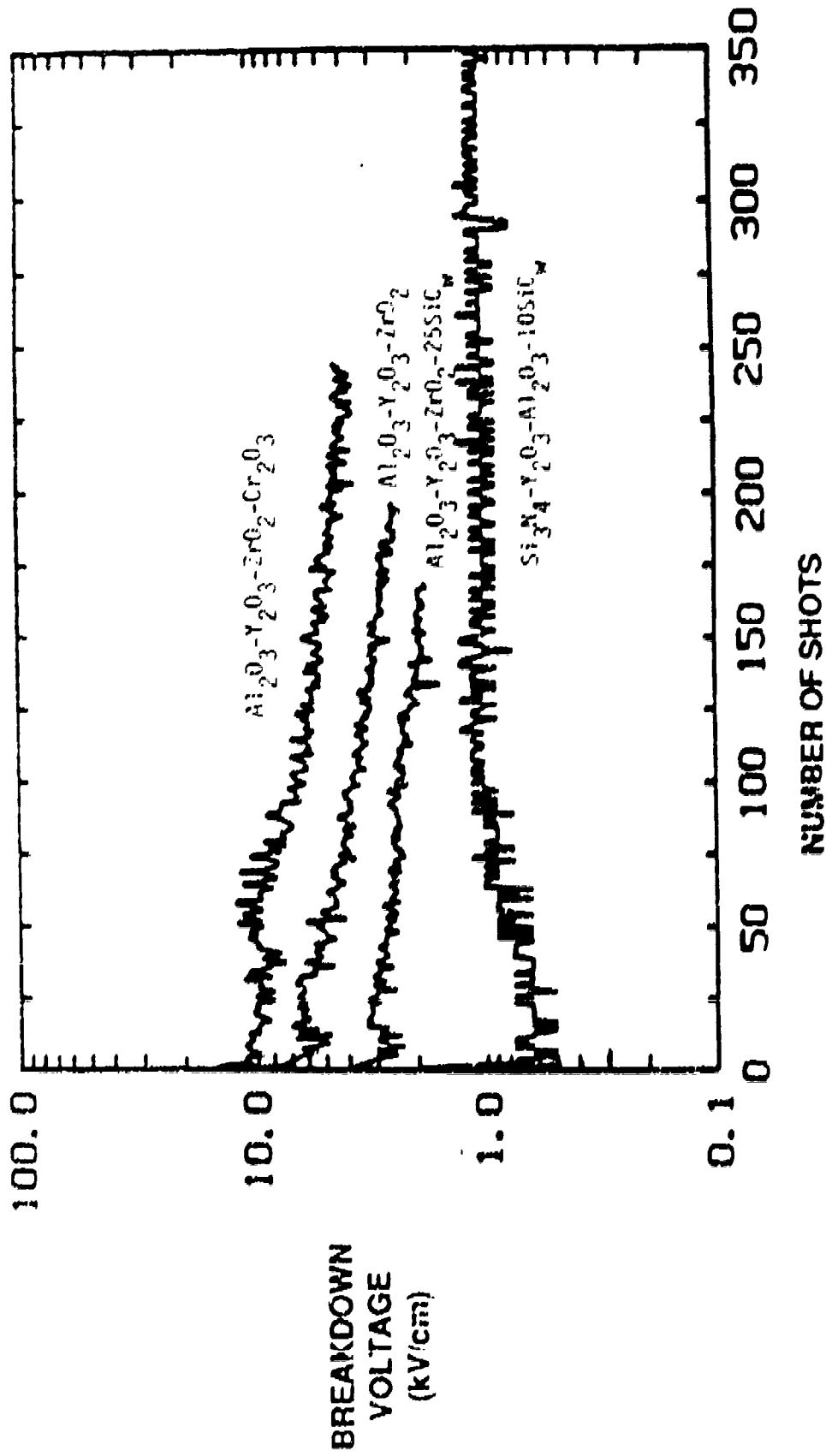


Figure 5.25. Summary of breakdown voltage resistance of advanced ceramic insulator materials taken from conum quality trends

6.2.2 Electrical Testing of Other Insulator Materials

During the course of the contract, various electrical breakdown tests were performed at TTU on a variety of insulating materials besides those that were candidate ceramic bore insulating materials. These tests included:

- Effect of ultraviolet radiation on surface breakdown
- Effect of UV absorber material on surface breakdown resistance
- Breakdown strength of conventional monolithic ceramics including mullite, cordierite and steatite
- A limited investigation of four different advanced polymeric insulating materials
- Measurements of the voltage standoff properties of pure alumina and two grades of commonly used glass-mica

These materials are of interest to areas of the railgun that are not exposed to the arc erosion or the abrasion and impact damage from the projectile, and thus were included in the program.

The research team at Texas Tech conducted a series of experiments to elucidate the role of ultraviolet radiation in surface arcing. When an arc crosses a material, it emits intense ultraviolet radiation which may produce chemical degradation of the material's surface which reduces its electrical resistance. Shown in Figure 6.26 is the ultraviolet spectrum of typical graphite and molybdenum electrodes. As can be seen, the molybdenum electrodes emit about 40 to 50% higher ultraviolet (UV) radiation intensity than the graphite electrodes. A G-10 insulator can survive up to three times as many arcs when the electrodes are graphite, as opposed to molybdenum. It is hypothesized that the reason for this is the harsher UV spectrum of the molybdenum electrodes lead to surface damage which lowers the voltage standoff strength of the G-10. An alternative explanation might be that molybdenum is vaporized during arcing and condenses onto the insulator surfaces, rendering them more conductive.

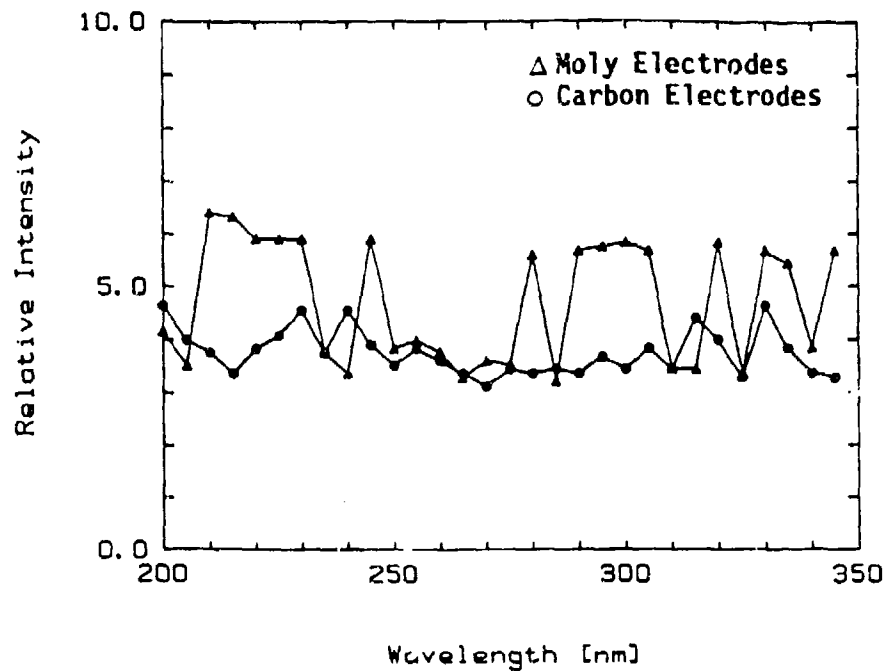


Figure 6.26 Spectrum intensity vs. wavelength (UV region) for molybdenum and graphite electrodes

It was further hypothesized that a UV absorber material could be used to protect the surface from the UV degradation. The commonly used organic material, benzophenone dissolved in ethanol, was used to treat the insulator surfaces. The test insulators were soaked in the benzophenone solution, dried, and subsequently tested. The test results for untreated and treated G-10 with molybdenum electrodes and untreated G-10 with graphite electrodes is shown in Figure 6.27. The lifetime of the G-10 with molybdenum electrodes was increased by almost a factor of three by treating the surface of the G-10 with the benzophenone. Also shown for reference is untreated G-10 with graphite electrodes illustrating the greater voltage standoff capability of the G-10 with graphite electrodes.

Limited tests were also performed on TTZ (transformation-toughened zirconia) insulators. This material withstood only one pulse in the voltage stand-off test. After soaking in the benzophenone, it survived two pulses. The benzophenone probably forms a molecular monolayer on the surface of the ceramic, but does not penetrate into it. It would, therefore, be expected to ablate away during the first arc exposure. Zirconia ceramics had been previously disqualified from the program on the basis of their poor surface voltage standoff performance.

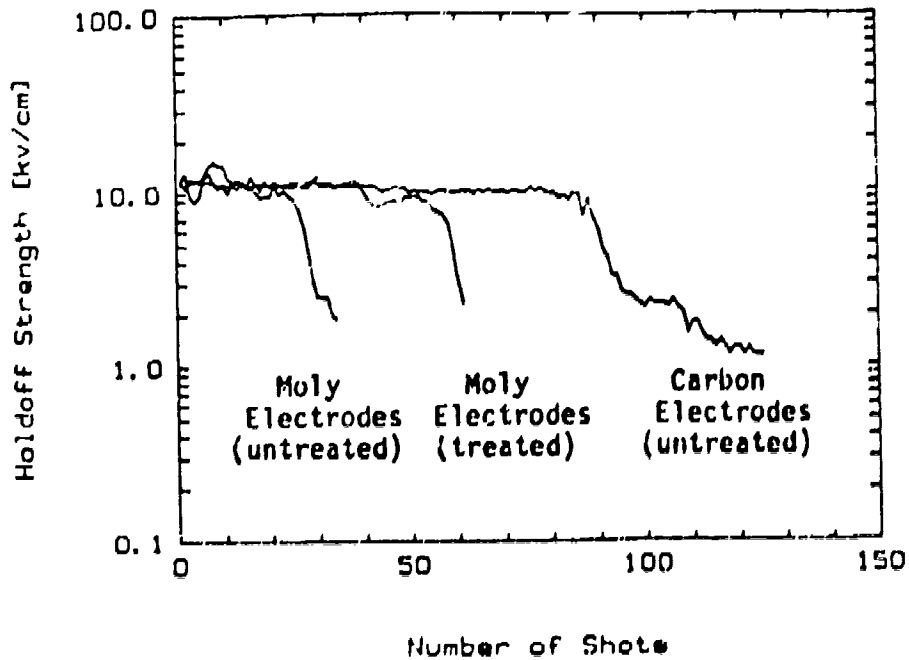


Figure 6.27 *Effect of graphite vs. molybdenum electrodes and treating of G-10 with benzophenone on the voltage stand-off capability of G-10 insulators*

The electrical testing also included some "conventional" ceramic materials in addition to the custom-formulated "advanced" ceramics. These materials were mullite (aluminum silicate), cordierite (magnesium aluminum silicate), and steatite (magnesium silicate). These materials are commonly used as electrical insulators in less demanding, lower voltage applications. Data from these tests is presented in Table 6.7. Graphs of the standoff voltage as a function of the number of arc pulses are plotted in Figures 6.28 through 6.30. All three materials retained substantial holdoff strength beyond 100 cycles. The steatite dropped below 70% of its initial holdoff strength after just 28 cycles, however. The performance of the mullite is similar to the results seen with the silicon nitride-30% mullite material tested previously. If electrical performance alone determined the selection of a railgun insulator material, mullite would be a leading candidate. However, this material has very low MOR strength and fracture toughness, so it does not merit further consideration.

TABLE 6.7 — Arc Exposure Data on Three Conventional Engineering Ceramics

	Mullite	Cordierite	Steatite
Electrode Material	Mo	Mo	Mo
Lifetime*	>137	100	28
Initial Breakdown Voltage (kV/cm)	9.45	7.81	13.86
Initial Breakdown Current (kA)	269	222	394
Average Pulse Rate (Hz)	0.6	0.8	0.7
Weight Loss of Insulator (g)	0.25	0.25	0.17
Weight Loss of Electrode (g)	0.06	0.02	0.05

* Lifetime is defined as the number of shots required to reduce the holdoff voltage to 70% of the initial breakdown voltage

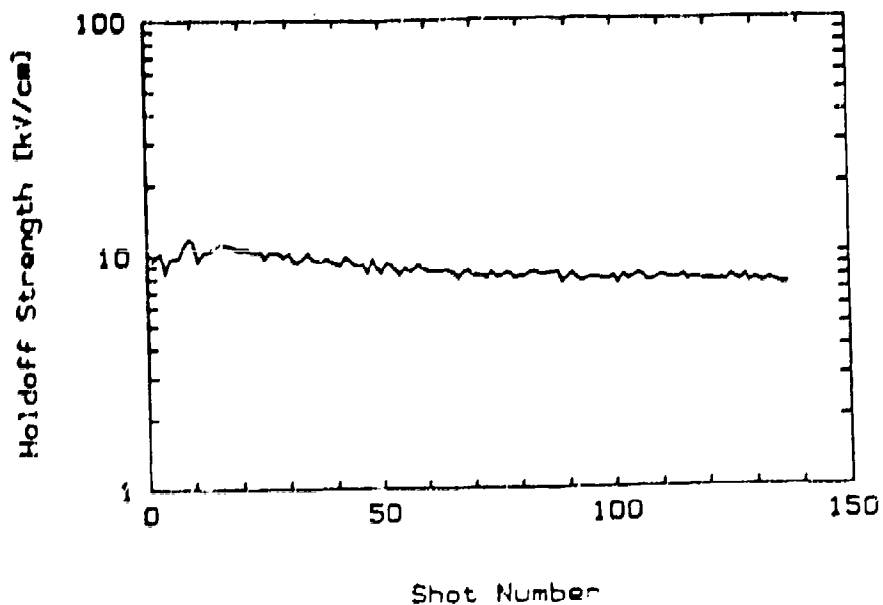


Figure 6.28 Voltage holdoff recovery behavior of mullite ceramic as measured at SDS III facility at TTU

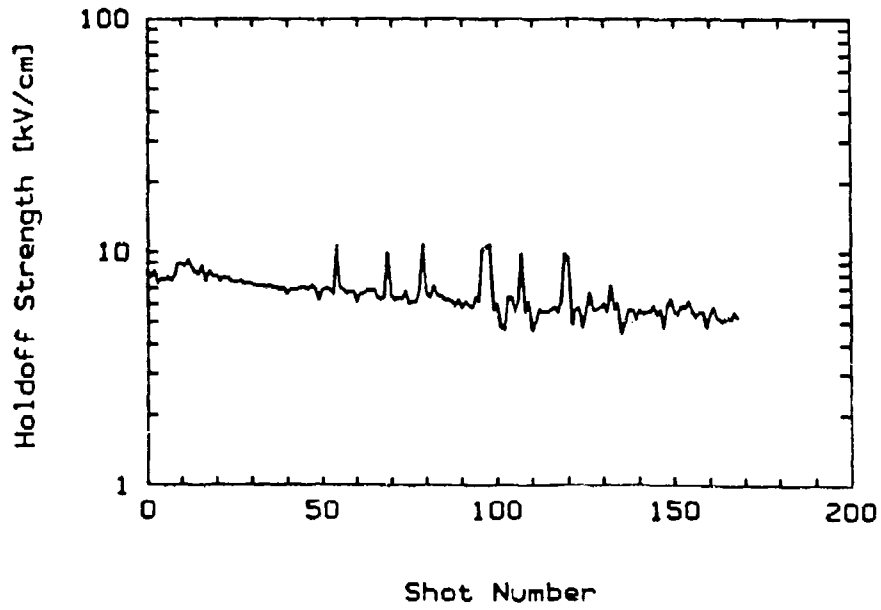


Figure 6.29 Voltage holdoff recovery behavior of cordierite ceramic as measured at SDS III facility at TTU

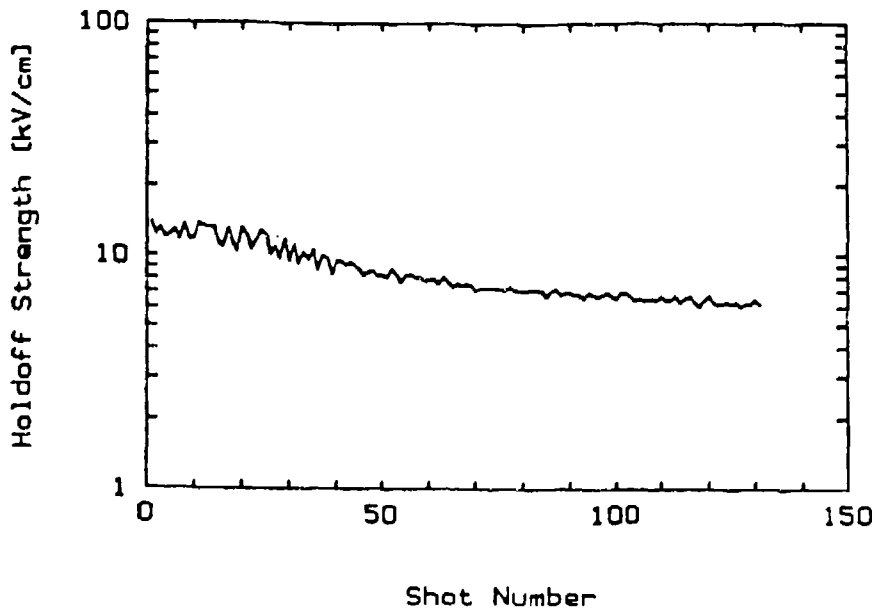


Figure 6.30 Voltage holdoff recovery behavior of steatite ceramic as measured at SDS III facility at TTU

A variety of other commercially available insulating materials was also studied to determine their high voltage surface standoff capabilities. These tests examined both polymeric and ceramic materials.

Four different advanced, state-of-the-art, organic insulating materials manufactured by the Polymer Corporation, Reading, PA, were tested in the standing arc SDS III electrical test facility as shown in Table 6.8. One material, Celezole U-60, became conductive after a single pulse, most likely due to formation of conductive carbon containing soot on its surface. The other three materials were tested to approximately 100 shots and the results are shown in Figures 6.31 through 6.33. It is difficult to directly compare the results of the organic insulator materials with those of the ceramics because of the much lower thermal conductivity of the organic insulators. The tests were performed at a frequency greater than 1 Hz and thus heat build up occurred. The ceramics, which have a much higher thermal conductivity and temperature resistance capability, are able to withstand a larger number of pulses without overheating their surfaces. The organic materials tended to overheat and degrade faster than if their surfaces were kept cool between pulses, however, a useful comparison can still be made between the different organic insulators.

TABLE 6.8 — Results of SDS Standing Arc Tests of Advanced Organic Insulator Materials

Material Trade Name	Material Composition	Result	Mass Loss (g)
Celezole U-60	unknown	Conductive after 1 pulse	—
Torlon 4203	polyamide-imide	Dropped to 2 kV/cm after 75 pulses	0.07
Ultem 1000	polyetherimide	Dropped to 5 kV after 110 pulses	0.22
Ultem 4001	polyetherimide	Cycled between 2 and 9 kV/cm up to 85 pulses	0.09

The Torlon (polyamide-imide resin) grade 4203 material (Figure 6.31) dropped from 14 kV/cm to 2 kV/cm holdoff strength after five shots and then cycled through levels of 2 to 9 kV/cm. This phenomena was probably due to burning off of surface layers of materials and exposing new material which increased the holdoff strength periodically. Both grades of Ultem (polyetherimide resin), 1000 and 4001 (Figures 6.32 and 6.33 respectively), revealed the same type of periodic behavior as the Torlon material, however, the Ultem materials exhibited greater voltage holdoff strengths than the Torlon material. The strengths exhibited by the Ultem 1000 material (above 4 kV/cm except for one point) demonstrates its usefulness in systems where arcs would play against it.

The mass losses exhibited by the organic insulator specimens compare with values of 0.01 to 0.04 grams for typical high quality ceramic specimens. And considering that the ceramic specimens are two to four times as dense as the organic insulators, the depth of eroded material is thus five to forty times less for the ceramics than the organic insulators.

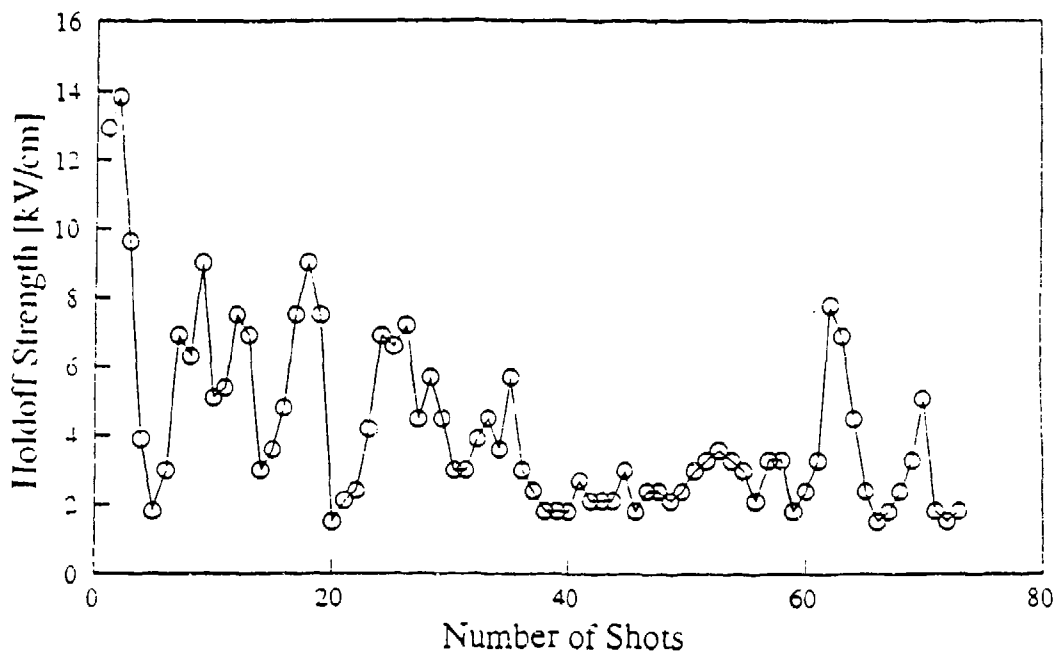


Figure 6.31 Voltage holdoff strength versus number of pulses for Torlon 4203 polymer.

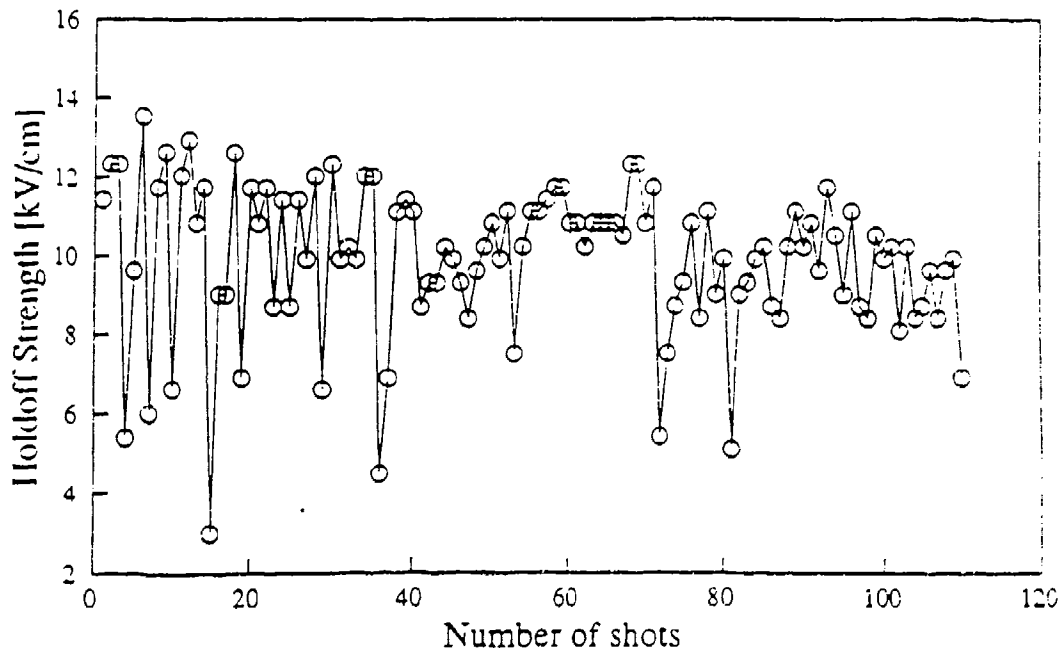


Figure 6.32 Voltage holdoff strength versus number of pulses for Ultem 1000 polymer.

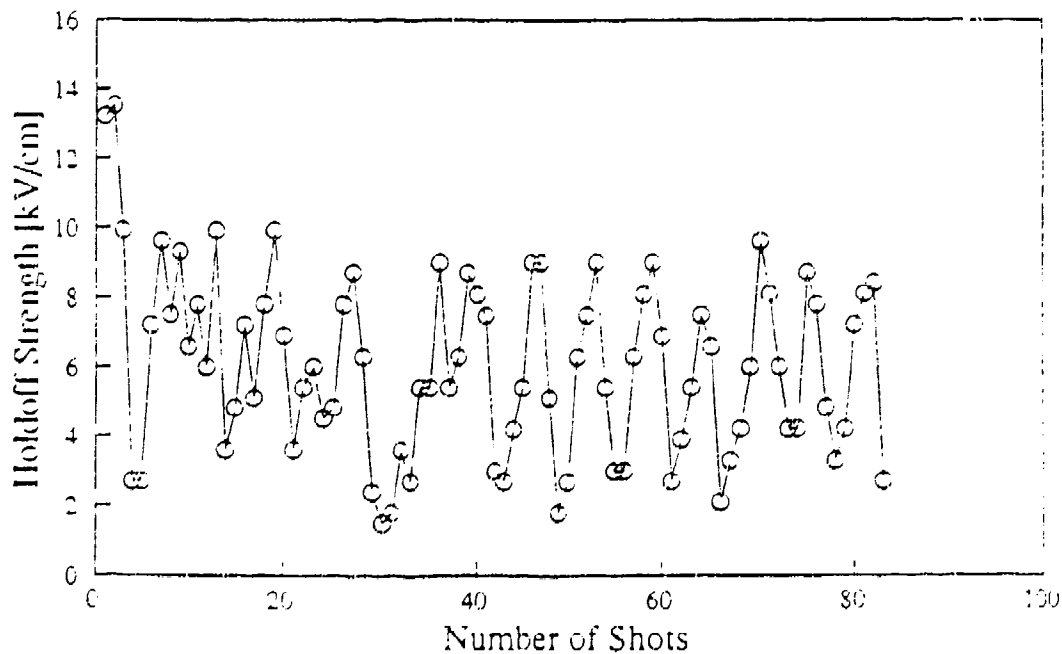


Figure 6.33 Voltage holdoff strength versus number of pulses for Ultem 4001 polymer.

The examination of commercially available ceramic high voltage insulator materials also included AD994, a relatively high purity alumina made by Coors Ceramics Company of Golden, Colorado, and two grades of Mycalex made by Mykroy-Mycalex Company in Clifton, New Jersey. The grade 400 Mycalex is made from natural flake mica in a glass matrix. The grade 1100 Mycalex is made from synthetic flake mica in a higher temperature glass matrix. The voltage breakdown strength versus number of pulses for these materials is shown in Figures 6.34 to 6.36. As expected, the pure alumina performed well, with little degradation in surface breakdown strength. The mica reinforced materials did not perform as well but still stayed above 5 kV/cm breakdown strength.

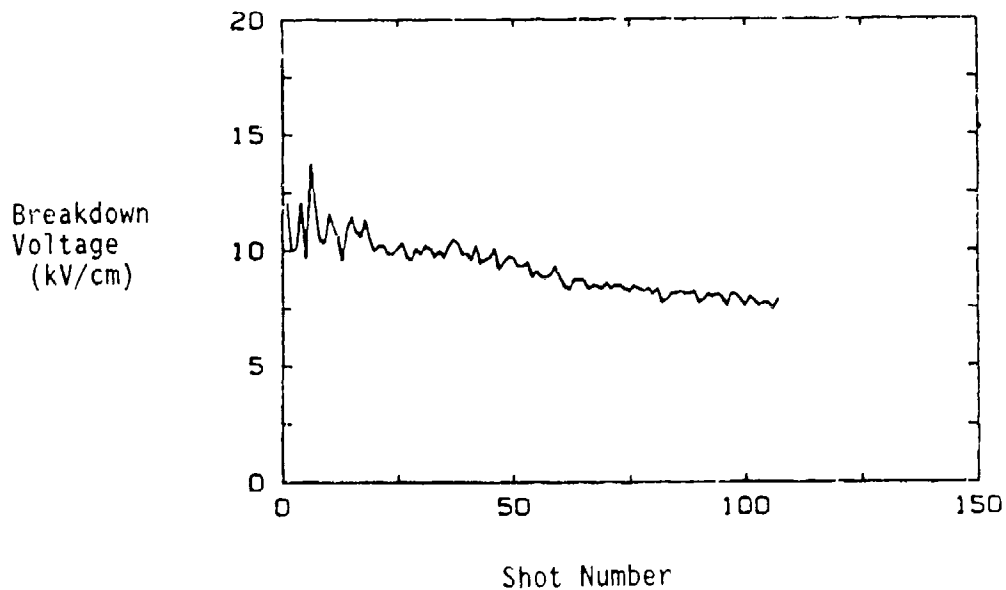


Figure 6.34 Surface voltage breakdown vs number of pulses for AD994 alumina.

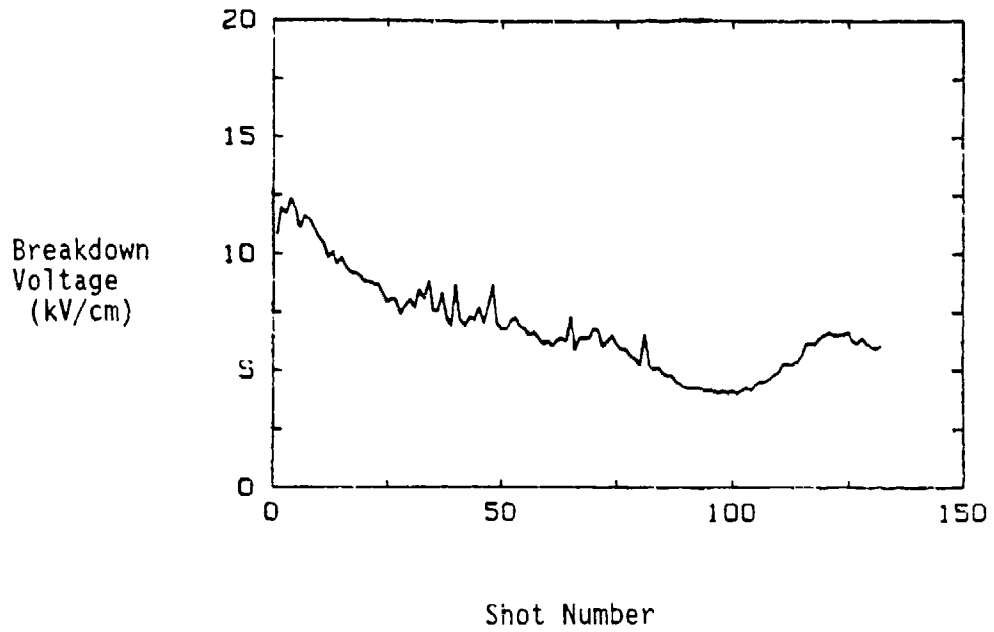


Figure 6.35 Surface voltage breakdown vs number of pulses for Mycalex 400 glass/mica composite.

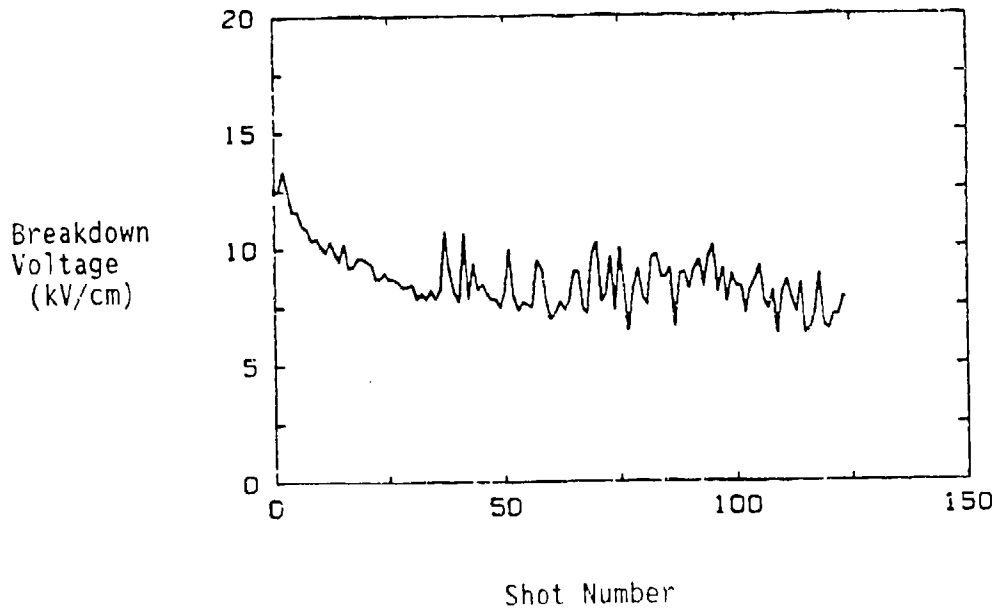


Figure 6.36 Surface voltage breakdown vs number of pulses for Mycalex 1100 glass/mica composite.

6.2.3 Conductor Materials

Early in the program before the decision was made to focus entirely on advanced ceramic insulator materials for EML bores, limited work was done on conductor materials for EML bores. This work centered on two different projects:

- Testing of electrode materials at Texas Tech University using their MAX I High Coulomb Stationary Arc Test Device
- Testing of sliding contact behavior of various conductors using a moving contact test facility at IAP Research, Inc. in Dayton, Ohio.

Each of these tests are described in this section.

The surface discharge electrode tests were conducted at the electrical engineering department at Texas Tech University (TTU) in Lubbock, Texas as part of the Doctoral Thesis work of Anthony Donaldson.²³ The tests were conducted in their MAX I Stationary Arc Test Device, which is a surface discharge switch device similar to that used for the testing of the insulating materials. Shown in Table 6.9 is a summary of eighteen different electrode materials that were tested at TTU. The pedigree of the materials is described in more detail in Table 6.10. The effective charge transferred per shot is a function of the resistance and the work function (energy required to remove an electron from the surface of the electrode) of each electrode material. Thus, the charge transferred was different for each specimen. The volume eroded data was determined by measuring the weight loss after repeated shots, and dividing it by the electrode material density and the number of shots. In order to normalize the test results, a third column in Table 6.9 gives the volume of material eroded per coulomb of electric charge transferred. The materials have been placed in order of increasing material erosion (per coulomb of transferred electric current). The most erosion-resistant materials are listed at the top, with decreasing performance seen as one moves down the list.

The tests summarized in this table were conducted at extremely high levels of charge transfer/area per shot. Such conditions are not representative of the electric current transfer in railgun conductor rails. For example a 6m length x 90mm bore railgun with a peak current of 2,500,000 amperes will transfer about 1,100 coulombs. This is about 22 times the 50 coulombs transferred per shot in the TTU tests (Table 6.9). However, the surface area of one of the conductor rails is about 600 times the area of the electrode test specimens, so that the charge transfer density was about 30 times higher in the electrode stationary arc tests than the average in railguns. However, in locations such as in the near breech region where the projectile is traveling relatively

slowly and the current is high, the difference in charge transfer density may only be five times greater for the stationary arc test than for railguns. Thus a typical railgun has a charge transfer (in local areas) of about 2 to 10 coulombs per shot, depending upon location in the bore. The greater charge transfer density in the electrode tests leads to gross surface melting, which makes the erosion/charge numbers in Table 6.9 inappropriate for direct application to railgun conductor design and materials selection. The tests are useful, nevertheless, for ranking the electrode materials in terms of relative performance.

TABLE 6.9 — MAX I High-Coulomb Stationary Arc Test Results

Electrode Material	Effective Charge/Shot (Coulombs)	Volume Eroded per Shot ($\text{cm}^3 \times 10^{-4}$)	Volume Eroded per Coulomb ($\text{cm}^3 \times 10^{-4} / \text{C}$)
CuW #1 + Ir	53.8	134	2.49
W #2	49.4	126	2.55
CuW #1 + Sb	37.4	97	2.59
CuW #3 (30W3)	56.7	149	2.63
CuW #1	54.0	148	2.74
CuW #2 (3W3)	53.8	149	2.77
W #1	51.2	156	3.05
CuW #1 + LaB ₆	56.5	215	3.81
Cu-Nb #2	51.8	248	4.79
Cu + LaB ₆	49.5	238	4.81
Cu-Nb #1	51.8	259	5.00
Cu-Nb + LaB ₆	55.8	338	6.06
Mo + LaB ₆	54.0	356	6.59
Cu-Al ₂ O ₃ (Al-60)	52.2	347	6.65
Mo	46.5	327	7.03
Cu-Ta	50.0	505	10.1
Cu-Al ₂ O ₃ (Al-15)	61.1	624	10.2
Cu #1	50.4	576	11.4

On the pages which follow, a series of eight graphs is presented in Figures 6.37 through 6.44 which shows the arc erosion performance of a large number of electrode materials. The experiments cover a wide range of charge per shot, and it is clear that when plotted on a log-log scale, the relationship between volume eroded per shot and charge per shot is generally quite linear.

TABLE 6.10 - Composition and Origin of Electrode Test Materials

Designation	Composition	Source
Cu + LaB ₆	97%Cu - 3%LaB ₆	Metallwerke Plansee GmbH.
CuNb	85%Cu - 15%Nb	Metallwerke Plansee GmbH.
CuNb + LaB ₆	83%Cu-14%Nb-3%LaB ₆	Metallwerke Plansee GmbH.
CuW + LaB ₆	66%W-31%Cu-3%LaB ₆	Metallwerke Plansee GmbH.
CuW #1 + Sb	66%W-31%Cu-3%Sb	Metallwerke Plansee GmbH.
CuW #2 (3W3)	68%W - 32%Cu	CMW Inc.
CuW #3 (30W3)	80%W - 20%Cu	CMW Inc.
CuNb #1	Cu-12%Nb	Supercon, Inc.
CuNb #2	Cu-12%Nb (finer filaments)	Supercon, Inc.

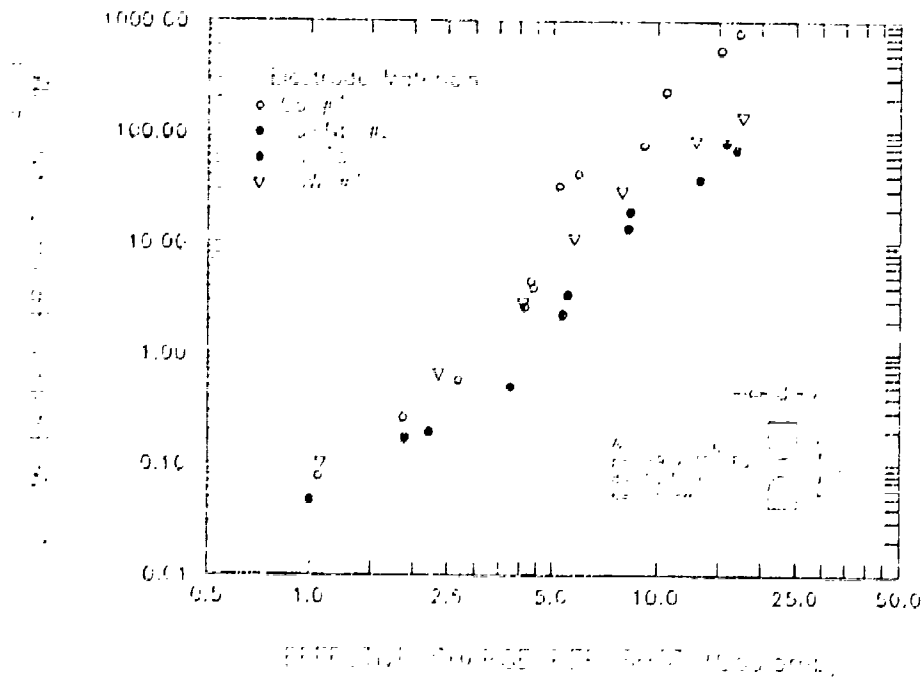


Figure 6.37 Stationary arc erosion test results for four copper-based hemispherical electrode materials tested in the Max I apparatus at TTU.

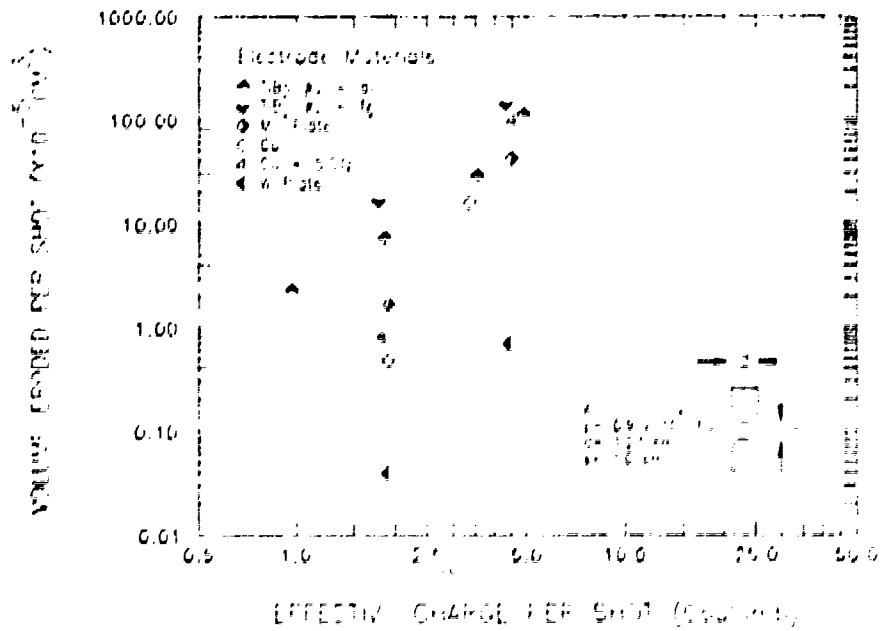


Figure 6.38 Stationary arc erosion test results for flat electrodes as a function of the effective charge per shot for five different conductor materials

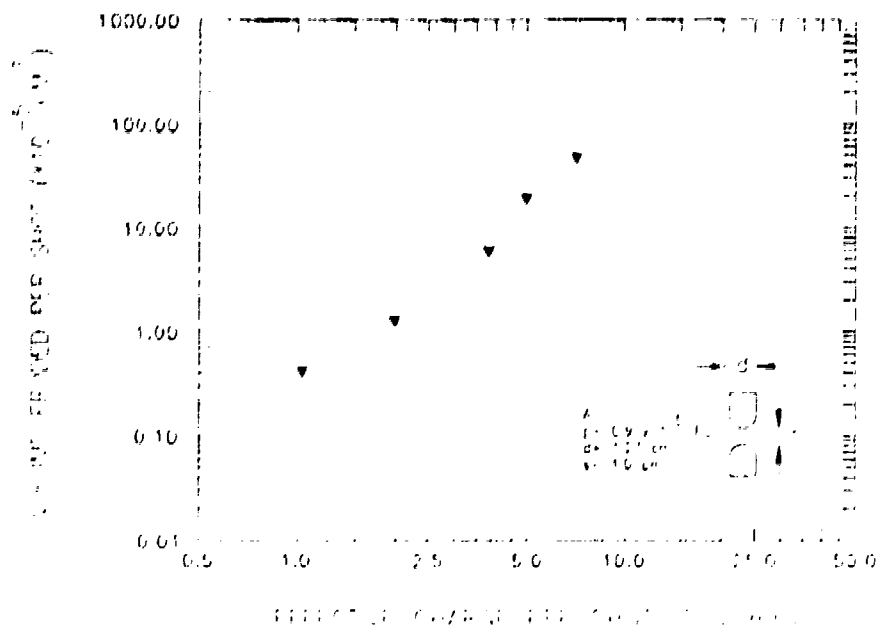


Figure 6.39 Stationary arc erosion test results for hemispherical electrodes as a function of the effective charge per shot for CuW + Re

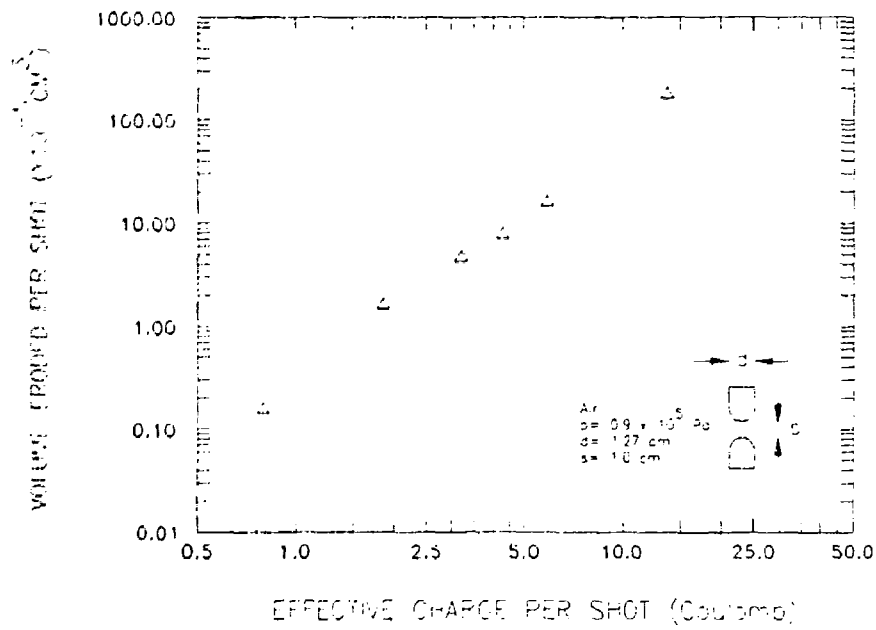


Figure 6.40 Stationary arc erosion test results for hemispherical electrodes as a function of the effective charge per shot for Tungsten alloy W #1

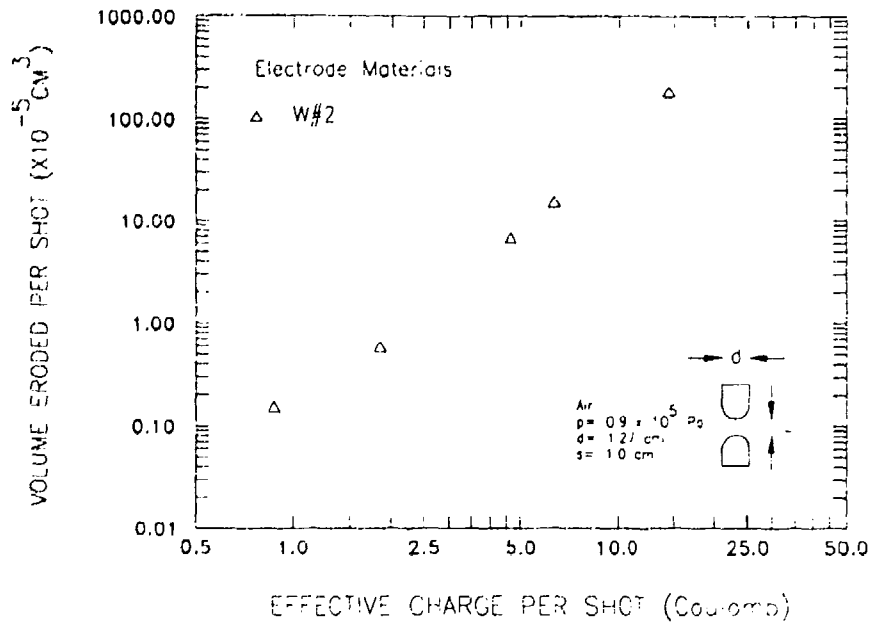


Figure 6.41 Stationary arc erosion test results for hemispherical electrodes as a function of the effective charge per shot for Tungsten alloy W #2 with its grains aligned perpendicular to the electrode surface.

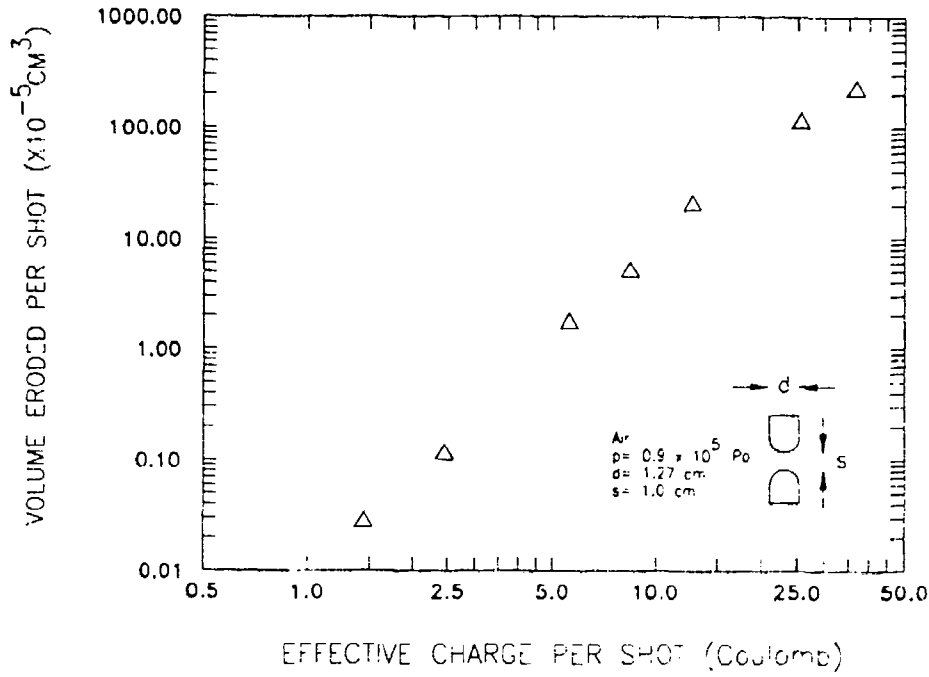


Figure 6.42 Stationary arc erosion test results for hemispherical electrodes as a function of the effective charge per shot for Dornier tungsten alloy W #3

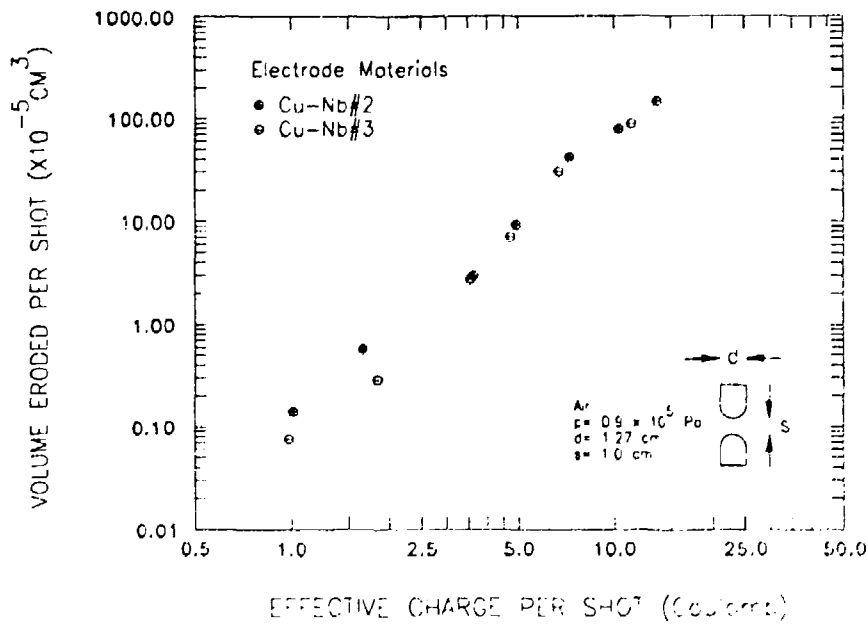


Figure 6.43 Stationary arc erosion test results for hemispherical electrodes as a function of the effective charge per shot for Supercon, Inc. Cu-Nb composites.

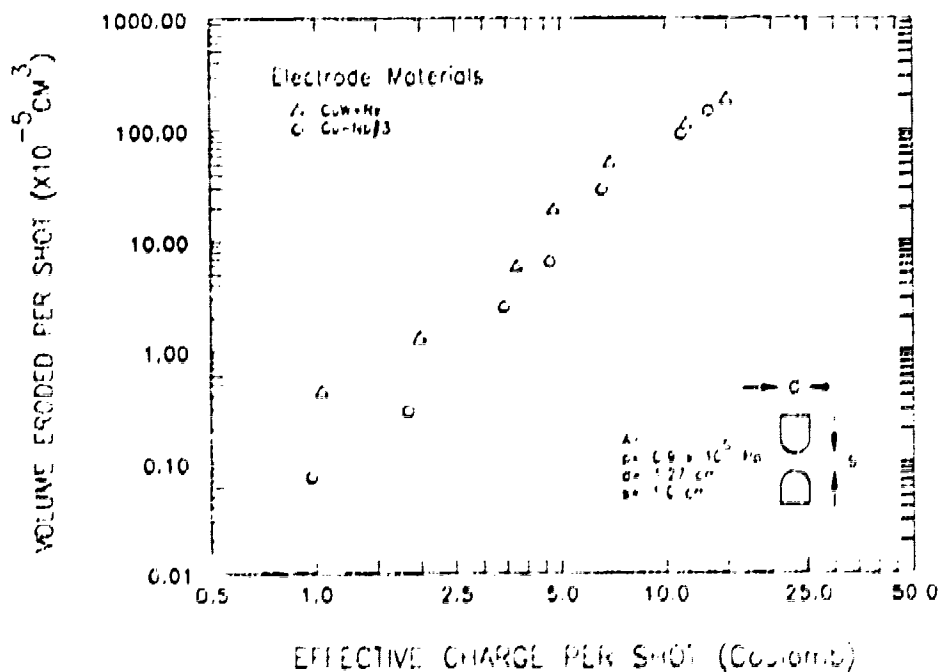


Figure 6.44 Stationary arc erosion test results for hemispherical electrodes as a function of the effective charge per shot for Cu-Nb compared to CuW + He.

Shown in Figure 6.42 is the volume of tungsten electrode alloy eroded per shot as a function of effective charge transfer (in coulombs) per shot. The tungsten alloy was W-6Ni-4Cu (by weight) and was designated W #3. As with previous tests, the total charge transfer per test point was about 1500 coulombs. Thus for the test point at 1 coulomb charge transfer per shot, about 1500 shots (pulses) were used to obtain the 1500 coulombs of total charge transfer. The total electrode volume eroded was then divided by 1500 to arrive at the volume of electrode material eroded per shot.

A tungsten alloy manufactured by CMW, Inc. of Indianapolis, Indiana (grade 1000) and a niobium reinforced copper alloy manufactured by Supercon Inc. of Shrewsbury, Massachusetts, exhibited greater arc erosion resistance at low coulomb levels than previously tested copper-tungsten alloys and different grades of niobium-copper. The materials were tested in the previously utilized Mark VI system at TTU using 1.27 cm (0.5 in) diameter hemispherical electrodes with a gap of 1 cm (0.39 in).

The copper niobium material (Cu-Nb #3) had a higher niobium filament density than the previously tested Cu-Nb #2 material. This was accomplished by further extrusion of the copper-niobium billet, thereby increasing the fineness of the filaments. It is possible that these finer filaments acted as better electron emitters and thus reduced erosion at the surface of the electrodes. However, as shown in Figure 6.43, after the

coulomb level reached about 5, the two materials (Cu-Nb #2 and Cu-Nb #3) behaved similarly. This was probably due to the melting of the niobium filaments at the surface, partially negating their emittance properties. The Cu-Nb #3 material is compared with previously tested CuW+Re material in Figure 6.44. The value of volume eroded per shot was significantly reduced at the lower coulomb levels. As discussed previously, a typical railgun environment has a charge transfer of about 2 to 10 coulombs per shot, depending on location in the bore.

As part of an advanced armature program that IAP Research, Inc. in Dayton, Ohio was conducting they agreed to test a conductive ceramic in their moving contact test facility. This device uses a current flowing from a stationary contact to a high speed rotating disk. The contact pressure between the stationary contact and the rotating disk is adjusted and measured at various electric current levels. Current densities of 100 to 1000 kA/cm² and armature speeds of 1 km/s can be evaluated in this facility. SPARTA produced five disks for test: one from the electrically conductive ceramic titanium diboride (TiB₂), one from pure molybdenum, one from the alumina dispersion strengthened copper alloy Glidcop Al60; and two from the copper alloy 110 to serve as a control. The disks were 5.0 in. (12.7 cm) in diameter with a 0.350 in. (0.89 cm) hole in their centers and were 0.25 in. (0.635 cm) thick.

Unfortunately there was not sufficient program funds at IAP to test the molybdenum and Glidcop disks but the titanium diboride disk was tested. At a peak current density of 790 kA/cm² the disk's perimeter was damaged and the tests stopped. The material exhibited a reasonably low contact resistance density which is important for solid armature railgun use. Because of the low ductility of the material the tests must be run very carefully to avoid overstressing the edges of the specimen. Thus, the 790 kA/cm² value may not be the true peak value.

6.3 Testing in the FLINT Railgun

6.3.1 Analysis and Modification of FLINT Gun Configuration

The FLINT gun is a small, square cross-section railgun which was used to test ceramic insulator materials produced in this program. It is located at the U.S. Army Research, Development and Engineering Center (ARDEC) at Picatinny Arsenal, New Jersey. The gun is built to the same design as the Plasma Utility Gun (PUG) at Eglin Air Force Base, Florida. The design of this gun makes replacement of bore insulators easy, and requires only simple rectangular shapes for these insulator panels. The purpose of the FLINT gun testing was to subject candidate ceramic insulator materials to the combined effects of all the mechanical, thermal, and electrical stresses present in an actual railgun. Before testing in the FLINT gun was begun, it was modified by replacing

some of the original insulator backup materials (G-10) with stiffer materials (graphite fiber reinforced epoxy) to reduce the deflections which the bore insulators would experience during firing.

A cross-section of the modified FLINT gun is shown in Figure 6.45. The insulator blocks were two different materials; bore facing blocks and backup blocks. The bore facing insulator rail was the test material while the backup insulator block was made from a directionally fiber reinforced resin matrix composite material. Requests for quotes were sent to several companies to determine the feasibility of using E-glass, S-glass, or a grade of graphite as the reinforcing fiber for the backup blocks. Graphite reinforced epoxy was selected as the replacement material. This material, oriented in such a direction as to provide the maximum stiffness between the side wall loading bolts and the bore insulator would offer a 5 to 12 times advantage in stiffness over conventionally used G-9, G-10, or G-11. This increased stiffness would result in reduced bending of the bore insulator ceramic test rail, which is very important for the survivability of the brittle ceramics. The conductor rails are backed by a 1.68 x 3.9 x 28 inch (4.3 x 10 x 71 cm) block made from the same materials used for the insulator backup blocks, graphite reinforced resin matrix composite. As in the case of the insulator sidewalls, this offers improved stiffness to reduce bore deflections.

An analysis of the stress state of the ARDEC FLINT gun was conducted. Actual material properties and barrel prestress states were used. The modified materials test section was compared with the previous design (and materials) used. The gun was modelled using a finite element code for the purpose of analyzing insulator deflections after upgrading with the higher modulus backup insulators. The properties of copper alloy Al60 (alumina dispersion strengthened) was used for the conductor rail modeling. The backup insulator was modeled as 62 v/o graphite in an epoxy matrix with 20% of the graphite fibers oriented along the bore length and 80% of the fibers perpendicular to the bore surfaces. The backup insulator properties were calculated using the computer modeling program ICAN (Integrated Composite Analyzer) based on the available property data of unidirectional layup graphite epoxy. The stresses and strains predicted by the model are mapped in Figure 6.46. Factors of up to 25 in reduction of displacement at the bore were calculated indicating the level of stiffening due to the modification.

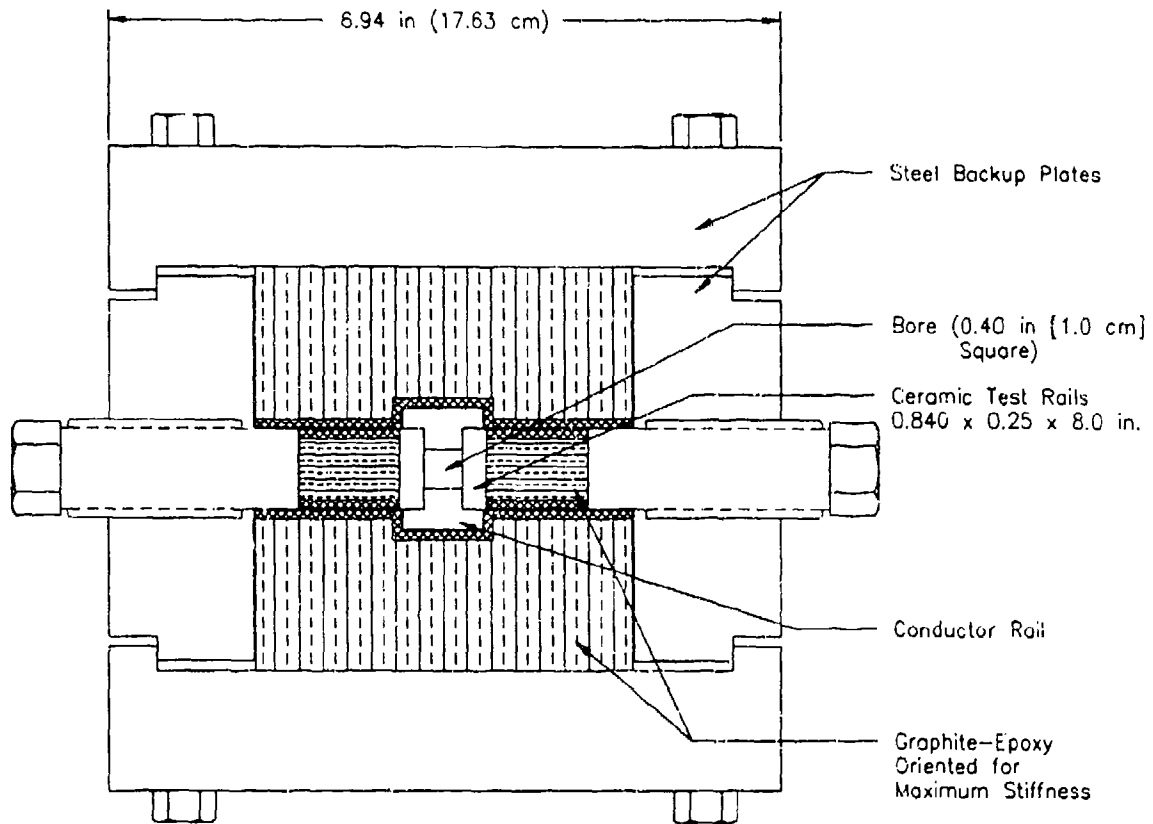


Figure 6.45 Cross-section of modified FLINT gun used for testing of advanced ceramics as bore insulators.

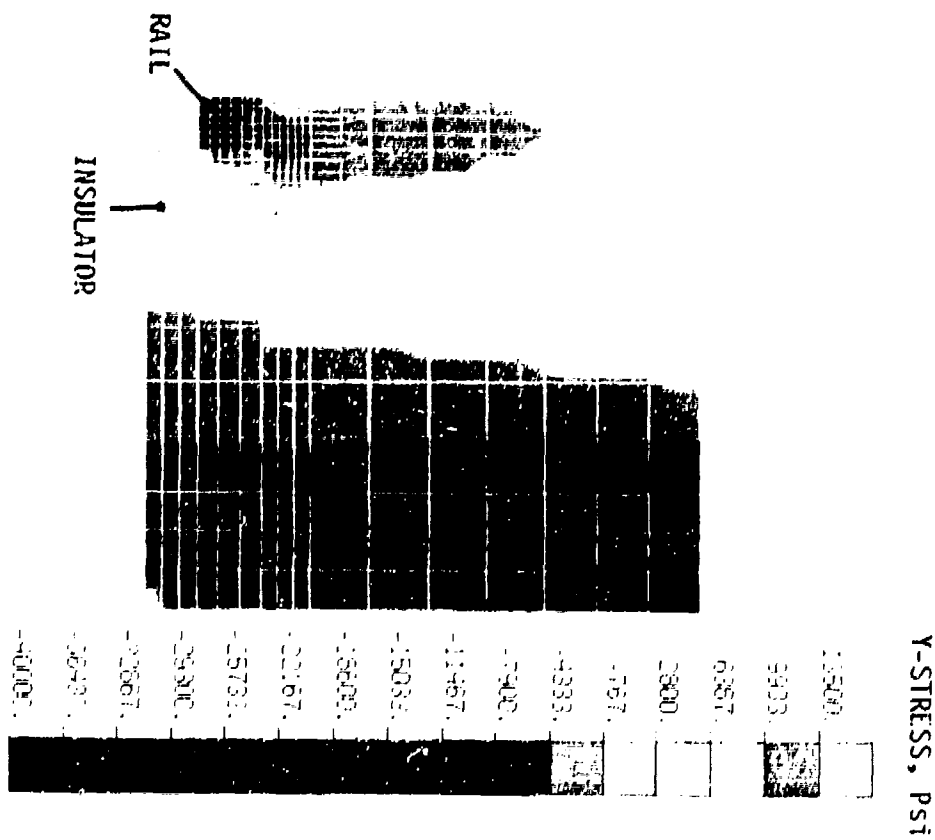
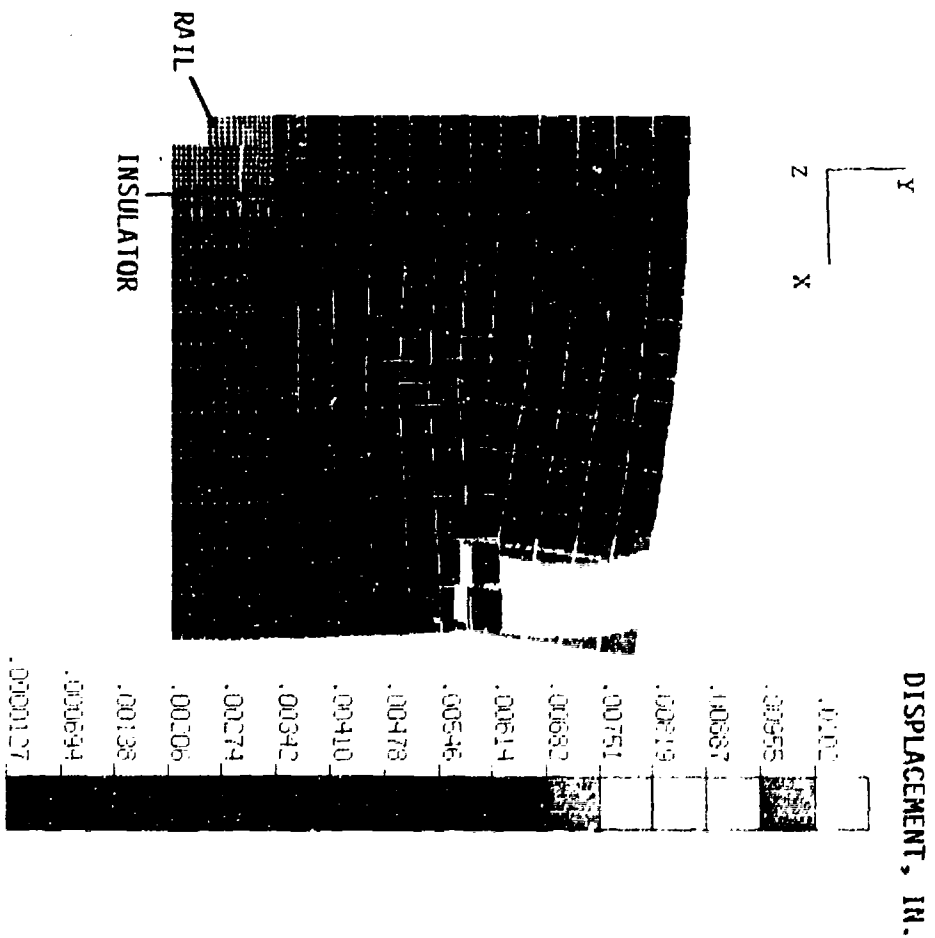


Figure 6.46 Finite element models of the cross-section of the modified FLINT gun barrel for testing of advanced ceramic insulator materials. Two different elastic moduli for the test bore insulator were used as inputs for the finite element runs: 175 and 345 GPa (25 and 50 Mpsi), with a Poisson ratio of 0.21 (typical value for ceramic materials). The rest of the barrel including the bolts and the top, bottom and side plates were modelled using the properties of steel.

The 2-D model of the barrel considers the interfaces between the barrel components as interface elements. This allowed us to examine the possibility of gap openings between the component materials such as between a conductor rail and a bore test insulator. Plasma and solid armature cases with 45 kpsi (310 MPa) bore pressure were analyzed. The effects of the originally designed prestresses of 30 ft-lb (41 N-m) torque on the side wall bolts and 60 ft-lb (81 N-m) torque on the top and bottom plate bolts were investigated, as well as the effects of doubling these values of torque. It was necessary to increase the prestress to maintain compression and to prevent separation between the rail and the test insulator (to prevent plasma leakage) during the plasma armature shots.

Figure 6.46 shows the predicted displacements and the Y direction (vertical) stresses of the modified FLINT gun utilizing a solid armature with a rail pressure of 45 kpsi (310 MPa) [350 kA/cm rail linear current density] and torque prestresses of 30 and 60 ft-lb (41 and 81 N-m). The elastic modulus of the test insulator was modeled as 50 Mpsi (345 GPa). The conductor rail deflects outward 0.002 in (0.05 mm) for the modified FLINT design compared to 0.050 in (0.125 mm) for the original square bore design. The maximum Y-stress of 32 kpsi (220 MPa) is localized at the rail and is below the yield strength of Al60 (83 kpsi (572 MPa) at room temperature). The Y-stresses in the graphite epoxy are below 4.5 kpsi (30 MPa), and the Y-stresses in the test insulator are below 13.5 kpsi (93 MPa). These values provide an adequate margin of safety against material failure.

6.3.2 Testing of Insulator Samples in FLINT

The railgun tests of advanced ceramic insulator rails in the FLINT railgun at ARDEC were conducted in August of 1989. The three pairs of rails tested are shown in Table 6.10. Shown in Figure 6.47 is a photograph of the first pair of rails after three shots in the FLINT gun. Quite a bit of difficulty was encountered in the assembly and alignment of the ceramic insulator rails in the gun. Shims had to be used in order to bring all the bore components into tight contact. The first set of test rails was successfully loaded into the gun and torqued to pre-set conditions. However, it was discovered that one of the shims had moved so it was decided to reassemble the bore components. Upon re-assembly and torquing of the top and side bolts, both insulators developed through-cracks in them. The cracks were not open, however, so it was decided to fire the gun. The gun firing did not cause the cracks to expand or to spall any material, thus a second and third shot were fired on the same set of rails.

TABLE 6.10 — Three Ceramic Insulator Samples Tested in the FLINT Gun

Test #	ID #	Composition	Outcome
1	N081	$\text{Al}_2\text{O}_3\text{-}0.25\text{Y}_2\text{O}_3\text{-}8\text{ZrO}_2$	Both rails broke during assembly, but no further damage occurred during three shots
2	4-253-4	$\text{Al}_2\text{O}_3\text{-}0.25\text{Y}_2\text{O}_3\text{-}8\text{ZrO}_2$	Rails loaded and fired three times successfully
3	N080	$\text{Al}_2\text{O}_3\text{-}0.25\text{Y}_2\text{O}_3\text{-}8\text{ZrO}_2\text{-}5\text{Cr}_2\text{O}_3$	One rail broke during assembly, but no further damage occurred during three shots

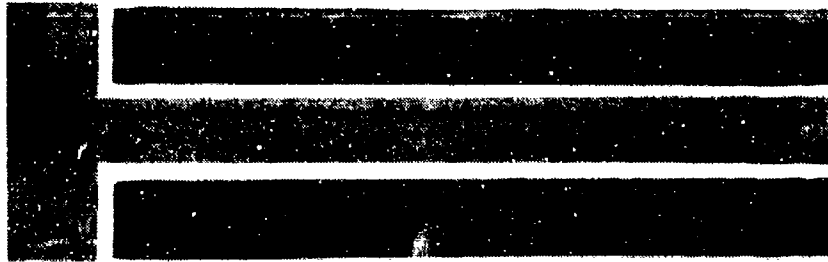


Figure 6.47 Photograph of the first pair of rails (N081) after three shots in FLINT gun at ARDEC.

The second pair of rails was successfully assembled into the FLINT gun and fired three shots with no damage. One of the rails from the third pair cracked at one location during assembly.

The first two sets of rails that were exposed were lower priority rails as they were used in order to establish set-up and test conditions for the railgun. The third set to be exposed were the higher performance materials selected from the results of the screening tests. At this point in the program, the FLINT testing was terminated because of budgetary limitations at ARDEC. The limited experience that was gained with the three pairs of samples that were tested indicate that advanced ceramics are indeed capable of withstanding the railgun environment. The cracking which did occur took place during

assembly, and not during gun operation, and even the pieces which did crack on assembly remained functional during the tests. This illustrates the importance of careful tolerancing of bore components and careful installation techniques during assembly when ceramic components are used.

This page is intentionally left blank.

SUMMARY AND CONCLUSIONS

This program focussed on the development of advanced ceramic materials for use as bore insulators for electromagnetic launchers. The results clearly demonstrated the feasibility of utilizing tailored property ceramics for this difficult application. Some valuable work was also accomplished on advanced conductor rail materials. Analysis conducted early in the program demonstrated the potential of the hard, stiff (high modulus), strong, and electrically insulating nature of advanced ceramics to dramatically improve the performance of EMLs. These properties are in contrast to those of currently utilized glass fiber reinforced polymer matrix materials which suffer significant ablation and erosion, have low stiffness, and are not capable of rep-rated operation with significant intershot rework.

The following items summarize the key results obtained and important conclusions reached during the program:

1. *Ceramic bore insulators lead to improved EML performance.* - Advanced ceramics, through the use of micro-architectural tailoring, can be utilized as rail-gun bore insulators to result in improved gun performance. Improvements arise because of their hardness (to prevent gouging and erosion by projectiles) and high melting or dissociation temperature, which leads to reduced ablation during exposure to the plasma, and thus dramatically increased bore lifetime. Less erosion and ablation leads to a smoother bore, which decreases the amount of damage the projectile sees while in bore due to balloting and abrasion. Another advantage is the increased stiffness, which reduces bore deflection and thus improves projectile/ bore interactions, gun efficiency and accuracy (less dispersion). Increased flexural strength resists the bending loads caused by plasma and electromagnetic pressures. Superior surface voltage standoff capability allows operation of a rep-rated gun without the need to remove conductive residue from the surface of the insulator between shots. Even guns that are not rep-rated would benefit as considerable time and effort is expended with current railguns in cleaning the bore between shots.

2. *Most advanced ceramics lose their surface voltage standoff capability after exposure to electrical arcs.* - The choice of ceramic material is severely restricted by the requirement for rep-rated surface voltage holdoff strength. This is most important for plasma armatures and less of a concern for solid armatures. Many ceramic materials dissociate under the intense heat pulse from the plasma arc, resulting in the formation of a conductive metallic film or nodules on the surface. This film can effectively short circuit the bore, preventing operation of the gun. A wide variety of ceramic materials evidence this behavior, such as silicon nitride, aluminum nitride, and ceramics with more than about 5% zirconia. Alumina-based materials do not exhibit this conductive film formation and do possess the necessary surface voltage standoff resistance necessary for use as EML bore insulators (plasma or solid armature).

3. *A microstructurally toughened alumina-zirconia-chromia ceramic was developed which satisfies all bore insulator requirements.* - Large, high quality pieces of $Al_2O_3 - 5\%ZrO_2 - 0.25\%Y_2O_3 - 5\%Cr_2O_3$ material were successfully fabricated. The material's microstructure revealed good distribution of constituents and phases for improved toughness, small grain size (for improved strength), and a mixed mode high energy fracture surface (leading to good toughness). The goal properties were all exceeded as shown in Table 7.1. The measured values were taken from the largest size pieces scaled-up in the program, 1.5 x 4.0 x 18.0 inches (3.8 x 10.2 x 45.7 cm). A patent for this material has been applied for.

The properties realized from this material were made possible through the microarchitectural designing (tailoring) of materials utilizing the concepts discussed in Section 5.1. These tailoring methods included the proper choice of matrix (alumina) for basic strength, toughness and electrical properties; the solid solution strengthening by the chromia (which also increased the surface voltage standoff strength); the grain size refining which resulted in an average grain size of 10 microns (0.0004 in.); the use of zirconia and yttria as glassy grain boundary phase forming materials in order to permit full consolidation at moderate temperatures; and the use of the same materials (zirconia and yttria) as second-phase strengtheners.

4. *The selected ceramic can be fabricated in full-scale rail segments without loss of properties.* - Strength values for experimental advanced ceramics are often reported for very small, laboratory-scale specimens which cannot be reproduced in useful sizes. The values listed in Table 7.1 were attained in the largest size form produced in the program, measuring 1.5 x 4.0 x 18.0 inches (3.8 x 10.2 x 45.7 cm). This size is representative of what would be needed for the actual fabrication of large railgun bore insulators.

TABLE 7.1 - Measured vs Goal Properties of Alumina-Zirconia-Chromia Bore Insulator Material

Property	Goal	Measured Value
99.9% Design Allowable Flexural (MOR) Strength,	50 kpsi (345 MPa)	68.1 kpsi (470 MPa)
Fracture Toughness	5.0 kpsi·in ^{1/2} (5.5 MPa·m ^{1/2})	5.3 kpsi·in ^{1/2} (5.8 MPa·m ^{1/2})
Elastic Modulus	40 Mpsi (275 GPa)	42 Mpsi (290 GPa)
Surface Voltage Standoff (after 100 arcs)	2 kV/cm	8 kV/cm

5. *Chromia additions produce superior voltage standoff in alumina ceramics.* - The addition of chromia to the alumina-based ceramics results in improved surface voltage standoff strength, especially for repetitive firing conditions. In addition the chromia acts as a solid solution strengthener and proper amounts added to alumina result in increased strength. The addition of SiC whiskers to the alumina, while improving mechanical properties, decreases the surface voltage standoff strength due to the intrinsic semiconducting nature of the SiC material.
6. *Whisker-reinforced silicon nitride was produced with remarkable mechanical properties.* - Relatively large panels (1.5 x 4.0 x 8.0 in. (3.8 x 10.2 x 20.4 cm) of silicon carbide whisker reinforced silicon nitride ceramic were also fabricated. The mechanical properties of this material were better than the alumina-chromia, with values of 98.8 kpsi (681 MPa) MOR strength (99.9% reliability), 8.8 kpsi·in^{1/2} (9.7 MPa·m^{1/2}) fracture toughness, and 45 Mpsi (311 GPa) modulus.
7. *Silicon nodules form on the surface of silicon nitride upon arc exposure, compromising its insulating ability.* - Silicon nitride based ceramics, despite their impressive mechanical properties, are only marginally adequate for use in EMLs because of the dissociation of the silicon nitride to form nodules of silicon metal on the surface exposed to the arc. These silicon nodules are not interconnected (even after multiple pulses) so the material possesses a finite surface voltage holdoff strength of about 1 kV/cm (with no cleaning between shots). This level of standoff strength may still be adequate for certain types of solid, hybrid, or transitioning armature guns. Another application would be to only use the material in the breech section of the gun in the length before a solid armature could transition to a plasma armature.

8. *Experimental ceramic insulators were successfully test-fired in the FLINT railgun.* Railgun insulator test segments (0.840 x 0.250 x 8.000 in. (2.13 x 0.635 x 20.32 cm)) were produced and successfully fired in the FLINT railgun at the U.S. Army Armament Research, Development and Engineering Center (ARDEC) at Picatinny Arsenal, New Jersey. The bore of this gun had been analyzed, the then currently used G-10 backup insulators replaced with directionally oriented graphite reinforced epoxy to reduce bore insulator deflection during a shot. These tests demonstrated the low ablation potential of the chromia/alumina material. Important lessons were learned about the need to design a system for the ceramics by proper tolerancing of components and proper installation techniques.
9. *An extensive series of candidate insulator materials was ranked for multiple arc exposure resistance.* - A wide variety of insulating materials: ceramics, resin matrix composites, and monolithic polymers was exposed to a rep-rated (approximately 1 Hz) plasma arc with a representative railgun current density at Texas Tech University. These tests were performed to assess their surface voltage standoff strength. The microscopic surface appearance of the exposed materials closely mirrored that seen in railgun exposed insulator materials. This demonstrates the validity of the apparatus for the electrical testing of railgun insulator materials.

Although the chief emphasis of this program was on the development of improved insulator materials, some valuable work was also performed in the evaluation of advanced conductor materials. The refractory metals tungsten, molybdenum, niobium, and rhenium were investigated in various combinations with copper. The refractory nonmetallic compounds lanthanum hexaboride and titanium diboride were also examined. The primary conclusions arising from this testing of conductor materials is as follows:

10. *Titanium diboride shows promise as an advanced conductor rail material.* - Electrically conductive ceramics show some potential for use as conductor rails for EMLs. Limited work in the program focused on the ceramic titanium diboride (TiB_2) which possesses an electrical conductivity of approximately 24% I.A.C.S. (i.e. about 24% as conductive as pure copper). No railgun tests were performed with the material but sliding contact tests conducted at I.A.P. Inc. in Dayton, Ohio demonstrated that the diboride material possessed excellent current passage characteristics and can accommodate a very large amount of electrical "action" (current integrated over time) before melting or dissociating. Much additional effort would be required to use the material as an actual railgun conductor rail because of its limited ductility and resistance to shock (thermal and mechanical).
11. *Some refractory metal materials were found to be more resistant to arc erosion than pure copper.* - There exist many materials with arc melting resistance superior to pure copper. SPARTA has conducted numerous prior programs that demonstrated the usefulness of cladding refractory metals (molybdenum, tungsten and

tantalum) on copper substrate for use as railgun conductor rails. High coulomb stationary arc tests conducted at Texas Tech University revealed that a wide variety of additional electrode materials (obtained from electrode manufacturers in the U.S. and overseas), not previously investigated for use as railgun conductors, possessed erosion resistance up to four times greater than copper. These materials are generally not available in the sizes and forms needed for rails, however, and much additional work is needed to turn them into viable rail candidates.

This page is intentionally left blank.

RECOMMENDATIONS FOR FUTURE WORK

SPARTA's program resulted in the development of a ceramic insulator material that meets the mechanical and electrical requirements for use as an electromagnetic railgun bore insulator. The feasibility of scale-up to sizes representative of those needed for use in current full scale guns was demonstrated. Additional issues still must be addressed before the ceramic material can be utilized with confidence in EMLs, however. These include:

1. *Demonstrate the affordable and repeatable production of full-scale ceramic insulator segments by methods such as near-net-shape forming.* - Only one large scale (1.5 x 4 x 18 in. (3.8 x 10.2 x 45.7 cm)) block was fabricated during the completed program. Additional blocks must be made and tested in order to demonstrate the reproducibility of the mechanical and physical properties. The large sizes made were hot-pressed as rectangular blocks. Specimens were cut from them with diamond tooling. The future ceramic bore insulator segment shapes may be somewhat complex, so their production by lower cost methods, such as near-net-shape forming is necessary. A study involving the hot-pressing of cylindrical shells or shell segments should be performed to demonstrate the retainment of mechanical and electrical properties in these somewhat more complex geometries.
2. *Demonstrate nondestructive flaw detection.* - The fracture toughness goal that was established in this program was based on the premise that any material would be discarded which was found to contain flaws larger than 0.010 inch (0.254 mm). If flaws this small cannot be reliably identified, then higher levels of fracture toughness will be required. A new x-ray inspection technology known as Microsoft X-ray has been developed and marketed by IRT Corp. in San Diego, California which is ideally suited to the inspection of thick ceramic parts. A flaw detection study should be conducted with this method (or other similar methods) on ceramic parts of the same dimensions and composition as those which will be used as bore insulators in a large railgun.
3. *Develop joints for railgun ceramic bore insulators.* - The maximum practical (technical and economic) length for advanced hot-pressed ceramics is about 40 inches (one meter). Thus, for full scale EMLs which may range in length from 20 to 100 feet (6 to 30 meters) multiple joints are needed in order to connect the

segments. These joints must resist the bending loads present as the projectile passes and must not permit the hot plasma (for a plasma, hybrid or transitioning armature gun) from penetrating the joint and leaving a conductive residue. Examples of joint types include butt, lap and beveled, all with or without grouting (ceramic cement). These joint designs impose additional tolerance constraints on the manufacturing method for the insulator segments. Different joint designs can be tested in a smaller gun (50 or 90 mm bore diameter) in order to economically evaluate a number of different joint concepts to down-select a single, best design.

4. *Select a cement composition.* - A study of different cement materials must be conducted. The cement must possess the same high voltage surface standoff strength and plasma ablation resistance as the bore insulators, as well as showing good strength and toughness. A variety of ceramic cements are commercially available which warrant scrutiny. It may also be advisable to examine epoxies, cyanate esters, and other polymers filled with ceramic particles. The same type of arc exposure tests which were performed at TTU to evaluate insulator materials should be repeated for cemented joints.
5. *Demonstrate ceramic insulator performance in full scale (90 or 120 mm bore diameter) railguns for multiple shots.* - The railgun shots completed during this program were conducted on short, thin ceramic segments backed by a high modulus support. It is necessary to test the full-scale pieces because the stress state will differ in the large pieces and problems of alignment, tolerancing, and precompression could not be addressed in the small gun. This demonstration would include use of joints and would probably consist of just a few segments in the breech end of the gun, where the harshest environment exists.
6. *Retrofit an existing full-scale round bore barrel with ceramic bore insulators.* - This would enable a demonstration of the effect of a full set of ceramic bore insulators on the efficiency, reproducibility, aiming accuracy, and lifetime of the barrel. In addition, the issue of honing of the ceramic segments while in place would be addressed.

It is a consensus in the electric gun community that railgun insulator performance has been a primary technical barrier in achieving the efficiency, accuracy and lifetime required in operational systems. The successful completion of the work recommended above would be a vital step in resolving the insulator problems and would add greatly to the advancement of electromagnetic launcher technology for use as reliable weapon or launch systems. It is estimated that the total length of such a program would be about two to three years for the full scale demonstration.

REFERENCES

1. S.N. Rosenwasser; "Recent Advances in Large Railgun Structures and Materials Technology", *IEEE Transactions on Magnetics*, 27(1):444-451 (1991).
2. S.N. Rosenwasser and R.D. Stevenson; "Selection and Evaluation of Insulator Materials for High-Performance Railgun Bores", *IEEE Trans Magnetics*, 22:1722-1729, (1986).
3. T.C. Derbidge et al. - Astron Research and Engineering, Inc.; "High Performance Insulator Materials for Electromagnetic Railguns", Final Report for Defense Nuclear Agency, DNA-TR-91-8, September 1991.
4. "Proceedings of the 1980 Conference on Electromagnetic Guns and Launchers"; *IEEE Transactions on Magnetics*, Volume 18 number 1, January 1982.
5. "Proceedings of the 2nd Symposium on Electromagnetic Launch Technology"; *IEEE Transactions on Magnetics*, Volume 20 number 2, March 1984.
6. "Proceedings of the 3rd Symposium on Electromagnetic Launch Technology"; *IEEE Transactions on Magnetics*, Volume 22 number 6, November 1986
7. "Proceedings of the 4th Symposium on Electromagnetic Launch Technology"; *IEEE Transactions on Magnetics*, Volume 25 number 1, January 1989.
8. "Proceedings of the 5th Symposium on Electromagnetic Launcher Technology"; *IEEE Transactions on Magnetics*, Volume 27 number 1, January 1991 pp 7-659.
9. D.B. Marshal; "Failure From Surface Flaws" in *Fracture in Ceramic Materials*, A.G. Evans, ed., Noyes Publ. Co., Park Ridge, NJ (1984), pp190-220.
10. J.T. Neil et al; "Improving the Reliability of Silicon Nitride: A Case Study", *Advanced Ceramic Materials*, 3:225-230 (1988).
11. R.D. Stevenson and S.N. Rosenwasser, "Development of Erosion Resistant Rails for Multishot Electromagnetic Launchers (Phase I)", AFATL TR-86-34, Air Force Armament Laboratory, Eglin Air Force Base, FL, 1986.
12. R.D. Stevenson et al, "Erosion Resistant rails for Multishot Electromagnetic Launchers", AFATL TR-89-62, Air Force Armament Laboratory, Eglin Air Force Base, FL, 1989.
13. R.D. Stevenson et al, "Development of High Performance, Erosion-Resistant Clad Conductor Rails", to be published by AFATL, Eglin AFB, FL, 1991.
14. D.L. Vrable et al, Design and Fabrication of an Advanced, Lightweight, High Stiffness, Railgun Barrel Concept, *IEEE Trans. Magnetics*, V27, 1991, pp. 470-475.
15. T.N. Tiegs and P.F. Becher; "Sintered Al_2O_3 / SiC Whisker Composites", *Am. Ceram. Soc. Bull.*, 66(2): 339-342 (1987).
16. J.H. Homeny, W.L. Vaughn, and M.K. Ferber; "Processing and Mechanical Properties of SiC Whisker / Al_2O_3 Matrix Composites", *Cer. Bull.* 66(2):333-338 (1987).
17. Military Standard MIL-STD-19421 (MR), "Strength of High Performance Ceramics at Ambient Temperature", (1983).
18. G.D. Quinn, et al; "Commentary on U.S. Army Standard Test Method for Flexural Strength of High Performance Ceramics at Ambient Temperatures", AMMRC 85-21, U.S. Army Materials and Mechanics Research Center, Watertown, MA., (1985).

19. G.K. Bansal and W.H. Duckworth; "Fracture Surface Energy Measurements by the Notch-Beam Technique", **Fracture Mechanics Applied to Brittle Materials: ASTM STP-678**, pp 38-46 (1979).
20. T.G. Engel; "High-Performance Insulator Materials for High-Current Switching Applications", *Proc. 7th IEEE Pulsed Power Conf. 1989* pp 336-340.
21. T.G. Engel et al; "Estimating the Erosion and Degradation Performance of Ceramic and Polymeric Insulator Materials in High-Current Arc Environments", *IEEE Trans Magnetics*, 27(1):533-537
22. S.N. Rosenwasser and R.D. Stevenson; "Selection and Evaluation of Insulator Materials for High-Performance Railgun Bores", *IEEE Trans Magnetics*, 22:1722-1729, (1986).
23. A.L. Donaldson; *Electrode Erosion in High Energy, High Current Transient Arcs*, Ph.D. Dissertation, Texas Tech Univ., December, 1990.

DISTRIBUTION LIST

No. of Copies	To
	Commander, U.S. Army Laboratory Command, 2800 Powder Mill Road, Adelphi, MD 20783-1145
1	ATTN: AMSLC-IM-TL
1	AMSLC-CT
	Commander, Defense Technical Information Center, Cameron Station, Building 5, 5010 Duke Street, Alexandria, VA 22304-6145
2	ATTN: DTIC-FDAC
	Director, Strategic Defense Initiative Organization, Office of the Secretary of Defense, Washington, DC 20310
1	ATTN: DSIO/SLKT, LTC M. Obal
1	Dr. John Stubstad
	U.S. Army Strategic Defense Command, P.O. Box 1500, Huntsville, AL 35807-3801
2	ATTN: SFAE-SD-GBI-I, David Montgomery
1	SFAE-SD-HED-A, Norven Goddard
1	SFAE-SD-HED-I, Robert Franklin
2	SFAE-SD-HVL, Stanley Smith
1	SFAE-SD-HPL, Col. Steve Kee
1	CSSD-KE-F, Joseph Butler
1	CSSD-KE-F, John R. Warden
1	CSSD-SL-K, Brian Hunter
2	CSSD-TM-H, Jimmy Derrick
1	CSSD-SL-S, Russel Freeman
1	CSSD-SL-K, Larry Atha
	Commander, USAMICOM, RD&E Center, Structures Directorate, Redstone Arsenal, AL 35898
1	ATTN: AMSMI-RD-ST-SAA, W. Nourse
	Institute for Defense Analysis, 1801 North Beauregard Street, Alexandria, VA 22311
1	ATTN: M. Rigdon
	McDonnell Douglas SSC, 5301 Bolsa Avenue, Huntington Beach, CA 92647
1	ATTN: J. Tracy
1	J. Davidson

- 1 SPARTA, Inc. 9455 Towne Centre Drive, San Deigo, CA 92121-1964
1 ATTN: Gary Wonacott
- Teledyne Brown Engineering Company, 300 Sparkman Drive, Huntsville, AL
35807-7007
- 1 ATTN: Charles Patty
- U.S. Army Armament RD&E Center, Picatinny Arsenal, NJ 07806-5000
- 1 ATTN: SFAE-SD-HVL, Curt Dunham
- Director, U.S. Army Materials Technology Laboratory, Watertown, MA
02172-0001
- 2 ATTN: SLCMT-TML
- 1 SLCMT-PRA
- 1 SLCMT-IMA-V
- 1 SLCMT-BM, John Dignam
- 1 SLCMT-BM, Robert Fitzpatrick, COR
- 1 Headquarters of DNA/RAEV, 6801 Telegraph Road, Alexandria, VA
22310-3398
ATTN: Maj. Jeffrey Cukr
- WL/MMSH, Eglin AFB FL 32542-5434
- 1 ATTN: Al Young
- 1 Nolan Taconi
- SDIO/TNI, The Pentagon, Room 1E 167, Washington D.C. 20301-7100
- 1 ATTN: Col. Peter Rustan
- Headquarters of DNA, Office of Technology Applications, 6801 Telegraph
Road, Alexandria, VA 22310-3398
- 1 ATTN: Col. Michael Downie

<p>U.S. Army Materials Technology Laboratory Watertown, Massachusetts 02172-0001</p> <p>DEVELOPMENT AND TESTING OF ADVANCED EM ACCELERATOR BORE MATERIALS</p>	<p>AD UNCLASSIFIED UNLIMITED DISTRIBUTION</p>	<p>Key Words Railgun Insulators EM Launchers Bore Materials Fracture Toughness Ceramics</p>	<p>R.D. Stevenson, S.N. Rosenwasser, and J.W. McCoy SPARTA, Inc. 9455 Towne Centre Drive San Diego, CA 92121</p> <p>Technical Report MTL TR 92-10, February 1992, 142pp. Illustrations, Contract DAAL04-86-C-0045</p> <p>Interim Report</p> <p>Electromagnetic railguns are being considered for a number of potential Strategic Defense, Theater Missile Defense and tactical missile applications. Bore materials, particularly insulators, limit the performance and lifetime of current railguns. A program was undertaken to develop improved advanced ceramic insulators. The program aim was to analytically determine the property goals required of bore insulators to meet railgun systems requirements; select and design initial candidate materials using micro-architectural tailoring; fabricate and test panels of the selected materials; iterate compositions and processing parameters to improve properties; and down-select to an optimal material and scale it up to a size required for near-term railguns. From the start of the program, it was realized that ceramics alone possessed the necessary properties to meet the system requirements. Through a combination of mechanical and electrical tests, a large number of ceramic materials were screened. Microstructurally toughened aluminum oxide based ceramics gave the best combination of mechanical and electrical properties. The addition of chromia to the base alumina-zirconia yttria composition improved the electrical properties with no compromise in mechanical properties. The alumina-chromia material was successfully scaled up to 1.5 x 4 x 18 inch pieces, representative of large railgun bore insulators. These scaled-up pieces also met the mechanical and electrical goal properties for railgun insulator operations. The additional work required to produce and qualify these insulator materials for reliable and cost effective high-energy railgun utilization was recommended.</p>
<p>U.S. Army Materials Technology Laboratory Watertown, Massachusetts 02172-0001</p> <p>DEVELOPMENT AND TESTING OF ADVANCED EM ACCELERATOR BORE MATERIALS</p>	<p>AD UNCLASSIFIED UNLIMITED DISTRIBUTION</p>	<p>Key Words Railgun Insulators EM Launchers Bore Materials Fracture Toughness Ceramics</p>	<p>R.D. Stevenson, S.N. Rosenwasser, and J.W. McCoy SPARTA, Inc. 9455 Towne Centre Drive San Diego, CA 92121</p> <p>Technical Report MTL TR 92-10, February 1992, 142pp. Illustrations, Contract DAAL04-86-C-0045</p> <p>Interim Report</p> <p>Electromagnetic railguns are being considered for a number of potential Strategic Defense, Theater Missile Defense and tactical missile applications. Bore materials, particularly insulators, limit the performance and lifetime of current railguns. A program was undertaken to develop improved advanced ceramic insulators. The program aim was to analytically determine the property goals required of bore insulators to meet railgun systems requirements; select and design initial candidate materials using micro-architectural tailoring; fabricate and test panels of the selected materials; iterate compositions and processing parameters to improve properties; and down-select to an optimal material and scale it up to a size required for near-term railguns. From the start of the program, it was realized that ceramics alone possessed the necessary properties to meet the system requirements. Through a combination of mechanical and electrical tests, a large number of ceramic materials were screened. Microstructurally toughened aluminum oxide based ceramics gave the best combination of mechanical and electrical properties. The addition of chromia to the base alumina-zirconia yttria composition improved the electrical properties with no compromise in mechanical properties. The alumina-chromia material was successfully scaled up to 1.5 x 4 x 18 inch pieces, representative of large railgun bore insulators. These scaled-up pieces also met the mechanical and electrical goal properties for railgun insulator operations. The additional work required to produce and qualify these insulator materials for reliable and cost effective high-energy railgun utilization was recommended.</p>

<p>U.S. Army Materials Technology Laboratory Watertown, Massachusetts 02172-0001</p> <p>DEVELOPMENT AND TESTING OF ADVANCED EM ACCELERATOR BORE MATERIALS</p>	<p>AD UNCLASSIFIED UNLIMITED DISTRIBUTION</p>	<p>Key Words Railgun Insulators EM Launchers Bore Materials Fracture Toughness Ceramics</p>	<p>R.D. Stevenson, S.N. Rosenwasser, and J.W. McCoy SPARTA, Inc. 9455 Towne Centre Drive San Diego, CA 92121</p> <p>Technical Report MTL TR 92-10, February 1992, 142pp. Illustrations, Contract DAAL04-86-C-0045</p> <p>Interim Report</p> <p>Electromagnetic railguns are being considered for a number of potential Strategic Defense, Theater Missile Defense and tactical missile applications. Bore materials, particularly insulators, limit the performance and lifetime of current railguns. A program was undertaken to develop improved advanced ceramic insulators. The program aim was to analytically determine the property goals required of bore insulators to meet railgun systems requirements; select and design initial candidate materials using micro-architectural tailoring; fabricate and test panels of the selected materials; iterate compositions and processing parameters to improve properties; and down-select to an optimal material and scale it up to a size required for near-term railguns. From the start of the program, it was realized that ceramics alone possessed the necessary properties to meet the system requirements. Through a combination of mechanical and electrical tests, a large number of ceramic materials were screened. Microstructurally toughened aluminum oxide based ceramics gave the best combination of mechanical and electrical properties. The addition of chromia to the base alumina-zirconia yttria composition improved the electrical properties with no compromise in mechanical properties. The alumina-chromia material was successfully scaled up to 1.5 x 4 x 18 inch pieces, representative of large railgun bore insulators. These scaled-up pieces also met the mechanical and electrical goal properties for railgun insulator operations. The additional work required to produce and qualify these insulator materials for reliable and cost effective high-energy railgun utilization was recommended.</p>
<p>U.S. Army Materials Technology Laboratory Watertown, Massachusetts 02172-0001</p> <p>DEVELOPMENT AND TESTING OF ADVANCED EM ACCELERATOR BORE MATERIALS</p>	<p>AD UNCLASSIFIED UNLIMITED DISTRIBUTION</p>	<p>Key Words Railgun Insulators EM Launchers Bore Materials Fracture Toughness Ceramics</p>	<p>R.D. Stevenson, S.N. Rosenwasser, and J.W. McCoy SPARTA, Inc. 9455 Towne Centre Drive San Diego, CA 92121</p> <p>Technical Report MTL TR 92-10, February 1992, 142pp. Illustrations, Contract DAAL04-86-C-0045</p> <p>Interim Report</p> <p>Electromagnetic railguns are being considered for a number of potential Strategic Defense, Theater Missile Defense and tactical missile applications. Bore materials, particularly insulators, limit the performance and lifetime of current railguns. A program was undertaken to develop improved advanced ceramic insulators. The program aim was to analytically determine the property goals required of bore insulators to meet railgun systems requirements; select and design initial candidate materials using micro-architectural tailoring; fabricate and test panels of the selected materials; iterate compositions and processing parameters to improve properties; and down-select to an optimal material and scale it up to a size required for near-term railguns. From the start of the program, it was realized that ceramics alone possessed the necessary properties to meet the system requirements. Through a combination of mechanical and electrical tests, a large number of ceramic materials were screened. Microstructurally toughened aluminum oxide based ceramics gave the best combination of mechanical and electrical properties. The addition of chromia to the base alumina-zirconia yttria composition improved the electrical properties with no compromise in mechanical properties. The alumina-chromia material was successfully scaled up to 1.5 x 4 x 18 inch pieces, representative of large railgun bore insulators. These scaled-up pieces also met the mechanical and electrical goal properties for railgun insulator operations. The additional work required to produce and qualify these insulator materials for reliable and cost effective high-energy railgun utilization was recommended.</p>